My Diploma Thesis

Martin Wiebusch

Contents

Introduction

Over the last two decades, the Standard Model of Particle Physics has been most successful in explaining a wide range of phenomena in particle physics. It describes the electromagnetic and weak interactions with an $SU(2) \times U(1)$ gauge theory, that undergoes a spontaneous breakdown to the $U(1)$ symmetry of electromagnetism. The strong interactions are described by Quantum Chromo-Dynamics (QCD), which is an $SU(3)$ gauge theory. So far no disagreements between experimental data and predictions of the Standard Model have been found. On the other hand, many parameters of the Standard Model are still only known to a very low precision. In particular, the elements of the Cabibbo-Kobayashi-Maskawa (CKM) matrix, that determine the couplings between quarks of different generations and the W bosons, are affected by large uncertainties. Consistency checks for the Standard Model and the search for physics beyond it require the exact determination of these parameters.

The uncertainties of the CKM matrix elements are not due to a lack of precise experimental data. Their origin are theoretical errors, which inevitably enter calculations, that try to determine observables related to weak hadronic decays from first principles. The main problem is, that perturbation theory fails to describe the dynamics of QCD at low energies. Thus, non-perturbative methods like numerical lattice simulations have to be applied, and these methods introduce their own numerical and systematic errors.

Particularly large theoretical uncertainties occur in the context of CP violating decays of neutral kaons. For almost 40 years the violation of CP symmetry in nonleptonic kaon decays like $K^0 \to \pi\pi$ has been known, but still the interplay between strong and weak interactions in these decays is not understood. Measurements [1, 2] of a nonzero ε'/ε parameter have underlined the necessity of a quantitative control of strong interaction effects in $K \to \pi\pi$ decays.

The starting point of most calculations of weak hadronic decay amplitudes like $K \to \pi\pi$ amplitudes is the effective Hamiltonian formalism. In this formalism, perturbative methods are used in conjunction with the operator product expansion (OPE) to derive a low energy effective theory. The Hamiltonian of this effective theory is expanded in a series of local operators O. The coefficients of the expansion (known as Wilson coefficients) encode the perturbative short distance effects, while the non-perturbative long distance effects are included in the matrix elements $\langle \pi\pi | O | K \rangle$ of the local operators. Lattice QCD offers, at least theoretically, a way to calculate these matrix elements numerically. However, the feasibility of these calculations and their numerical precision are limited by the available computing power.

In principle, it is possible to use chiral perturbation theory to express the two pion matrix elements $\langle\pi\pi|O|K\rangle$ in terms of one pion matrix elements $\langle\pi|O|K\rangle$, which are less problematic from the numerical point of view. This strategy is outlined in [3]. In practice, it can only be done to leading order in the chiral expansion. Therefore, direct lattice computations of $\langle\pi\pi|O|K\rangle$ matrix elements are desirable. Such calculations have been performed in the quenched approximation by Boucaud et al. [4], according to a strategy outlined in [5].

Ultimately, we want to compute the $\langle\pi\pi|O|K\rangle$ matrix elements in full, i.e. unquenched, QCD. Today's computing power allows the generation of unquenched gauge configurations on sufficiently large and fine lattices by means of hybrid Monte Carlo algorithms. The first step in a lattice computation of $\langle\pi\pi|O|K\rangle$ matrix elements is to gain control over the various statistical and systematic errors that are due to the final two pion state. Thus, in this work, we study the propagation of a two pion state. We calculate the pion four point correlation function, from which the energy shift of the two pion state can be extracted. The four point function is calculated in two different ways. Following the conventional method, we use a point source for the two pions and compute the correlation function with local propagators. For an isospin 0 state, the four point correlation function can not be obtained from local propagators, due to contributions from disconnected diagrams. In this case, the wall propagator method introduced in [6] is a possible solution. To investigate the applicability of the wall propagator method on unquenched gauge configurations, we also create the two pion state with a wall source at $t = 0$ and try to calculate the $I = 2$ correlation function with wall propagators.

The rest of this work is organised in the following way: The first chapter gives a phenomenological overview of CP violation in the neutral kaon system and it's impact on the determination of the CKM matrix elements. *Chapter 2* provides an introduction to the concepts and strategies related to the computation of weak hadronic decay amplitudes. We will see how the effective Hamiltonian formalism can be used to combine the virtues of both, perturbative calculations and numerical lattice simulations. *Chapter 3* introduces the lattice formulation of QCD. In *chapter 4*, we discuss the various numerical algorithms related to this work. The results of our computations are presented in *chapter 5*.

Chapter 1

CP Violation in the Standard Model

In the Standard Model, the strength of interactions between quarks and the W bosons is determined by the elements of the CKM matrix V. Certain choices for the CKM matrix elements allow transitions, that violate CP symmetry. It is possible to define physical observables, that measure the strength of CP violation in a specific transition. Here, we will consider decays of kaons into two or three pions and define two such observables, ε and ε'.

Obviously, experimental measurements of observables like ε and ε' put certain constraints on the elements of the CKM matrix. The CKM matrix is unitary by definition, and this imposes further relations between its elements. In particular, the experimental constraints could disagree with the requirement of unitarity. This provides an experimental method to check the validity of the Standard Model and may eventually yield evidence for physics beyond the Standard Model.

With the current uncertainties, the experimental results are compatible with a unitary CKM matrix. The uncertainties, however, are mostly due to our inability to make exact theoretical predictions for QCD effects at low energies. Without these *theoretical errors*, experimental results would be much more constraining and could already have led to evidence for physics beyond the Standard Model.

We start this chapter with a discussion of CP violating decays and particle-antiparticle mixing in the neutral kaon system. This leads us to the definition of the CP violating observables ε and ε'. To understand, how measurements of these observables constrain the CKM matrix, we briefly review the weak Lagrangian of the Standard Model and introduce the two most commonly used parametrisations of the CKM matrix. Then we discuss the *unitarity triangle*, which is a graphical representation of a relation between the CKM matrix elements, that follows from unitarity. We will see how the shape of the unitarity triangle is restricted by the values of certain observables, in particular ε and ε'.

1.1 The Neutral Kaon System

Kaons are bound states between an s or $\bar{s}$ quark and a first generation quark (u, d or their antiparticles). The quark content of the neutral K mesons is

$$K^0 \sim d\bar{s} \qquad , \qquad \bar{K}^0 \sim s\bar{d} \quad . \tag{1.1}$$

They form a particle-antiparticle pair, which means that they are swapped under charge conjugation.

$$\mathsf{C}\left|K^0\right\rangle \propto \left|\bar{K}^0\right\rangle \qquad , \qquad \mathsf{C}\left|\bar{K}^0\right\rangle \propto \left|K^0\right\rangle \quad . \tag{1.2}$$

In this section, we only consider particles at rest. Therefore, $\left|K^0\right\rangle$ and $\left|\bar{K}^0\right\rangle$ denote one particle states with momentum 0. The strong interactions of the Standard Model are symmetric under parity transformations and the neutral Kaon states are defined as eigenstates of the strong Hamiltonian with parity -1.

$$\mathsf{P}\left|K^0\right\rangle = -\left|K^0\right\rangle \qquad , \qquad \mathsf{P}\left|\bar{K}^0\right\rangle = -\left|\bar{K}^0\right\rangle \quad . \tag{1.3}$$

We can absorb any phases from the charge conjugation in the definition of $\left|K^0\right\rangle$ and $\left|\bar{K}^0\right\rangle$. Then their transformation behaviour under CP transformations is

$$\mathsf{CP}\left|K^0\right\rangle = -\left|\bar{K}^0\right\rangle \qquad , \qquad \mathsf{CP}\left|\bar{K}^0\right\rangle = -\left|K^0\right\rangle \quad . \tag{1.4}$$

Now, we can construct a basis of CP eigenstates $\left|K^0_+\right\rangle$ and $\left|K^0_-\right\rangle$ as

$$\left|K^0_\pm\right\rangle = \frac{1}{\sqrt{2}}(\left|K^0\right\rangle \mp \left|\bar{K}^0\right\rangle) \qquad , \qquad \mathsf{CP}\left|K^0_\pm\right\rangle = \pm\left|K^0_\pm\right\rangle \quad . \tag{1.5}$$

Because the strong interactions are symmetric under CP transformations, the CP eigenstates are also eigenstates of the strong Hamiltonian.

Pions are bound states between a quark and an anti-quark of the first generation. Like the Kaons, they are pseudo-scalars, i.e. odd under parity transformations. If the masses of the two light quarks, m_u and m_d, are equal, the Standard Model Hamiltonian is symmetric under $SU(2)_{\text{flavour}}$ transformations, which mix the u and d quarks. When considering mesons, $m_u = m_d$ is a valid approximation, because the quark masses are negligible with respect to the typical binding energies inside a meson. Like spin eigenstates, we can characterise $SU(2)_{\text{flavour}}$ eigenstates by two quantum numbers I and I_3, which are called *isospin* and *isospin 3-component*, respectively. In this approximation, the one-pion states $\left|\pi^+\right\rangle$, $\left|\pi^-\right\rangle$ and $\left|\pi^0\right\rangle$ are defined as isospin eigenstates, i.e.

$$\begin{aligned}
\left|\pi^+\right\rangle &= \left|I=1, I_3=+1\right\rangle = -\left|\bar{d}u\right\rangle \quad , \\
\left|\pi^0\right\rangle &= \left|I=1, I_3=0\right\rangle \quad = \frac{1}{\sqrt{2}}(\left|\bar{u}u\right\rangle - \left|\bar{d}d\right\rangle) \quad , \\
\left|\pi^-\right\rangle &= \left|I=1, I_3=-1\right\rangle = +\left|\bar{u}d\right\rangle \quad ,
\end{aligned} \tag{1.6}$$

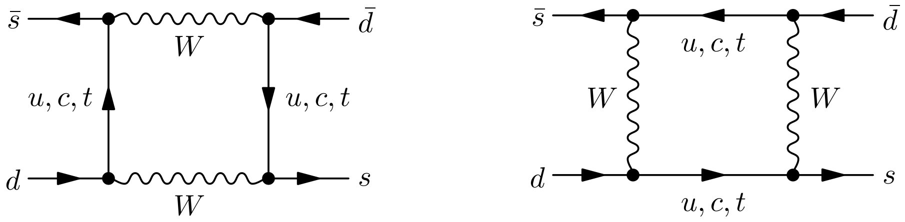

Figure 1.1: Standard Model box diagrams that allow K^0-$\bar{K}^0$ mixing.

where $|\bar{q}_1 q_2\rangle$ denotes a bound state between the quarks $\bar{q}_1$ and q_2 with (spacial) spin 0 and parity -1. Note that the anti-quarks transform according to the $\bar{2}$ representation of $SU(2)$, which is equivalent, but not equal to the usual 2 representation. In (1.6) we used the fact that the doublet $(-\bar{d}, \bar{u})$ transforms, like (u, d), according to the 2 representation of $SU(2)$.

The weak interactions allow transitions between the K^0 and the $\bar{K}^0$ state and decays like $K \to \pi\pi$ and $K \to \pi\pi\pi$. These transitions involve flavour changes and are mediated by the W bosons. *Figure 1.1* shows the box diagrams responsible for K^0-$\bar{K}^0$ transitions. *Figure 1.2* shows two examples for diagrams contributing to $K \to \pi\pi$ and $K \to \pi\pi\pi$ decays, respectively.

For an effective description of the neutral Kaon system, we now have to consider linear superpositions of the states $|K^0\rangle$ and $|\bar{K}^0\rangle$.

$$|\phi, t\rangle = \phi_1(t) \left|K^0\right\rangle + \phi_2(t) \left|\bar{K}^0\right\rangle \quad . \tag{1.7}$$

Because of the decays, the probability of finding a Kaon is no longer conserved. The effective time development operator of the Kaon system is therefore non-unitary and

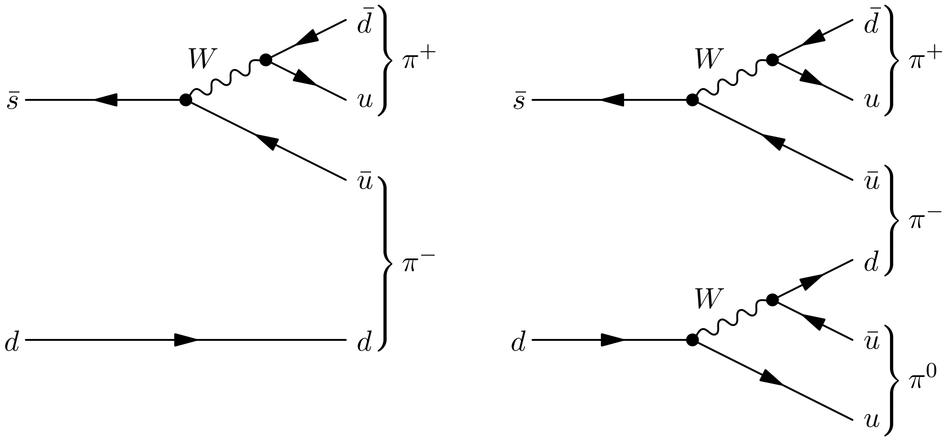

Figure 1.2: Standard Model diagrams, that contribute to Kaon decays (left: $K \to \pi\pi$, right: $K \to \pi\pi\pi$)

must be expressed in terms of a non-hermitian Hamiltonian H.

$$|\phi, t\rangle = e^{-iHt} |\phi, 0\rangle \quad . \tag{1.8}$$

In the basis of $|K^0\rangle$ and $|\bar{K}^0\rangle$, H can be written as a complex 2×2 matrix.

$$H = \begin{pmatrix} \langle K^0| H |K^0\rangle & \langle K^0| H |\bar{K}^0\rangle \\ \langle \bar{K}^0| H |K^0\rangle & \langle \bar{K}^0| H |\bar{K}^0\rangle \end{pmatrix} = \begin{pmatrix} H_{11} & H_{12} \\ H_{21} & H_{22} \end{pmatrix} \quad . \tag{1.9}$$

In experiments, we are dealing with energy eigenstates. Therefore, we have to diagonalise the matrix H. Because H is non-hermitian, the eigenvalues are complex and the eigenstates are not orthogonal. Let $|K_L^0\rangle$ and $|K_S^0\rangle$ denote the eigenstates of H. By choosing their phases appropriately, we can always make sure that

$$\langle K_L^0 | K_L^0\rangle = \langle K_S^0 | K_S^0\rangle = 1 \quad , \quad \langle K_L^0 | K_S^0\rangle \geq 0 \quad . \tag{1.10}$$

We can write the eigenvalues as

$$M_L - \frac{i}{2}\Gamma_L \quad , \quad M_S - \frac{i}{2}\Gamma_S \qquad \text{with } M_L, M_S \geq 0,\ \Gamma_S \geq \Gamma_L \geq 0 \quad . \tag{1.11}$$

Then

$$e^{iHt} |K_L^0\rangle = e^{-(\Gamma_L/2)t} e^{-iM_L t} |K_L^0\rangle \quad , \quad e^{iHt} |K_S^0\rangle = e^{-(\Gamma_S/2)t} e^{-iM_S t} |K_S^0\rangle \quad . \tag{1.12}$$

We see that M_L and M_S are the masses of the states $|K_L^0\rangle$ and $|K_S^0\rangle$, while Γ_L and Γ_S are their decay widths.

Empirically, the values of Γ_L and Γ_S differ by a factor of ca. 573. It is therefore relatively easy to isolate the $|K_L^0\rangle$ states experimentally. At a sufficiently large distance from a Kaon source, we can be sure that most of the $|K_S^0\rangle$ states have already decayed. To verify CP violation experimentally, we can exploit the fact that Pions are odd under parity transformations. If CP was an exact symmetry, the mass eigenstates $|K_L^0\rangle$ and $|K_S^0\rangle$ would be equal to the CP eigenstates $|K_+^0\rangle$ and $|K_-^0\rangle$. Furthermore, $|K_+^0\rangle$ could only decay into CP even states, while $|K_-^0\rangle$ would only decay into CP odd states. Two Pions can only form a CP even state, whereas three Pions are always CP odd. Therefore, the only possible decays would be $K_+^0 \to \pi\pi$ and $K_-^0 \to \pi\pi\pi$.

As first discovered in 1964 by Christenson, Fitch and Turlay, [7], the K_L^0 decays dominantly into three Pions, but with a small probability of ca. $3 \cdot 10^{-3}$ also into two Pions. First, that means that K_L^0 is *almost* CP odd, while K_S^0 is *almost* CP even, i.e.

$$|K_S^0\rangle \approx |K_+^0\rangle \quad , \quad |K_L^0\rangle \approx |K_-^0\rangle \quad . \tag{1.13}$$

There are two possible contributions to the small branching ratio for $K_L^0 \to \pi\pi$. First, $|K_L^0\rangle$ can contain a small component of $|K_+^0\rangle$. In this case, we speak of CP *violation in mixing* or *indirect* CP *violation.* A second possibility is that the weak interactions allow decays like $K_-^0 \to \pi\pi$, where a CP odd state decays directly into a CP even state. In this case we speak of CP *violation in decays* or *direct* CP *violation.*

1.2 CP Violating Observables

It is possible to define two physical observables, ε and ε', that measure the the two types of CP violation discussed above, respectively. Unlike scattering cross sections, which are calculated from the squared moduli of transition matrix elements, these observables are not automatically independent of the phases we choose for the initial and final states. As physical observables can not depend on the phases of state vectors, we have to define ε and ε' in such a way that all phases of the initial and final states cancel.

For defining physical observables we should consider decays of the mass eigenstates $|K_L^0\rangle$ and $|K_S^0\rangle$. Let's therefore write these states in terms of $|K^0\rangle$ and $\left|\bar{K}^0\right\rangle$. To do this, we exploit the fact that the Standard Model Hamiltonian is invariant under CPT transformations. The time reflection is represented by an *anti*-unitary operator T. Because $|K^0\rangle$ and $\left|\bar{K}^0\right\rangle$ are zero momentum states, their transformation behaviour is simply

$$\mathsf{T}\left|K^0\right\rangle = e^{i\zeta}\left|K^0\right\rangle \quad , \quad \mathsf{T}\left|\bar{K}^0\right\rangle = e^{i\zeta}\left|\bar{K}^0\right\rangle \quad , \tag{1.14}$$

where ζ is an undetermined phase. To extract conditions for the matrix elements of H from CPT symmetry, we have to keep in mind that, in accordance with the definition of anti-unitary operators, the time reflection interchanges initial and final states. If $|f\rangle$ and $|i\rangle$ are arbitrary states, CPT symmetry requires

$$\langle f|\, H\, |i\rangle = \langle i|\, (\mathsf{CPT})^\dagger H (\mathsf{CPT})\, |f\rangle \quad . \tag{1.15}$$

By choosing $|K^0\rangle$ and $\left|\bar{K}^0\right\rangle$ as initial and final states and applying T and CP according to (1.4) and (1.14), we get relations among the matrix elements of H. For $|f\rangle = |K^0\rangle$ and $|i\rangle = \left|\bar{K}^0\right\rangle$ or vice versa, (1.15) yields nothing, but for $|f\rangle = |i\rangle = |K^0\rangle\, , \left|\bar{K}^0\right\rangle$, we get

$$H_{11} = H_{22} \qquad \Rightarrow \qquad M_{11} = M_{22} \quad , \quad \Gamma_{11} = \Gamma_{22} \quad . \tag{1.16}$$

With these conditions, the energy eigenstates $|K_L^0\rangle$ and $|K_S^0\rangle$ can be written as

$$\left|K_S^0\right\rangle = \frac{\left|K_+^0\right\rangle + \bar{\varepsilon}\left|K_-^0\right\rangle}{\sqrt{1+|\bar{\varepsilon}|^2}} = \frac{(1+\bar{\varepsilon})\left|K^0\right\rangle - (1-\bar{\varepsilon})\left|\bar{K}^0\right\rangle}{\sqrt{2(1+|\bar{\varepsilon}|^2)}} \quad , \tag{1.17a}$$

$$\left|K_L^0\right\rangle = \frac{\left|K_-^0\right\rangle + \bar{\varepsilon}\left|K_+^0\right\rangle}{\sqrt{1+|\bar{\varepsilon}|^2}} = \frac{(1+\bar{\varepsilon})\left|K^0\right\rangle + (1-\bar{\varepsilon})\left|\bar{K}^0\right\rangle}{\sqrt{2(1+|\bar{\varepsilon}|^2)}} \quad . \tag{1.17b}$$

Note that $\bar{\varepsilon}$ depends on the phase conventions we imposed on $|K^0\rangle$ and $\left|\bar{K}^0\right\rangle$. It is therefore not a physical observable. From (1.13) we know, however, that the energy eigenstates $|K_L^0\rangle$ and $|K_S^0\rangle$ are almost parallel to the CP eigenstates. Therefore, it is possible to choose the phases of $|K_L^0\rangle$ and $|K_S^0\rangle$ in such a way that $|\bar{\varepsilon}| \ll 1$. In particular, there is a phase convention for $|K_L^0\rangle$ and $|K_S^0\rangle$ in which $\bar{\varepsilon}$ is equal to the observable quantity ε, which we will define below.

Let us now proceed with the final states. It is sufficient to consider decays into two Pions. For convenience, we choose isospin eigenstates as final states. The one Pion states have already been defined in (1.6). As we are considering zero momentum states, the spacial part of wave function for the two pion system is always even under exchange of the two Pions. To satisfy the Pauli principle, the isospin part of the wave function must also be even under particle exchange. This excludes the $I = 1$ states, so that the total isospin of the two Pion state has to be either 0 or 2. Furthermore, for Pions the value of I_3 is equal to their electric charge. As our initial states are neutral Kaons, charge conservation implies that we only have to consider pion states with $I_3 = 0$. In terms of tensor products of one pion states $|\pi\rangle\,|\pi\rangle$ they are given by

$$\begin{aligned}
|\pi\pi,0\rangle \equiv |\pi\pi, I=0, I_3=0\rangle &= \frac{1}{\sqrt{3}}\left|\pi^+\right\rangle\left|\pi^-\right\rangle + \frac{1}{\sqrt{3}}\left|\pi^-\right\rangle\left|\pi^+\right\rangle - \frac{1}{\sqrt{3}}\left|\pi^0\right\rangle\left|\pi^0\right\rangle \quad ,\\
|\pi\pi,2\rangle \equiv |\pi\pi, I=2, I_3=0\rangle &= \frac{1}{\sqrt{6}}\left|\pi^+\right\rangle\left|\pi^-\right\rangle + \frac{1}{\sqrt{6}}\left|\pi^-\right\rangle\left|\pi^+\right\rangle + \sqrt{\frac{2}{3}}\left|\pi^0\right\rangle\left|\pi^0\right\rangle \quad .
\end{aligned} \tag{1.18}$$

The coefficients are the usual Clebsch-Gordan coefficients for two (iso)spin 1/2 particles.

Now we define the *decay amplitudes* as matrix elements of the Hamiltonian between Kaon and Pion states. Let

$$\begin{aligned}
A_{0L} &= \left\langle\pi\pi,0\middle|H\middle|K_L^0\right\rangle \quad , \qquad A_{2L} = \left\langle\pi\pi,2\middle|H\middle|K_L^0\right\rangle \quad ,\\
A_{0S} &= \left\langle\pi\pi,0\middle|H\middle|K_S^0\right\rangle \quad , \qquad A_{2S} = \left\langle\pi\pi,2\middle|H\middle|K_S^0\right\rangle \quad .
\end{aligned} \tag{1.19}$$

The two observables ε and ε' are then defined by

$$\varepsilon = \frac{A_{0L}}{A_{0S}} \cdot \frac{\langle K^0 | K_S^0\rangle}{\langle K^0 | K_L^0\rangle} \quad , \tag{1.20a}$$

$$\varepsilon' = \frac{A_{2L}A_{0S} - A_{0L}A_{2S}}{\sqrt{2}A_{0S}^2} \cdot \frac{\langle K^0 | K_S^0\rangle}{\langle K^0 | K_L^0\rangle} \quad . \tag{1.20b}$$

They are invariant under independent re-phasing of the initial and final states.

$$\begin{aligned}
\left|K_L^0\right\rangle &\to e^{i\gamma_L}\left|K_L^0\right\rangle \quad , \qquad |0\rangle \to e^{i\gamma_0}\,|0\rangle \quad ,\\
\left|K_S^0\right\rangle &\to e^{i\gamma_S}\left|K_S^0\right\rangle \quad , \qquad |2\rangle \to e^{i\gamma_2}\,|2\rangle \quad .
\end{aligned} \tag{1.21}$$

Therefore, ε and ε' do not depend on the phase conventions imposed on the initial and final states, as it should be the case for physical observables. Furthermore, it is possible to choose the phases of $|K_L^0\rangle$ and $|K_S^0\rangle$ in such a way that the factor $\langle K^0 | K_S^0\rangle \,/\, \langle K^0 | K_L^0\rangle = 1$. Then, the expressions for ε and ε' simplify to

$$\varepsilon = \frac{A_{0L}}{A_{0S}} \quad , \tag{1.22a}$$

$$\varepsilon' = \frac{A_{2L}A_{0S} - A_{0L}A_{2S}}{\sqrt{2}A_{0S}^2} \quad . \tag{1.22b}$$

In what sense does ε measure CP violation in mixing while ε' measures CP violation in decay? To answer this, we substitute (1.17) in the expressions (1.22) and expand to first order in $\bar{\varepsilon}$. With

$$\begin{aligned} A_{0+} &= \langle \pi\pi, 0 \big| H \big| K^0_+ \rangle \quad , \quad & A_{2+} &= \langle \pi\pi, 2 \big| H \big| K^0_+ \rangle \quad , \\ A_{0-} &= \langle \pi\pi, 0 \big| H \big| K^0_- \rangle \quad , \quad & A_{2-} &= \langle \pi\pi, 2 \big| H \big| K^0_- \rangle \quad , \end{aligned} \tag{1.23}$$

we get

$$\varepsilon \approx \frac{A_{0-}}{A_{0+}} + \bar{\varepsilon} \left(1 - \frac{A^2_{0-}}{A^2_{0+}} \right) \quad , \tag{1.24a}$$

$$\varepsilon' \approx \left(\frac{A_{2-}}{A_{0+}} - \frac{A_{0-} A_{2+}}{A^2_{0+}} \right) \left(1 - 2\bar{\varepsilon}\, \frac{A_{0-}}{A_{0+}} \right) \quad . \tag{1.24b}$$

Assume that there is no CP violation in decays. That means that transitions from CP odd to CP even states are forbidden and

$$A_{0-} = A_{2-} = 0 \quad . \tag{1.25}$$

In this case, we have

$$\varepsilon = \bar{\varepsilon} \quad , \quad \varepsilon' = 0 \quad . \tag{1.26}$$

If there was no CP violation at all, we also had $\bar{\varepsilon} = 0$ and therefore $\varepsilon = \varepsilon' = 0$. Empirically, the ratio ε'/ε is of the order 10^{-3}. If the effects of CP violation in decays are much smaller than the effects of CP violation in mixing, then ε will be dominated by effects of CP violation in mixing. For ε' on the other hand, all terms are proportional to CP violating amplitudes. It is therefore a direct measure of CP violation in decays.

How do we make theoretical predictions for ε and ε'? The first step is to calculate the mixing parameter $\bar{\varepsilon}$. As it defines the eigenvectors $|K^0_L\rangle$ and $|K^0_S\rangle$, it can be calculated from the matrix elements of H between the states $|K^0\rangle$ and $|\bar{K}^0\rangle$, as shown in (1.9). These matrix elements have been calculated very successfully [8, 9, 10] using lattice simulations in combination with *effective Hamiltoninans* obtained from *Operator Product Expansions* (see section 2.1). The value of ε is directly related to $\bar{\varepsilon}$. In fact, as already mentioned above, we can choose the phases of $|K^0_L\rangle$ and $|K^0_S\rangle$ in such a way [CITE] that $\bar{\varepsilon} = \varepsilon$. Once we know $\bar{\varepsilon}$, we can substitute (1.17) and (1.18) in (1.20) to express ε' in terms of the amplitudes $\langle \pi\pi, 0 \big| H \big| K^0 \rangle$, $\langle \pi\pi, 2 \big| H \big| K^0 \rangle$, $\langle \pi\pi, 0 \big| H \big| \bar{K}^0 \rangle$ and $\langle \pi\pi, 2 \big| H \big| \bar{K}^0 \rangle$.

In practice, the process is a bit more complex, because various empirical laws can be used to simplify the equations and improve the accuracy of the theoretical predictions. The most important empirical input comes from the $\Delta I = 1/2$ rule. The Kaons contain only one light quark, which gives them an isospin of 1/2. Now, experiments tell us that the majority of the two Pion states generated in $K \to \pi\pi$ decays have isospin 0. Until today there is no convincing explanation for this rule, though it is believed that

		1. generation	2. generation	3. generation
leptons	charged leptons	e	μ	τ
	neutrinos	ν_e	ν_μ	ν_τ
quarks	up type	u	c	t
	down type	d	s	b

Table 1.1: Fermionic fields of the Standard Model

the reason can be found in the non-perturbative dynamics of the strong interactions. Therefore, the $\Delta I = 1/2$ rule is another great challenge for non-perturbative methods such as lattice QCD.

For a detailed derivation of equations that relate ε and ε' to matrix elements of H, see for example the reviews by Chau or Nir, [11, 12].

1.3 The Standard Model Lagrangian

Currently, the field theory which is most successful at describing the observed particles and their interactions, is the *Standard Model of Particle Physics*. In principle, it allows us to calculate the amplitudes in (1.19) and thus make theoretical predictions for ε and ε'. There are, however, great technical problems in the calculation of the amplitudes, which are all related to the fact that perturbation theory fails to describe the dynamics of quarks at low energies. This issue will be discussed in *chapter 2*. To understand how CP symmetry is broken in the Standard Model, let us briefly review the structure of the Standard Model Lagrangian.

The Standard Model is a $SU(3)_C \times SU(2)_L \times U(1)_Y$ gauge theory, that undergoes a spontaneous breakdown to a $SU(3)_C \times U(1)_Q$ symmetry at the *electroweak breaking scale* of ca. 250 GeV. The subscripts Y and Q stand for hypercharge and electric charge, respectively, and $SU(3)_C$ is the colour symmetry of QCD. The fermionic fields of the Standard Model are listed in *table 1.1*. Additionally, the Standard Model contains the gauge bosons required by the $SU(3)_C \times SU(2)_L \times U(1)_Y$ gauge group and one scalar Higgs doublet. Under $SU(3)_C$, the leptons and Higgs fields transform as singlets. Each of the quark fields has three components in colour space and transforms according to the fundamental 3 representation of $SU(3)_C$. The conjugated fields $\bar{u}$, $\bar{d}$ etc. transform according to the $\bar{3}$ representation. Under $SU(2)_L$, the right handed spinor components transform different from the left handed components. The right handed components are singlets under $SU(2)_L$. The Higgs fields and the left handed quark and lepton pairs of each generation form doublets under $SU(2)_L$.

The interaction terms of the Standard Model Lagrangian can be divided in three classes: QCD terms, electroweak terms and Higgs terms. The QCD terms couple the quark fields to the gauge bosons of the $SU(3)_C$ group (gluons). The electroweak terms couple the various electroweak currents to the W and Z bosons and the photons. The Higgs terms include all interactions that involve the scalar Higgs fields. When the Higgs field acquires a vacuum expectation value, these terms generate the mass terms for fermions and the W and Z bosons.

Among the electroweak terms, we distinguish terms involving charged currents and terms involving neutral currents. We write

$$\mathcal{L}_{\text{int}}^{\text{EW}} = \mathcal{L}_{\text{int}}^{\text{CC}} + \mathcal{L}_{\text{int}}^{\text{NC}} \quad , \tag{1.27}$$

where the superscripts 'CC' and 'NC' stand for charged current and neutral current, respectively. The neutral current interactions can be written as

$$\mathcal{L}_{\text{int}}^{\text{NC}} = -eA_\mu J_{\text{em}}^\mu + \frac{g_2}{\cos\theta_W} Z_\mu^0 J_Z^\mu \quad . \tag{1.28}$$

The fields A_μ and Z_μ are associated with the photons and the Z^0 bosons, respectively, and θ_W, e and g_2 denote the Weinberg angle, the electromagnetic and the weak coupling constant. The currents J_{em}^μ and J_Z^μ are

$$J_{\text{em}}^\mu = \sum_f Q_f \, \bar{\psi}_f \gamma^\mu \psi_f \quad , \tag{1.29a}$$

$$J_Z^\mu = \frac{1}{2} \sum_f \Big(T_f^3 \, \bar{\psi}_f \gamma^\mu (1-\gamma^5) \psi_f \; - \; 2Q_f \sin^2\theta_W \, \bar{\psi}_f \gamma^\mu \psi_f \Big) \quad , \tag{1.29b}$$

where the index f runs over all fermion fields in *table 1.1* and ψ_f denotes the related field. The Q_f are the electric charges and T_f^3 the third components of the weak isospin, i.e. the eigenvalue of the third generator of the $SU(2)_L$ group. The factor $(1-\gamma^5)$ projects out the left handed components of the spinors. The charged current interactions can be written as

$$\mathcal{L}_{\text{int}}^{\text{CC}} = \frac{g_2}{\sqrt{2}} (W_\mu^+ J_+^\mu + W_\mu^- J_-^\mu) \quad , \tag{1.30}$$

where W_μ^+ and W_μ^- are the gauge fields associated with the W bosons. The charged currents are

$$J_+^\mu = \frac{1}{2} \sum_{i,j} \Big(V_{ij} \, \bar{u}_i \gamma^\mu (1-\gamma^5) d_j \; + \; \delta_{ij} \, \bar{\nu}_i \gamma^\mu (1-\gamma^5) \ell_j \Big) \quad , \tag{1.31a}$$

$$J_-^\mu = \frac{1}{2} \sum_{i,j} \Big(V_{ij}^* \, \bar{d}_j \gamma^\mu (1-\gamma^5) u_i \; + \; \delta_{ij} \, \bar{\ell}_j \gamma^\mu (1-\gamma^5) \nu_i \Big) \quad , \tag{1.31b}$$

where u_i, d_i, ν_i and ℓ_i denote the up type quark, the down type quark, the neutrino and the charged lepton of the i-th generation, respectively, and the indices i and j run over the three generations. The coefficients V_{ij} are the elements of the CKM matrix.

The corresponding matrix for the leptonic terms is the identity matrix. This choice is necessary to obtain massless neutrinos.[1]

We see that the off diagonal elements of the CKM matrix describe the coupling between quarks of different generations and the W bosons. It is exactly this type of vertex, that allows the CP violating transitions and decays sketched in *figures 1.1 and 1.2*. We therefore expect to get some constraints on the CKM matrix elements from measurements of CP violating observables.

1.4 Parametrisation of the CKM Matrix

Before we discuss the way, in which CP violating observables constrain the CKM matrix, we should express it in terms of independent parameters. We will introduce the *Standard Parametrisation* [13], as proposed by the Particle Data Group, and the *Wolfenstein parametrisation* [14].

First, let's introduce a different notation for the CKM matrix elements. Rather than writing V_{ij} with $i, j \in \{1, 2, 3\}$, we can define

$$V = \begin{pmatrix} V_{ud} & V_{us} & V_{ub} \\ V_{cd} & V_{cs} & V_{cb} \\ V_{td} & V_{ts} & V_{tb} \end{pmatrix} \quad . \tag{1.32}$$

This notation is more instructive, as, for instance, V_{us} determines the coupling between a W boson, a u and an s quark.

A general unitary 3×3 matrix has 9 independent real parameters. We can write three of them as rotation angles θ_{12}, θ_{13} and θ_{23}. These are just the parameters of a rotation matrix in three real dimensions. The other six parameters appear as phase factors of the form $e^{i\phi}$. Five of these phases can be absorbed into the definition of the quark fields. The remaining phase is usually called δ. In terms of θ_{12}, θ_{13}, θ_{23} and δ, the matrix V can be written as

$$V = \begin{pmatrix} c_{12}c_{13} & s_{12}c_{13} & s_{13}e^{-i\delta} \\ -s_{12}c_{23} - c_{12}s_{23}s_{13}e^{i\delta} & c_{12}c_{23} - s_{12}s_{23}s_{13}e^{i\delta} & s_{23}c_{13} \\ s_{12}s_{23} - c_{12}c_{23}s_{13}e^{i\delta} & -c_{12}s_{23} - s_{12}c_{23}s_{13}e^{i\delta} & c_{23}c_{13} \end{pmatrix} \quad , \tag{1.33}$$

where $s_{ij} = \sin\theta_{ij}$ and $c_{ij} = \cos\theta_{ij}$. Furthermore, we can choose the phases of the quark fields in such a way, that c_{ij} and s_{ij} are positive numbers. From experiments, we know that $0 \leq \delta \leq \pi$ and that s_{13} and s_{23} are of order 10^{-3} and 10^{-2}, respectively.

[1]Recent observations of *neutrino oscillations* prove that neutrinos are actually not massless. However, their masses are very small and we are only concerned with hadronic physics in this work, so we will deliberately ignore this fact.

Consequently, $c_{13} \approx c_{23} \approx 1$. In this approximation, it is more convenient to choose the following independent parameters:

$$s_{12} = |V_{us}| \quad , \quad s_{13} = |V_{ub}| \quad , \quad s_{23} = |V_{cb}| \quad , \quad \delta \quad . \tag{1.34}$$

The phase δ is also called the CP *violating phase*. To see, why it is called so, we have to work out, how the quark terms in $\mathcal{L}_{\text{int}}^{\text{CC}}$ transform under CP. From elementary Dirac algebra, we know that

$$(\mathsf{CP})\, \bar{\psi}_i \gamma^\mu \psi_j \, (\mathsf{CP})^\dagger = -\bar{\psi}_j \gamma_\mu \psi_i \quad , \tag{1.35a}$$

$$(\mathsf{CP})\, \bar{\psi}_i \gamma^\mu \gamma^5 \psi_j \, (\mathsf{CP})^\dagger = -\bar{\psi}_j \gamma_\mu \gamma^5 \psi_i \quad , \tag{1.35b}$$

$$(\mathsf{CP})\, W_\mu^\pm \, (\mathsf{CP})^\dagger = -W_\mp^\mu \quad , \tag{1.35c}$$

where ψ_i and ψ_j are arbitrary Dirac spinors. Therefore

$$(\mathsf{CP})(V_{ij}\, \bar{u}_i \gamma^\mu (1-\gamma^5) W_\mu^+ d_j)(\mathsf{CP})^\dagger = V_{ij}\, \bar{d}_j \gamma^\mu (1-\gamma^5) W_\mu^- u_i \quad , \tag{1.36a}$$

$$(\mathsf{CP})(V_{ij}^*\, \bar{d}_j \gamma^\mu (1-\gamma^5) W_\mu^- u_i)(\mathsf{CP})^\dagger = V_{ij}^*\, \bar{u}_i \gamma^\mu (1-\gamma^5) W_\mu^+ d_j \quad . \tag{1.36b}$$

We see that, if $V_{ij} = V_{ij}^*$, the CP transformation just swaps the quark terms in the Lagrangian. For $V_{ij} \neq V_{ij}^*$, the Lagrangian is *not* invariant under CP transformations. In the parametrisation (1.33), the only non real expression is the phase factor $e^{i\delta}$. Consequently, the phase δ parametrises the CP violation in the Standard Model and for $\delta = 0$, CP would be an exact symmetry.

For phenomenological applications, people often use the *Wolfenstein parametrisation* [14]. It is an approximate parametrisation, in which each matrix element is expanded as a power series in the parameter s_{12}. It's independent parameters are

$$\lambda = s_{12} \quad , \quad A = \frac{s_{23}}{s_{12}^2} \quad , \quad \rho = \frac{s_{13}}{s_{12}s_{23}} \cos\delta \quad , \quad \eta = \frac{s_{13}}{s_{12}s_{23}} \sin\delta \quad . \tag{1.37}$$

In terms of these parameters, the CKM matrix V can be written as

$$V = \begin{pmatrix} 1 - \frac{1}{2}\lambda^2 - \frac{1}{8}\lambda^4 & \lambda & A\lambda^3(\bar{\rho} - i\bar{\eta}) \\ -\lambda & 1 - \frac{1}{2}\lambda^2 - \frac{1}{8}\lambda^4(1+4A^2) & A\lambda^2 \\ A\lambda^3(1-\bar{\rho}+i\bar{\eta}) & -A\lambda^2 + A\lambda^4(\frac{1}{2} - \bar{\rho} - i\bar{\eta}) & 1 - \frac{1}{2}A^2\lambda^4 \end{pmatrix} + \mathcal{O}(\lambda^5) \quad , \tag{1.38}$$

where

$$\bar{\rho} = \rho(1 - \frac{\lambda^2}{2}) \quad , \quad \bar{\eta} = \eta(1 - \frac{\lambda^2}{2}) \quad . \tag{1.39}$$

Presently, the parameter λ is known to a relatively high precision. Measurements of semileptonic decays of s and b particles give

$$\lambda = 0.224 \pm 0.0036 \quad , \tag{1.40a}$$

$$A = 0.83 \;\; \pm 0.02 \quad . \tag{1.40b}$$

Note that, due to the smallness of λ, the expansion in (1.38) is valid up to a very high precision. Our current knowledge about $\bar{\rho}$ and $\bar{\eta}$ is much worse, though there have been intense efforts in the last years to constrain the allowed values for these parameters. The most recent values are[2]

$$\bar{\rho} = 0.178 \pm 0.046 \quad , \tag{1.40c}$$

$$\bar{\eta} = 0.341 \pm 0.028 \quad . \tag{1.40d}$$

1.5 The Unitarity Triangle

In the Standard Model, the CKM matrix is constructed from unitary matrices, that diagonalise the couplings between the quark fields and the Higgs field. Consequently, the CKM matrix itself is unitary.[3]

The unitarity of the CKM matrix imposes certain conditions on it's elements V_{ij}. One of these conditions is

$$V_{ud}V_{ub}^* + V_{cd}V_{cb}^* + V_{td}V_{tb}^* = 0 \quad . \tag{1.41}$$

If we divide (1.41) by $V_{cd}V_{cb}^*$, we get

$$1 + \frac{V_{ud}V_{ub}^*}{V_{cd}V_{cb}^*} + \frac{V_{td}V_{tb}^*}{V_{cd}V_{cb}^*} = 0 \quad . \tag{1.42}$$

This equation can be represented diagrammatically as a triangle in the complex plane. In the Wolfenstein parametrisation, $V_{ud}V_{ub}^*/V_{cd}V_{cb}^*$ is related to the parameters $\bar{\rho}$ and $\bar{\eta}$ by

$$-\frac{V_{ud}V_{ub}^*}{V_{cd}V_{cb}^*} = \bar{\rho} + i\bar{\eta} \quad . \tag{1.43}$$

The resulting triangle is shown in *figure 1.3*. The base points B and C are fixed at $(0,0)$ and $(1,0)$. The coordinates of it's apex A are $(\bar{\rho}, \bar{\eta})$.

There is a multitude of experimental observables, which can be used to constrain the possible values of $\bar{\rho}$ and $\bar{\eta}$ and thus, the position of the point A in *figure 1.3*. An overview over these restrictions is given in *figure 1.4*. The plot is strongly idealised, as all errors have been neglected. (For an explanation of the individual constraints, see the recent paper [17] of the *CKMfitter group*, from which I copied the plot.) We see how the unitarity triangle provides, in principle, a consistency check for the Standard Model. If the Standard Model is correct, all curves have to intersect at the apex of the triangle. In particular, we see what constraints the observed values of ε and ε' put on the unitarity triangle.

[2] both given in [15]

[3] For more explicit information about the construction of the CKM matrix, see chapter 20 of [16], in particular section 3.

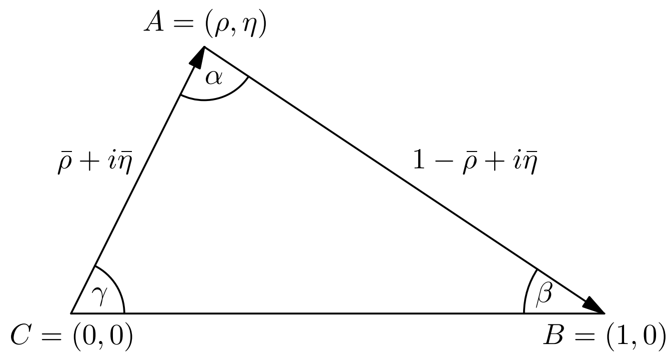

Figure 1.3: The unitarity triangle. A graphical representation of the condition (1.42), which follows from the unitarity of the CKM matrix. $\bar\rho$ and $\bar\eta$ are related to $V_{ud}V_{ub}^*/V_{cd}V_{cb}^*$ by (1.43).

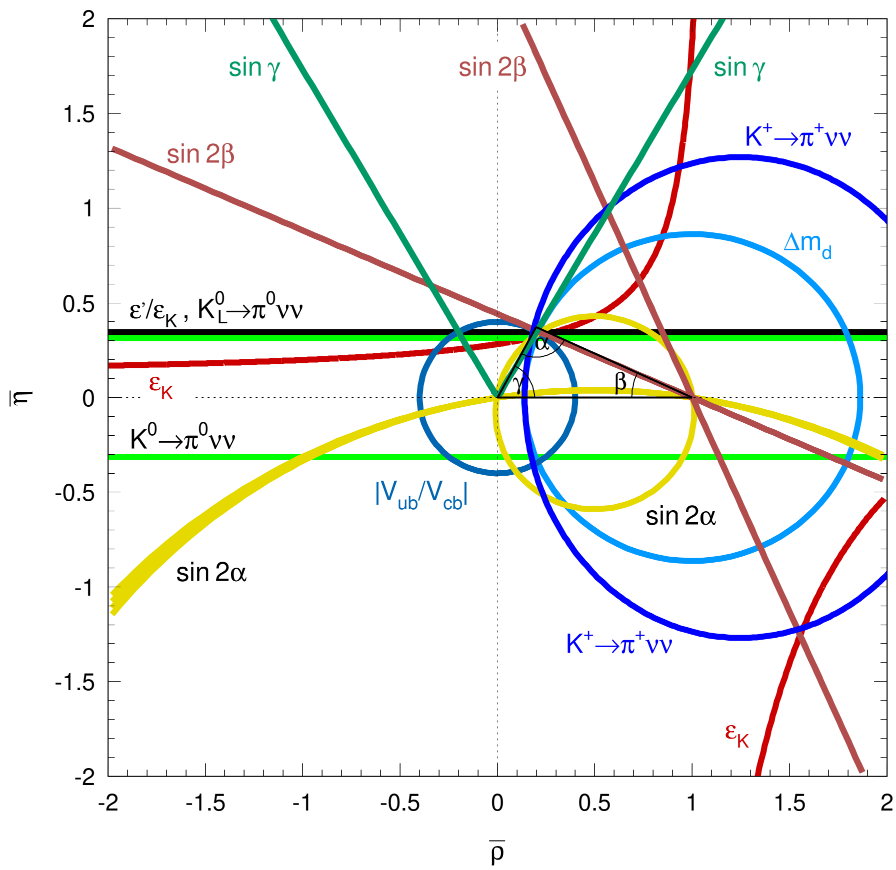

Figure 1.4: The idealised unitarity triangle. (Plot taken from [17].) The position of the apex is restricted in different ways by observables measured in K and B-meson decays, K^0-$\bar{K}^0$ and B^0-$\bar{B}^0$ mixing. Experimental and theoretical errors have been neglected in this plot. The Standard Model requires all curves to intersect in one point, which provides, in principle, a strong test for the validity of the Standard Model.

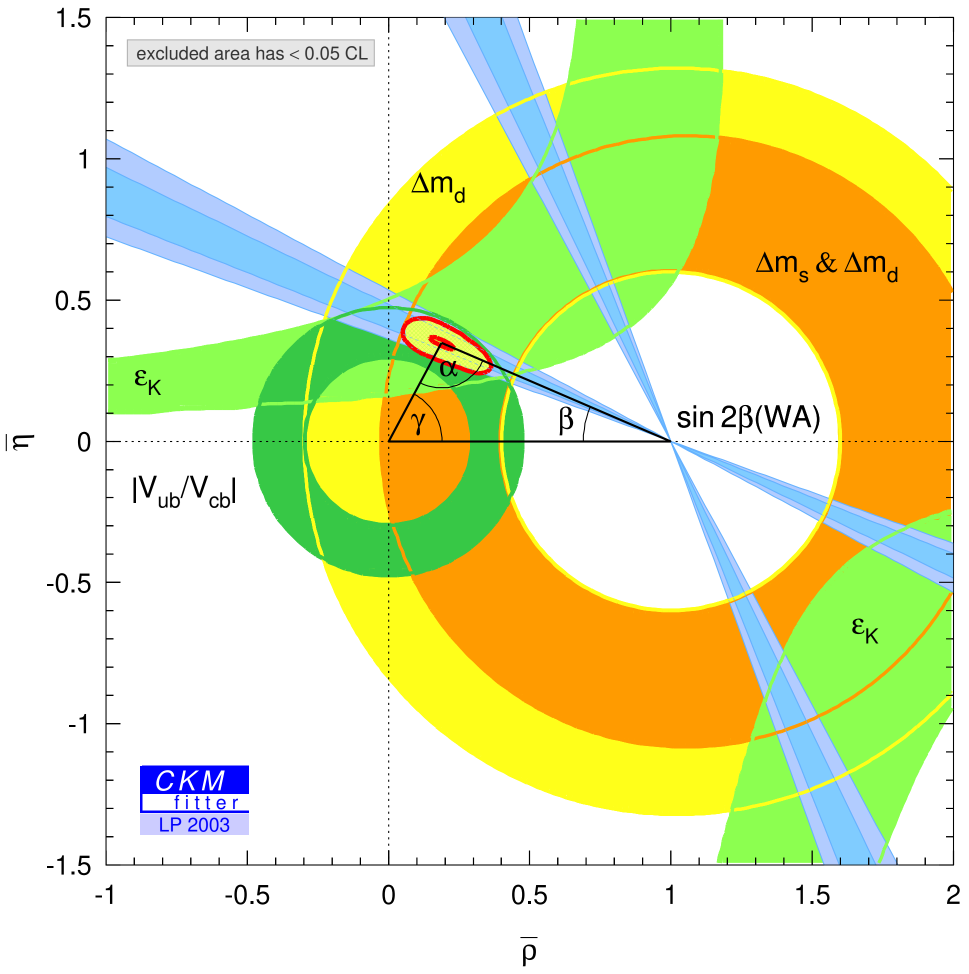

Figure 1.5: Constraints on the unitarity triangle. (Picture from the web page of [17])

Figure 1.5 shows a more realistic plot, which accounts for the current errors of the observed quantities. If the Standard Model is consistent, the apex of the unitarity triangle should lie in a region, where all the bands overlap. The plot only includes those observables, whose errors are sufficiently small to provide the currently strongest constraints. For several years, the strongest constraints came from the four quantities

- $|\varepsilon| = (2.28 \pm 0.013) \cdot 10^{-3}$ from K^0-$\bar{K}^0$ mixing
- $|V_{ub}/V_{cb}| = 0.086 \pm 0.008$ from charmless to charmed semileptonic B decays
- the mass difference Δm_d of the B_d system ($B_d = \bar{b}d$)
- the mass difference Δm_s of the B_s system ($B_s = \bar{b}s$)

In 2002, CP violation in B mesons was discovered by two groups [18, 19]. Since then, the quantity $\sin 2\beta$ (β being the angle in *figure 1.3*) can be determined very accurately from $B_d \to J/\Psi\ K_S$ decays. The world average from this decay mode is $\sin 2\beta = 0.734 \pm 0.054$ [20].

With the exception of $\sin 2\beta$, the constraints from all the observables mentioned above are affected by *theoretical errors*. That means that the equations that relate the observed quantities to $\bar{\rho}$ and $\bar{\eta}$ contain *hadronic matrix elements*, which have to be calculated at energies much lower than Λ_{QCD}, the scale at which QCD becomes non-perturbative. Therefore, non-perturbative methods like lattice simulations are required to calculate the hadronic matrix elements, and these methods bring in their own statistical and systematic errors. In fact (except for $\sin 2\beta$), the overall errors shown in *figure 1.5* are currently dominated by the theoretical errors, so that improvements in the experimental data would not significantly improve our knowledge about $\bar{\rho}$ and $\bar{\eta}$. To overcome this situation is a great challenge for non-perturbative QCD methods in general and lattice QCD in particular.

Chapter 2

Computation of Weak Hadronic Amplitudes

The fundamental problem in the calculation of weak hadronic amplitudes, like $K \to \pi\pi$ amplitudes, is that it requires control over a large range of energy scales. The strong interactions between the quarks are characterised by their binding energy of order 1 GeV, while the actual transition is mediated by a W boson, whose mass is of order 100 GeV. At a scale of 1 GeV, the strong interactions are non-perturbative. Thus, we need non-perturbative methods like numerical lattice simulations to deal with the low energy QCD effects. It would, however, be impracticable to include the weak effects at the 100 GeV scale in the same simulations. On the other hand, the weak interactions can be treated perturbatively, and at their characteristic scale, 100 GeV, QCD becomes perturbative as well. So, the obvious strategy is to calculate the high energy effects perturbatively and then use lattice methods to include the low energy effects. In this chapter, I'll sketch how this strategy is realised in practice.

In the first section, I explain the *Operator Product Expansion* (OPE) method, which provides the formal framework for the "joint venture" of perturbative and non-perturbative methods. In the second section, we will discuss the issue of *renormalisation* for matrix elements calculated in lattice and continuum formulations of field theories. We will see, that some kind of *matching* is required to make the two approaches compatible. In the third section, I describe the relation between physical matrix elements and *euclidean correlation functions*, which are the quantities that we get from numerical lattice simulations.

2.1 The Operator Product Expansion

The *Operator Product Expansion* (OPE) provides the formal framework for the separation of high energy and low energy contributions to physical amplitudes. It allows us to use perturbation theory to construct an *effective theory* for low energies. Then, lattice methods can be used to calculate transition amplitudes in this effective theory.

To get an idea of the structure of this effective theory, we will now use the OPE method to remove the heavy W fields from the Standard Model Lagrangian. The first step is to apply the path integral formalism[1] and *integrate out* the W fields. In the *unitary gauge*, we can write the part of the Standard Model Lagrangian involving the W fields as

$$\mathcal{L}^W = W_\mu^+ \big(g^{\mu\nu}(\partial^2 + m_W^2) - \partial^\mu\partial^\nu\big) W_\nu^- + \frac{g_2}{\sqrt{2}}(J_\mu^+ W_+^\mu + J_\mu^- W_-^\mu) \quad , \tag{2.1}$$

where J_μ^+ and J_μ^- are defined in (1.31). The path integral over the W fields,

$$Z^W = \int [dW^+][dW^-] \; \exp\left(i \int d^4x \, \mathcal{L}^W(x)\right) \quad , \tag{2.2}$$

is a Gauss integral. It's solution is, up to an irrelevant normalisation factor,

$$Z^W = \exp\left(-i \int d^4x \, d^4y \, \frac{g_2^2}{2} J_\mu^-(x) \Delta^{\mu\nu}(x-y) J_\nu^+(y)\right) \quad , \tag{2.3}$$

where $\Delta^{\mu\nu}(x-y)$ is the W propagator

$$\begin{aligned} \Delta^{\mu\nu}(x-y) &= \int \frac{d^4k}{(2\pi)^4} \, \frac{1}{k^2 - m_W^2} \left(\frac{k^\mu k^\nu}{m_W^2} - g^{\mu\nu}\right) e^{-ik(x-y)} \\ &\equiv \int \frac{d^4k}{(2\pi)^4} \, \tilde{\Delta}^{\mu\nu}(k) \, e^{-ik(x-y)} \quad , \end{aligned} \tag{2.4}$$

defined by the equation

$$\big(g_{\mu\nu}(\partial^2 + m_W^2) - \partial_\mu\partial_\nu\big)\Delta^{\nu\rho}(x) = \delta_\mu^\rho \, \delta^{(4)}(x) \quad . \tag{2.5}$$

To solve the full theory, we still have to perform the path integrals over all the other fields Φ.

$$\begin{aligned} Z &= \int [d\Phi] \; e^{iS'} \cdot Z^W \\ &= \int [d\Phi] \; \exp\left(iS' - i \int d^4x \, d^4y \, \frac{g_2^2}{2} J_\mu^-(x) \Delta^{\mu\nu}(x-y) J_\nu^+(y)\right) \quad , \end{aligned} \tag{2.6}$$

where S' denotes all the terms of the Standard Model action S, that do not depend on the W fields. In other words, we can write the Standard Model action S as

$$S = S' - \int d^4x \, d^4y \, \frac{g_2^2}{2} J_\mu^-(x) \Delta^{\mu\nu}(x-y) J_\nu^+(y) \quad . \tag{2.7}$$

[1] For more information on the path integral formalism, see *section 3.2* of this work or, for example, chapter 9 of [16].

We see that we can not calculate the remaining path integrals with the usual Gaussian method, because the second term in (2.7) is not local. Therefore, we have to expand it as a series of local operators. To do this, we first expand the momentum space propagator $\tilde{\Delta}^{\mu\nu}(k)$ as

$$\tilde{\Delta}^{\mu\nu}(k) = -\frac{1}{m_W^2}\left(\frac{k^\mu k^\nu}{m_W^2} - g^{\mu\nu}\right)\left(1 + \frac{k^2}{m_W^2} + \frac{k^4}{m_W^4} + \ldots\right) \quad . \tag{2.8}$$

Then, after substituting (2.8) in (2.4), we can replace k^μ by $i\partial^\mu$ and obtain

$$\Delta^{\mu\nu}(x) = \frac{1}{m_W^2}\left(\frac{\partial^\mu \partial^\nu}{m_W^2} + g^{\mu\nu}\right)\left(1 - \frac{\partial^2}{m_W^2} + \frac{\partial^4}{m_W^4} - \ldots\right)\delta^{(4)}(x) \quad . \tag{2.9}$$

Now, we can substitute this series in (2.7) and use partial integration to let the derivatives act on the currents J_μ^+ and J_ν^-. After partial integration, we can get rid of the delta function $\delta^{(4)}(x-y)$ by performing the integral over y. Then, all operators are evaluated at x and we are left with a series of local operators. The full series is identical to the Standard Model Action. By aborting the series at a certain power n of $1/m_W^2$, we systematically ignore terms proportional to $(1/m_W^2)^n$, which should be a good approximation at energies much smaller than m_W. Now we could proceed and apply the same strategy to other heavy particles of the Standard Model, like the Z boson or even the heavy quarks t, b etc. In the latter case, one speaks of *heavy quark effective theories* (HQET).

Let's summarise this. In the calculation above, we have "integrated out" the W field from the Standard Model. It does no longer appear as a dynamic degree of freedom, but is replaced by a series of effective operators or *vertices*. Transitions, which used to be mediated by the W boson, are now mediated by the effective vertices. Thus, the calculation of weak amplitudes boils down to calculating matrix elements of the effective operators. Depending on the desired initial and final states. This can be done in perturbation theory, with non-perturbative lattice simulations, or, as we will see below, with a mixture of both.

So far our discussion of the OPE has been quite formal. Let's therefore finish this section with a small example. Consider the simple electroweak process

$$c \to s u \bar{d} \quad . \tag{2.10}$$

We apply the OPE method to the W fields, as shown above, and include only terms of order $1/m_W^2$. Then the process (2.10) is mediated through a series of four quark vertices, namely

$$\mathcal{L}_{scud} = \frac{G_F}{\sqrt{2}} V_{cs}^* V_{ud} \sum_{i,j} (\bar{s}^i c^i)_{V-A} (\bar{u}^j d^j)_{V-A} \quad , \tag{2.11}$$

where, the indices $i, j = 1, 2, 3$ are colour indices. The subscript $V-A$ stands for "vector minus axial". For two arbitrary spinors ψ and ψ' we define

$$(\bar{\psi}\psi')_{V-A} \equiv \bar{\psi}\gamma^\mu(1-\gamma^5)\psi' \quad . \tag{2.12}$$

For a perturbative tree level calculation, the only thing we have to do is read off the Feynman rule from (2.11). However, at higher orders, there occurs the problem of divergent loop integrals, and *renormalisation* methods have to be applied to "remove" these divergences. This issue is discussed in the next section.

2.2 Renormalisation and Matching

In this section we will see, how lattice and perturbative methods can work together in the calculation of weak amplitudes. To understand this, it is important to view the lattice formulation of QCD as one of many possible *renormalisation schemes*. Perturbative calculations could be done in the lattice renormalisation scheme, but for large calculations this becomes impracticable. The obvious advantage of the lattice formulation is, however, that it allows numerical, non-perturbative computations. It is therefore important to know how to convert quantities between different renormalisation schemes. This will be discussed later on. First, we briefly review the systematics of renormalisation.

One distinguishes *infrared* and *ultraviolet divergences*. The infrared divergences are due to a divergence of the integrand as the loop momentum k approaches zero. It can be shown, that infrared divergences always cancel each other, as long as one calculates "physically sensible" amplitudes. The ultraviolet divergences are a much more serious problem. They appear, if the integrand does not vanish quickly enough, as the loop momentum approaches infinity. They usually don't cancel, and most people interpret this as an indication, that the theory under consideration fails at high energies and should only be viewed as the low energy limit of a superior theory. In the following, I will only talk about ultraviolet divergences.

The process of renormalisation can be divided in three steps, where the last step is optional.

Step 1. The first step to deal with divergent loop integrals is to introduce an ad hoc prescription to make all loop integrals finite. This step is called *regularisation*. For example, one can introduce an arbitrary scale Λ and restrict the loop integral to four-momenta k with $(k^0)^2+(k^1)^2+(k^2)^2+(k^3)^2 < \Lambda$. The original theory, and therewith the original divergences, is restored in the limit $\Lambda \to \infty$. Therefore, Λ is called the *cutoff parameter*. The lattice formulation of QCD can also be viewed as a regularisation prescription. By discretising the space and time coordinates and restricting all fields to a four-dimensional box with periodic boundary conditions, all path integrals become just finite dimensional integrals. The original ultraviolet divergences are restored in the limit, where the lattice spacing a approaches zero. Therefore, on the lattice, the lattice spacing a is the cutoff parameter. For perturbative calculations, the most popular regularisation prescription is *dimensional regularisation*. It has the nice feature, that it does not break Lorentz or gauge symmetry. There, the basic idea is to introduce for all relevant expressions a smooth dependence on the number d of space-time dimensions. This can be done in such a way that the loop integrals, considered as analytic functions of the (complex) dimension d, have an isolated pole at $d = 4$. Then, the theory can be regularised by performing all calculations in $d = 4 - 2\varepsilon$ dimensions. The original theory is restored in the limit $\varepsilon \to 0$, so ε is the cutoff parameter of dimensional regularisation.

Step 2. Once we have regularised the theory, all transition amplitudes will depend explicitly on the cutoff parameter, and some will diverge in the limit, where the cutoff is removed. But for a certain class of theories (to which the Standard Model does belong), it is possible to remove the divergences of all physical observables by introducing a cutoff dependence for the parameters of the theory, like masses, coupling constants and scaling factors of the fields. This process is called *tuning*. In most cases, the parameters diverge as the cutoff is removed, but this does not matter, as long as all physically observable quantities remain finite in the limit of vanishing cutoff. Theories, for which the divergences of physical observables can be removed in this way, are called *renormalisable theories*. However, for a given regularisation, the requirement of physical observables being finite may not fix the cutoff dependence of the parameters uniquely. A prescription, that tells us how to choose between different ways to tune the parameters, is called a *renormalisation scheme*. For a given cutoff, the value of a certain observable can be different for different renormalisation schemes, but the limit it approaches, if we remove the cutoff, has to be the same for all schemes.

Step 3. In dimensional regularisation, it is convenient to trade, in a third step, the cutoff parameter for another parameter called the *renormalisation scale* μ. To do this, one rewrites the Lagrangian in terms of *renormalised*, cutoff independent fields, masses and coupling constants. The cutoff dependence is included through *renormalisation factors*. For a theory with fields ϕ_i, masses m_i and coupling constants g_i, we replace

$$\begin{aligned} \phi_i(\varepsilon) &\to Z_{\phi_i}(\varepsilon,\mu)\phi_i(\mu) \quad , \\ m_i(\varepsilon) &\to Z_{m_i}(\varepsilon,\mu)m_i(\mu) \quad , \\ g_i(\varepsilon) &\to Z_{g_i}(\varepsilon,\mu)\mu^{\varepsilon}g_i(\mu) \quad . \end{aligned} \tag{2.13}$$

The renormalisation scale μ is an arbitrary quantity of mass dimension 1. The factor μ^{ε} is necessary to keep the Lagrangian dimensionless. As μ appears explicitly in the renormalised Lagrangian, physical observables will depend explicitly on μ. Again, this explicit dependence has to be cancelled by an implicit dependence through the other parameters of the theory.

Let's now return to our example from the last section, the $c \to su\bar{d}$ transition. *Figure 2.1* shows the three types of loop diagrams, that contribute, at first order in the strong

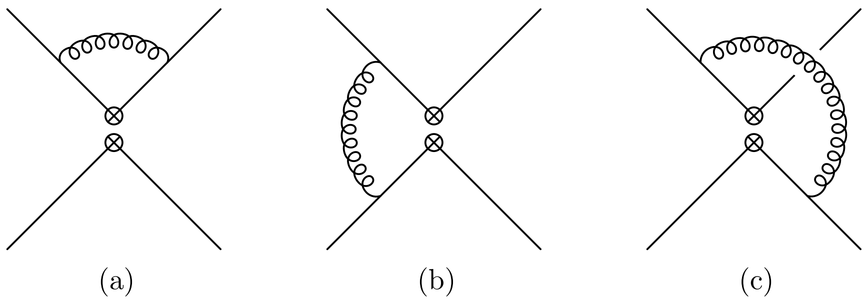

Figure 2.1: One loop corrections for the vertex (2.11)

coupling α_s, to the renormalisation of the vertex (2.11). In addition to the diagrams in *figure 2.1*, there are also one loop insertions to the external legs, which contribute to field and mass renormalisation. If we would substitute the Feynman rules, we'd see that the diagrams (b) and (c) in *figure 2.1* allow transitions with a different colour structure than the tree level diagram. At tree level, we get transitions of

$$\text{type 2:} \qquad c^i \to s^i u^j \bar{d}^j \quad , \tag{2.14}$$

where i and j are colour indices. With one loop corrections included, we also get transitions of

$$\text{type 1:} \qquad c^i \to s^j u^i \bar{d}^j \quad . \tag{2.15}$$

The reason for this is, that the vertex factors for the quark-gluon vertices contain the $SU(3)$ generators T^a. Basic $SU(3)$ algebra yields

$$\sum_a T^a_{ir} T^a_{js} = -\frac{1}{6}\delta_{ir}\delta_{js} + \frac{1}{2}\delta_{is}\delta_{jr} \quad . \tag{2.16}$$

The second term is responsible for the transitions of type 1.

Obviously, because of the different colour structure, the one loop divergences in the diagrams (b) and (c) of *figure 2.1* can not be completely cancelled by tuning the coupling constant of the vertex (2.11). To make the theory finite, we have to introduce another vertex with a colour structure of type 1 and remove the remaining divergences by tuning its coupling constant. The interaction Lagrangian then takes the general form

$$\mathcal{L}_{csud} = \frac{G_F}{\sqrt{2}} V^*_{cs} V_{ud} (C_1 O_1 + C_2 O_2) \quad , \tag{2.17}$$

where C_1 and C_2 are coupling constants. In the context of operator product expansions, they are also called *Wilson coefficients*. The related operators are

$$O_1 = \sum_{i,j} (\bar{s}^i c^j)_{V-A} (\bar{u}^i d^j)_{V-A} \quad , \tag{2.18a}$$

$$O_2 = \sum_{i,j} (\bar{s}^i c^i)_{V-A} (\bar{u}^j d^j)_{V-A} \quad . \tag{2.18b}$$

At tree level, i.e. at order zero in the strong coupling α_s, there are no transitions of type 1 and thus $C_1 = 0$ and $C_2 = 1$. Only at higher orders in α_s we get contributions from O_1. Therefore, one says that the operators O_1 and O_2 *mix under renormalisaton.*

With the Lagrangian (2.17), we could now calculate the amplitude for the $c \to su\bar{d}$ transition by applying the steps 1 to 3 described above. I will only quote the results here. For a detailed derivation, see chapter 5 of [21]. With dimensional regularisation in the $\overline{\text{MS}}$ scheme, the coupling constants C_1 and C_2 are

$$C_1(\mu) = -3\frac{\alpha_s(\mu)}{4\pi}\ln\frac{m_W^2}{\mu^2} \quad , \quad C_2(\mu) = 1 + \frac{\alpha_s(\mu)}{4\pi}\ln\frac{m_W^2}{\mu^2} \quad . \tag{2.19}$$

To simplify the result for the $c \to su\bar{d}$ transition amplitude, we assume that all quark masses vanish and that all external particles have the same (off shell) four momentum p with $p^2 < 0$. Let $|i\rangle$ and $|f\rangle$ be the initial and final states, respectively. Then, we obtain the transition amplitude T_{fi} from the Lagrangian (2.11).

$$T_{fi} \equiv \langle f|T|i\rangle = \frac{G_F}{\sqrt{2}}V_{cs}^* V_{ud}\Big(C_1(\mu)O_{1\,fi}(\mu) + C_2(\mu)O_{2\,fi}(\mu)\Big) \quad , \tag{2.20}$$

where $O_{1\,fi}$ and $O_{2\,fi}$ are the matrix elements of the operators O_1 and O_2. To first order in α_s, we have

$$O_{1\,fi}(\mu) = \left(1 + \frac{11}{3}\cdot\frac{\alpha_s(\mu)}{4\pi}\ln\frac{\mu^2}{-p^2}\right)O_{1\,fi}^{(0)} + \left(-3\frac{\alpha_s(\mu)}{4\pi}\ln\frac{\mu^2}{-p^2}\right)O_{2\,fi}^{(0)} \quad , \tag{2.21a}$$

$$O_{2\,fi}(\mu) = \left(1 + \frac{11}{3}\cdot\frac{\alpha_s(\mu)}{4\pi}\ln\frac{\mu^2}{-p^2}\right)O_{2\,fi}^{(0)} + \left(-3\frac{\alpha_s(\mu)}{4\pi}\ln\frac{\mu^2}{-p^2}\right)O_{1\,fi}^{(0)} \quad , \tag{2.21b}$$

where $O_{1\,fi}^{(0)}$ and $O_{2\,fi}^{(0)}$ are the μ independent tree level matrix elements.

From the results (2.19) and (2.21) we see, that only the Wilson coefficients depend on the large W mass m_W. In the renormalised matrix elements $O_{1\,fi}$ and $O_{2\,fi}$, there appears only the renormalisation scale μ. This is true for any choice of the initial and final states, because the matrix elements are calculated in an effective theory, which "knows" the m_W scale only through the Wilson coefficients. In this particular sense, the operator product expansion allows us to separate high energy physics from low energy physics: The contributions from high energy scales (like the W mass) are included in the Wilson coefficients, which are universal, i.e. do not depend on our choice of the initial and final states. Transition amplitudes are expressed in terms of the Wilson coefficients and matrix elements of effective operators O_i. The matrix elements depend only on low energy scales (quark and lepton masses etc.) and the renormalisation scale μ.

Let me stress again, that the calculations leading to (2.19) and (2.21) were done with *Dimensional Regularisation* (DR) and the $\overline{\text{MS}}$ renormalisation scheme. Analogous calculations can be performed in *Lattice Perturbation Theory* (LPT), i.e. by using lattice regularisation instead of dimensional regularisation. The LPT results for matrix elements and coupling constants will differ from the analogous results obtained with dimensional regularisation. Only the transition amplitudes T_{fi} are independent of the regularisation prescription, which is as it should be, since $|T_{fi}|^2$ are physical observables.

Now, our strategy for calculating weak amplitudes is obvious. We compute matrix elements numerically on the lattice and then substitute them in algebraic expressions obtained in (continuum) perturbation theory. The latter is usually done with dimensional regularisation in the $\overline{\rm MS}$ scheme (DR/$\overline{\rm MS}$). The matrix elements we compute numerically on the lattice are matrix elements calculated to all orders in LPT, and for a fixed lattice spacing a ($\sim 1\,\mathrm{fm}$). (But, of course, they are affected by other types of errors.) If we want to substitute matrix elements from numerical lattice simulations in DR/$\overline{\rm MS}$ calculations, we need to know how to convert LPT matrix elements to DR/$\overline{\rm MS}$ matrix elements. This conversion or *matching* can be done by comparing the (algebraic) results for one loop corrections to matrix elements calculated in LPT or DR/$\overline{\rm MS}$, respectively. The relation between LPT matrix elements and their DR/$\overline{\rm MS}$ counterparts can be written as follows (see chapter 3 of [22]):

$$(O_i^{\overline{\rm MS}})_{fi}(\mu) = \sum_j Z_{ij}(a\mu) \cdot (O_j^{\rm LPT})_{fi}(a) \quad , \tag{2.22}$$

where $O_i^{\overline{\rm MS}}$ and $O_j^{\rm LPT}(a)$ denote complete sets of operators that mix under DR/$\overline{\rm MS}$ or LPT renormalisation, respectively, and the functions Z_{ij} depend on the dimensionless quantity $a\mu$ and the bare (cutoff dependent) parameters of the theory.

To make the joint venture between numerical lattice computations and perturbative calculations efficient, one has to make sure that the errors produced by both methods are of the same order of magnitude. For perturbative calculations, the main source of errors is the abortion of the perturbative expansion at a certain power of the coupling constant. If the coupling constant is too large, then contributions from higher order diagrams are no longer suppressed and the perturbation series diverges. This is precisely what happens in QCD, if we choose the renormalisation scale μ to be smaller than $\Lambda_{\rm QCD} \approx 200\,\mathrm{MeV}$. In numerical lattice computations, an important source of errors are *cutoff effects*. In LPT, they would appear as terms proportional to positive powers of the lattice spacing a and thus vanish in the limit $a \to 0$. In numerical simulations, however, we have to use a fixed, non-zero lattice spacing. Therefore, terms proportional to a will contribute to the numerical results for matrix elements. To obtain meaningful results from a lattice simulation, the energy scale induced by the lattice spacing a should be bigger than the energy scales which are relevant for the considered quantity. For matrix elements of the operators O_i, this scale is given by μ, as can be seen in (2.21). In practice, μ should be in the range

$$\Lambda_{\rm QCD} < \mu \lesssim \frac{\pi}{a} \quad . \tag{2.23}$$

The most common choice is

$$\mu = \frac{1}{a} \quad . \tag{2.24}$$

2.3 Correlation Functions and Matrix Elements

In the last section, we talked about the problem of converting or *matching* lattice matrix elements to continuum renormalisation schemes like the $\overline{\text{MS}}$ scheme. This problem is also called the *ultraviolet problem*, as it deals with the effects of the finite lattice spacing a, which introduces an ultraviolet cutoff to the lattice regularised theory. In lattice simulations, we have to make two other modifications to the original theory. First, it is not possible to describe the evolution of operators in real time. We can only calculate their evolution along an *imaginary* time axis. Usually, for a given field theory on Minkowski space, one can find a corresponding theory on a space-time with euclidean metric, so that the imaginary time behaviour of the first is equal to the real time behaviour of the latter. The second modification is, that all fields are restricted to a box of finite extent in (euclidean) space and time, usually with periodic boundary conditions. The problem of extracting physically meaningful quantities from such *euclidean finite volume field theories* is often referred to as the *infrared problem*, because the finite spacial volume introduces an infrared cutoff to the field theory. That is the problem we will discuss in this section.

As we will see in *chapter 3*, lattice methods allow us to calculate *euclidean Greens functions G*. These are traces of the form

$$G^{\text{E}} = \text{Tr}(e^{-HT} O) \quad , \tag{2.25}$$

where O is an operator, that consists of time ordered products of field operators. H is the Hamiltonian of the considered (euclidean finite volume) field theory and $T > 0$ the (euclidean) time extent of the lattice.

Assume that we have a field theory in *Minkowski* space with a Hamilton operator H and a vacuum state $|0\rangle$. Let $J(t)$ be an operator that consists of products of field operators at (Minkowski) time t. If we are interested in Pions, we would choose $J(t)$ so, that $J^\dagger(t)\,|0\rangle$ has the largest possible overlap with a one Pion state. In general, one has to choose J in such a way that the lightest state created by $J^\dagger$ is the state we are interested in. This is most conveniently done by choosing the *symmetry properties* of J appropriately. Assume that G_i $(i = 1 \ldots n)$ are symmetry generators, and the state we are interested in is the lightest state with corresponding quantum numbers γ_i. Then, if we choose $J^\dagger(t)$ so that $[G_i, J^\dagger(t)] = \gamma_i J(t)\ \forall i$, it follows immediately, that $J^\dagger(t)\,|0\rangle$ has the quantum numbers γ_i. For example, the Pion is the lightest state with parity -1 and isospin 1. Therefore, to create a pion, we choose $J^\dagger(t)$ in such a way that $[\mathsf{P}, J^\dagger(t)] = -J^\dagger(t)$ and $[I^2, J^\dagger(t)] = 1 \cdot (1+1) J^\dagger(t)$, where P is the parity operator and I^2 the Casimir operator of the isospin group.

Note that the evolution of J in real time is described by

$$J(t) = e^{iHt} J(0) e^{-iHt} \quad . \tag{2.26}$$

To let J evolve along the negative imaginary time axis, we define $J^{\mathrm{E}}(\tau),\ \tau \in \mathbb{R}$ as

$$J^{\mathrm{E}}(\tau) = e^{H\tau} J(0) e^{-H\tau} \quad . \tag{2.27}$$

Then, we define the *two point correlation function* C_2 as

$$C_2(\tau; T) = \mathrm{Tr}\left\{e^{-HT} J^{\mathrm{E}}(\tau) J^{\mathrm{E}\dagger}(0)\right\} \quad , \tag{2.28}$$

with $T > t > 0$. Note that C_2 is a euclidean Greens function, i.e. of the form (2.25). Now, assume that $\{|n\rangle\}$ is a complete set of energy eigenstates with

$$H\,|n\rangle = E_n\,|n\rangle \quad . \tag{2.29}$$

Note that the symbol n is not a simple index, but represents all quantum numbers, that might be necessary to identify a specific energy eigenstate. For infinite volume theories, it will even include continuous variables like momenta. In that case, a sum over n implies integrals over the continuous variables. Writing the trace in (2.28) explicitly and inserting a complete set of states between J and $J^\dagger$ gives

$$C_2(\tau; T) = \sum_{n,k} \langle k|\, e^{-HT} J^{\mathrm{E}}(\tau)\,|n\rangle\,\langle n|\,J^{\mathrm{E}\dagger}(0)\,|k\rangle \quad . \tag{2.30}$$

To express C_2 in terms of $J(0) \equiv J^{\mathrm{E}}(0)$, we use (2.27) and get

$$\begin{aligned} C_2(\tau; T) &= \sum_{n,k} \langle k|\, e^{-H(T-\tau)} J(0)\, e^{-H\tau}\,|n\rangle\,\langle n|\,J(0)\,|k\rangle \\ &= \sum_{n,k} |\,\langle k|\,J(0)\,|n\rangle\,|^2\, e^{-E_k(T-\tau)} e^{-E_n\tau} \quad . \end{aligned} \tag{2.31}$$

Now let $|n_0\rangle$ denote the lowest energy state that is created by $J^\dagger$ and let E_0 be it's energy, i.e. $\langle n_0|\,J^\dagger(0)\,|0\rangle \neq 0$ and $E_0 < E_n$ for all n with $\langle n|\,J^\dagger(0)\,|0\rangle \neq 0$. Then, from (2.30), we get

$$\begin{aligned} C_2(\tau; T) &= \sum_{n,k} |\,\langle k|\,J(0)\,|n\rangle\,|^2 e^{-E_k(T-\tau)} e^{-E_n\tau} \\ &= |\,\langle 0|\,J(0)\,|n_0\rangle\,|^2\,(e^{-E_0\tau} + e^{-E_0(T-\tau)}) + D + \ldots \\ &= |\,\langle 0|\,J(0)\,|n_0\rangle\,|^2\, e^{-E_0T/2} \cosh\big(E_0(\tau - T/2)\big) + D + \ldots \quad . \end{aligned} \tag{2.32}$$

The constant D is related to diagonal matrix elements of $J(0)$. If, in the sum in the first line, $|n\rangle$ is equal to $|k\rangle$, the τ dependent exponentials cancel. Thus, the leading term in D is proportional to e^{-E_dT}, where E_d is the energy of the lightest state $|d\rangle$, for which $\langle d| J(0) |d\rangle \neq 0$. The dots in (2.32) indicate contributions from states created by $J^\dagger$, that are more massive than $|n_0\rangle$. They are proportional to $e^{-E\tau}$ or $e^{-E(T-\tau)}$, where $E > E_0$. If there is a sufficiently large gap between E_0 and the next higher energy eigenvalue E, we can neglect those contributions in the area where both τ and $T-\tau$ are large enough. Then, we can extract the energy E_0 and the form factor $\langle 0| J(0) |\pi\rangle$ from the correlation function (2.28).

For finite volume field theories, the energy spectrum is discrete, so there will always be a gap of finite size between two energy eigenstates. However, in infinite volumes, the energy spectrum is continuous. For one particle states, one can exploit translational symmetry and create particles with a specific momentum. The spectrum of one particle or bound states with a fixed momentum is again discrete. The real problem are two or more particle states, because in an infinite volume their relative momenta are continuous variables, and even after fixing the total momentum, the energy spectrum of many particle states remains continuous.

In lattice simulations, we are always forced to consider a finite volume theory. The classical way to extract physically meaningful quantities from lattice simulations is to extrapolate the lattice results to infinite volumes, i.e. consider the limit $L \to \infty$, where L is the edge length of the spacial box. However, in this limit, the energy gaps between many particle states vanish and we get problems to isolate individual energy eigenstates. In 1990 L. Maiani and M. Testa showed [23] that in the case where the two particle state is at the lower end of the continuous spectrum, i.e. where the relative momentum of the particles is zero, the contributions from higher states are suppressed by inverse powers of $\sqrt{\tau}$. They also concluded that, if there is a continuum of states below the considered two particle state, no physically meaningful results can be extracted from correlation functions. These considerations were done for *infinite volumes*.

Another approach is to derive equations that relate quantities from finite volume theories in an analytical way to quantities in infinite volume theories. The most popular example is probably the *Lüscher formula* [24], which relates the phase shift for two Pion scattering in an infinite volume to the energy of a two pion state in a finite volume. In 2000, Lellouch and Lüscher derived another formula [25], which relates finite volume matrix elements of local operators, like those obtained from operator product expansions, to the corresponding infinite volume ones, and which is valid for matrix elements between two particle states. Thus, physical (infinite volume) transition amplitudes between two particle states can be obtained from matrix elements calculated in finite volumes, where the energy spectrum is discrete.

We have already seen that, in a finite volume, we can extract the energy of a state $|n_0\rangle$ and the form factor $\langle 0| J(0) |n_0\rangle$ from the two point correlation function (2.28). To calculate matrix elements of an operator $O(t)$, which is a combination of field operators at (Minkowski) time t, we have to consider *three point correlation functions*. Assume that $J_f(t)$ and $J_i(t)$ are combinations of field operators at time t, which annihilate the desired initial and final states (in the same sense, in which J annihilated $|n_0\rangle$ in the discussion above). Furthermore, let $J_f^{\mathrm{E}}(\tau)$, $J_i^{\mathrm{E}}(\tau)$ and $O^{\mathrm{E}}(\tau)$ be defined in analogy to (2.27). Then, we define the three point correlation function as

$$C_3(\tau_2, \tau_1; T) = \mathrm{Tr}\left\{e^{-HT} J_f^{\mathrm{E}}(\tau_2) O^{\mathrm{E}}(\tau_1) J_i^{\mathrm{E}\dagger}(0)\right\} \quad , \tag{2.33}$$

with $T > \tau_2 > \tau_1 > 0$. Then, C_3 is also a euclidean Greens function, i.e. of the form (2.25). Inserting complete sets of energy eigenstates, we get

$$C_3(\tau_2, \tau_1; T) = \sum_{n,k,\ell} \langle n| e^{-HT} J_f^{\mathrm{E}}(\tau_2) |k\rangle \langle k| O^{\mathrm{E}}(\tau_1) |\ell\rangle \langle \ell| J_i^{\mathrm{E}\dagger}(0) |n\rangle \quad . \tag{2.34}$$

Let $|i\rangle$ and $|f\rangle$ be the lowest energy states created by $J_i^\dagger$ and $J_f^\dagger$, respectively, and let E_i and E_f be their energies. Then, in the simplest case, where $O(0)$ can not create or annihilate the states $|f\rangle$ and $|i\rangle$ itself, we obtain in analogy to (2.30)

$$\begin{aligned} C_3(\tau_2, \tau_1; T) &= \langle 0| e^{-H(T-\tau_2)} J_f(0) e^{-H\tau_2} |f\rangle \langle f| e^{H\tau_1} O(0) e^{-H\tau_1} |i\rangle \langle i| J_i^\dagger(0) |0\rangle + \ldots \\ &= \langle 0| J_f(0) |f\rangle \langle f| O(0) |i\rangle \langle i| J_i^\dagger(0) |0\rangle \, e^{-E_f(\tau_2-\tau_1)} e^{-E_i\tau_1} + \ldots \end{aligned} \tag{2.35}$$

where the dots indicate contributions from states with higher energies, which can be neglected for $\tau_1 \gg \tau_2 \gg 0$. Assume that we have extracted the energies E_i and E_f and the matrix elements $\langle 0| J_f(0) |f\rangle$ and $\langle 0| J_i(0) |i\rangle$ from two point correlation functions like (2.28). Then we can use the three point correlation function (2.33) to obtain the matrix element $\langle f| O(0) |i\rangle$. This is also possible if $|f\rangle$ is a two particle state, as long as the time extent of the lattice is such, that τ_1 and τ_2 can become large compared to the size of the energy gap that separates E_f from the next higher energy eigenvalue. But in any case, the first step is to determine E_f and the form factor $\langle 0| J_f(0) |f\rangle$ from a two point correlation function, where now $|f\rangle$ is a two particle state. This is the motivation for studying two pion propagators on the lattice.

Chapter 3

Lattice Regularised QCD

In the last chapters, the importance of numerical lattice simulations, in particular for the calculation of hadronic matrix elements, has been mentioned repeatedly. Before we can do such simulations, we have to formulate a lattice regularised version of QCD. This is the aim of this chapter.

QCD is a typical example of a *non-abelian gauge theory*. Therefore, in the first section, we review the crucial steps in the construction of non-abelian gauge theories. The second section discusses the *path integral formalism*, which is the starting point of all lattice calculations. In the last section, we introduce the *lattice formulation of QCD* as a way to explicitly calculate the partition functional Z from the path integral formalism. For the implementation of fermions on the lattice, we restrict ourselves to Wilson fermions, as this is the type of fermions we will be using later on.

3.1 Non-abelian Gauge Theories

QCD is a local $SU(3)$ gauge theory of fermionic matter fields. In local gauge theories, the interactions between the matter fields are mediated by bosonic exchange particles called *gauge bosons*. The couplings between the fields follow the requirement, that the theory is symmetric under a group of *local* gauge transformations, i.e. transformations, that mix the field components locally, but in a way that is different from point to point.

Let's start by introducing some notations. We consider a field theory with $n = n_f \cdot N_c$ fermion fields. We call n_f the *number of flavours* and N_c the *number of colours*. In QCD, the number of colours is 3. The Standard Model has six quark flavours (see *table 1.1*), but in lattice simulations we usually include only the lightest flavours. We denote the fermion fields as $\psi^f_{i\alpha}$, where $f = 1 \ldots n_f$ labels the flavour, $i = 1 \ldots N_c$ the colour and $\alpha = 1 \ldots 4$ is the spinor index. Whenever possible, we will use α, β, γ for spinor indices, i, j, k for colour indices and f, g, h for flavour indices. If not stated otherwise, summation over repeated indices is implied. The spinor indices will often be suppressed, for example in contractions with γ matrices like $\bar{\psi}_i^f \gamma^\mu \psi_j^g$. Likewise, we will suppress the flavour index in statements that are true for each flavour separately.

Assume that we have chosen the fields so that the mass matrix is diagonal, and assume that fields of the same flavour f have the same mass m_f. Then, the non-interacting Lagrangian is

$$\mathcal{L}_0 = \sum_{f,i} \bar{\psi}_i^f (i\partial\!\!\!/ - m_f)\psi_i^f \quad . \tag{3.1}$$

This Lagrangian is invariant under *global $SU(N_c)$ gauge transformations*, defined by

$$\psi_i \to \Lambda_{ij}\psi_j \quad , \tag{3.2}$$

where Λ is an element of the fundamental representation of $SU(N_c)$[1], i.e. a unitary matrix with $\det\Lambda = 1$. To see that the Lagrangian (3.1) is invariant under such transformations, note that

$$\bar{\psi}_i = \psi_i^\dagger\gamma^0 \to (\Lambda_{ij}\psi_j)^\dagger\gamma^0 = \psi_j^\dagger\gamma^0\Lambda_{ji}^\dagger = \bar{\psi}_j\Lambda_{ji}^\dagger \tag{3.3}$$

and therefore

$$\begin{aligned}\bar{\psi}_i(i\partial\!\!\!/ - m)\psi_i \to \quad & \bar{\psi}_j\Lambda_{ji}^\dagger(i\partial\!\!\!/ - m)\Lambda_{ik}\psi_k \\ &= \bar{\psi}_j\Lambda_{ji}^\dagger\Lambda_{ik}(i\partial\!\!\!/ - m)\psi_k \\ &= \bar{\psi}_j(i\partial\!\!\!/ - m)\psi_j \quad .\end{aligned} \tag{3.4}$$

The possible transformations can be parametrised by real parameters ω^a ($a = 1\dots r$). The number r of parameters is called the *rank* of the group. The corresponding matrices Λ can be written as

$$\Lambda = e^{-i\omega^a T^a} \qquad \text{with } T^a \text{ hermitian.} \tag{3.5}$$

The hermitian matrices T^a are called *generators*. They satisfy *commutation relations* of the form

$$[T^a, T^b] = if^{abc}T^c \quad . \tag{3.6}$$

The coefficients f^{abc} are called *structure constants*. They are a property of the group and therefore the same in all it's representations. For compact semi-simple groups like $SU(N_c)$, we can choose the parametrisation in such a way that the structure constants are totally anti-symmetric ($f^{abc} = f^{[abc]}$), and that the generators are orthogonal with respect to the trace, i.e.

$$\mathrm{Tr}(T^aT^b) = \frac{1}{2}\delta^{ab} \quad . \tag{3.7}$$

The linear (r-dimensional) space of the generators together with the commutation bracket forms the fundamental representation of the *Lie algebra* of $SU(N_c)$. There

[1] As an excellent introduction to Lie groups and representations, I recommend [26].

is also a canonical way to define a representation of the $SU(N_c)$ group on the space of its generators, namely

$$T^a \to \Lambda T^a \Lambda^\dagger \quad . \tag{3.8}$$

This representation is called the *adjoint representation.* The trace from (3.7) is invariant under these transformations.

Now, we define *local* gauge transformations by making the transformation matrices space-time dependent.

$$\psi_i(x) \to (\Lambda\psi)_i(x) \equiv \Lambda_{ij}(x)\psi_j(x) \equiv (e^{-i\omega^a(x)T^a})_{ij}\psi_j(x) \quad . \tag{3.9}$$

Let $\mathcal{G}_{\text{loc}}$ denote the set of local gauge transformations, i.e. the set of mappings $\Lambda : \mathbb{R}^4 \to SU(N_c)$. It has a group structure, too, if we define the group multiplication as

$$(\Lambda_1\Lambda_2)(x) = \Lambda_1(x)\Lambda_2(x) \quad . \tag{3.10}$$

We therefore call $\mathcal{G}_{\text{loc}}$ the *local gauge group.* For *infinitesimal* elements Λ of $\mathcal{G}_{\text{loc}}$, where all $\Lambda(x)$ are only infinitesimally different from unity, we can use (3.5) and write the transformation law (3.9) as

$$\psi_i(x) \to \psi_i(x) - i\omega^a(x)T^a_{ij}\psi_j(x) \quad , \tag{3.11}$$

Here, the parameters $\omega^a(x)$ are infinitesimal for all x and all a.

Is the Lagrangian (3.1) also invariant under local gauge transformations? We see immediately, that the mass terms $m\bar{\psi}_i(x)\psi_i(x)$ are invariant, because the transformation matrices $\Lambda(x)$ and $\Lambda^\dagger(x)$ cancel independently at every x. However, to make the derivative terms invariant, too, the field derivatives $(\partial_\mu\psi_i)(x)$ would have to transform into $\Lambda_{ij}(x)(\partial_\mu\psi_j)(x)$. But this is not possible, because $(\partial_\mu\psi_i)(x) \to (\partial_\mu\Lambda_{ij}\psi_j)(x)$ and the derivative also acts on the (now x dependent) Λ_{ij}. From a less algebraic point of view, we might say that a field derivative at x cannot have a simple transformation behaviour, because the derivative operator compares fields at (infinitesimally) different points in space-time, which transform independently under local gauge transformations.

To make the theory invariant under local gauge transformations, we have to construct a *covariant derivative operator* D_μ in such a way, that $(D_\mu\psi)(x)$ transforms like a vector field under Lorentz transformations and as a fundamental under local gauge transformations, i.e.

$$(D_\mu\psi)_i(x) \to \Lambda_{ij}(x)(D_\mu\psi)_j(x) \quad . \tag{3.12}$$

Ultimately, this is done by introducing the *gauge fields* $A^a_\mu(x)$, which transform as vectors under Lorentz transformations and under infinitesimal local gauge transformations according to

$$A^a_\mu(x) \to A^a_\mu(x) - f^{abc}A^b_\mu(x)\omega^c(x) - \frac{1}{g}(\partial_\mu\omega^a)(x) \quad . \tag{3.13}$$

Then, a covariant derivative satisfying (3.12) is defined through

$$(D_\mu \psi)_i = \partial_\mu \psi_i - ig A^a_\mu T^a_{ij} \psi_j \quad . \tag{3.14}$$

I will now take some time to motivate the definitions (3.13) and (3.14), because the relevant arguments will also be instructive for the implementation of gauge fields in the lattice regularised theory.

We already saw that the main obstacle in the transition from a global to a local gauge symmetry is, that fields at different points x and y in space-time become incomparable, because they are transformed by independent matrices $\Lambda(x)$ and $\Lambda(y)$. An obvious solution is to introduce for each pair of points x and y a *connector* $U(x,y)$. Connectors are $SU(N_c)$ matrices, which satisfy

$$U(x,x) = \mathbb{1} \qquad , \qquad U(y,x) = [U(x,y)]^\dagger \quad , \tag{3.15}$$

and which transform in the following way under local gauge transformations:

$$U(x,y) \to (\Lambda U)(x,y) \equiv \Lambda(x) U(x,y) \Lambda^\dagger(y) \quad . \tag{3.16}$$

Then, we can define the covariant derivative through

$$(D_\mu \psi)(x) = \lim_{a\to 0} \frac{1}{a}\big(U(x, x+a\hat{\mu})\psi(x+a\hat{\mu}) - \psi(x)\big) \quad , \tag{3.17}$$

where $\hat{\mu}$ denotes the space-time unit vector in μ direction. From the properties (3.15) and (3.16) of the connectors, it follows immediately that the covariant derivative (3.17) satisfies the condition (3.12). For an infinitesimal four vector ε, the connectors $U(x, x+\varepsilon)$ will be infinitesimal $SU(N_c)$ transformation matrices. Therefore, they can be written in terms of the generators T^a as

$$U(x, x+\varepsilon) = \mathbb{1} - ig A^a_\mu(x) T^a \varepsilon^\mu \quad . \tag{3.18}$$

The coefficients $A^a_\mu(x)$ are the *gauge fields*. The constant g can at this stage be regarded as an arbitrary normalisation constant for the gauge fields. Later, we will see that it plays the role of a coupling constant. Setting $y = x + \varepsilon$ in (3.16) and using the expansion (3.18), one immediately obtains the transformation behaviour (3.13) for the gauge fields. Furthermore, if we substitute the expansion (3.18) in (3.17), we obtain the equation (3.14). Thus, our two definitions for the covariant derivative, (3.17) and (3.14), are equivalent.

To construct a kinetic term for the gauge fields, we have to find a local combination of gauge field derivatives, which is invariant under Lorentz and local gauge transformations. Such a quantity can be obtained from the commutator $[D_\mu, D_\nu]$ of two covariant derivatives. Using (3.14), we get

$$\begin{aligned}
[D_\mu, D_\nu] &= [\partial_\mu, \partial_\nu] - ig[\partial_\mu, A^a_\nu T^a] - ig[A^a_\mu T^a, \partial_\nu] + (ig)^2 [A^b_\mu T^b, A^c_\nu T^c] \\
&= -ig(A^a_{\nu,\mu} T^a - A^a_{\mu,\nu} T^a - ig A^b_\mu A^c_\nu [T^b, T^c]) \\
&= -ig(A^a_{\nu,\mu} - A^a_{\mu,\nu} - ig f^{abc} A^b_\mu A^c_\nu) T^a \\
&= -ig F^a_{\mu\nu} T^a \quad ,
\end{aligned} \tag{3.19}$$

where $F^a_{\mu\nu}$ is the *field strength tensor*

$$F^a_{\mu\nu}(x) = (\partial_\mu A^a_\nu)(x) - (\partial_\nu A^a_\mu)(x) - igf^{abc}A^b_\mu(x)A^c_\nu(x) \quad . \tag{3.20}$$

Note that, in (3.19), the symbols A^a_μ, $A^a_{\nu,\mu}$ and T^a should be understood as multiplication operators, whose action on a field ψ is defined by

$$(A^a_\mu\psi)(x) = A^a_\mu(x)\psi(x) \quad , \tag{3.21a}$$

$$(A^a_{\nu,\mu}\psi)(x) = (\partial_\mu A^a_\nu)(x)\psi(x) \quad , \tag{3.21b}$$

$$(T^a\psi)_i(x) = T^a_{ij}\psi_j(x) \quad . \tag{3.21c}$$

On the right hand sides, $A^a_\mu(x)$, $(\partial_\mu A^a_\nu)(x)$ and T^a_{ij} denote the ordinary gauge fields, gauge field derivatives and generator components. From these definitions, we immediately get the commutation relations, that were used in (3.20).

$$[T^a, A^b_\mu] = [T^a, A^b_{\nu,\mu}] = [T^a, \partial_\mu] = 0 \quad , \tag{3.22a}$$

$$[T^a, T^b] = if^{abc}T^c \quad , \tag{3.22b}$$

$$[\partial_\mu, A^a_\nu] = A^a_{\nu,\mu} \quad . \tag{3.22c}$$

In any case, we see from (3.19), that the commutator of covariant derivatives acts like a multiplication operator in position space, namely

$$([D_\mu, D_\nu]\psi)(x) = -igF^a_{\mu\nu}(x)T^a\psi(x) \equiv -igF_{\mu\nu}(x)\psi(x) \quad . \tag{3.23}$$

$F_{\mu\nu}(x)$ is a matrix in colour space, i.e. it carries two colour indices. From the transformation behaviour of $(D_\mu\psi)(x)$ it follows that the components of $F^\dagger_{\mu\nu}(x)F^{\mu\nu}(x)$ transform as scalar fields under Lorentz transformations. Furthermore, we can obtain a gauge invariant quantity by taking the trace over colour indices. Therefore, the following quantity behaves like a scalar field under Lorentz and local gauge transformations.

$$\frac{1}{2}\operatorname{Tr}(F^\dagger_{\mu\nu}F^{\mu\nu}) = \frac{1}{2}F^a_{\mu\nu}F^{\mu\nu}_b \operatorname{Tr}(T^aT^b) = \frac{1}{4}F^a_{\mu\nu}F^{\mu\nu}_a \equiv \frac{1}{4}F^2 \quad . \tag{3.24}$$

As it contains derivatives of the gauge fields A^a_μ, it may serve as a kinetic term. Thus, the following Lagrangian is Lorentz invariant and invariant under local gauge transformations:

$$\mathcal{L} = -\frac{1}{4}F^2 + \sum_f \bar\psi^f(i\not{D} - m_f)\psi^f \quad . \tag{3.25}$$

The covariant derivative $\not{D}$ carries colour and spinor indices, which are contracted with the quark fields $\bar\psi$ and ψ. For $N_c = 3$, this is the Lagrangian of QCD.

For certain choices of the fermion masses m_f, the Lagrangian (3.25) has additional *global* symmetries. If all fermion masses are equal, it is symmetric under an $SU(n_f)$ group of transformations, that mix fermion fields of different flavours.

$$\psi^f \to U^{fg}\psi^g \qquad \text{with } U \in SU(n_f). \tag{3.26}$$

For $n_f = 2$, this is the famous *isospin symmetry*. If all fermion masses are zero, we can even mix the left and right handed components ψ_L^f and ψ_R^f of the spinors independently. Then, the Lagrangian (3.25) is invariant under a $SU(n_f)_L \times SU(n_f)_R$ group of transformations of the following form:

$$\psi_L^f = U_L^{fg}\psi_L^g \qquad , \qquad \psi_R^f = U_R^{fg}\psi_R^g \quad , \tag{3.27}$$

with $U_L \in SU(n_f)_L$ and $U_R \in SU(n_f)_R$. This symmetry is called *chiral symmetry*. It is generally believed that, in the quantised theory, it is spontaneously broken to a single $SU(n_f)$ group. In this case, the *Goldstone theorem* requires the existence of massless bosonic particles, the so called *Goldstone bosons*. Further information on spontaneous symmetry breaking and the Goldstone theorem can be found in [16] or the original paper [27] by Goldstone, Salam and Weinberg. In the real world, the chiral symmetry of QCD is also broken explicitly, since the masses of the quarks are nonzero. However, the quark masses are small compared to the to the masses of the lightest mesons, so chiral symmetry is still a good *approximate* symmetry. Thus, we should find a set of very light hadrons, that can be identified with the Goldstone bosons related to the spontaneous breakdown of chiral symmetry. In fact, the pions are much lighter than all other hadrons, so they seem to be the right candidates.

3.2 Path Integral Quantisation

In the last section, we constructed the Lagrangian of QCD. This Lagrangian fully determines a *classical* field theory, which is symmetric under Poincaré transformations and local $SU(3)$ gauge transformations. To *quantise* this theory, we have to promote the fields and their conjugate momenta to operators, which satisfy canonical commutation (fermionic fields) or anti-commutation (bosonic fields) relations. For the gauge fields, this is not possible, if we treat all four (Lorentz) components of A_μ^a as independent degrees of freedom. Some *gauge fixing* condition has to be imposed, that reduces the dynamical degrees of freedom of the gauge fields. Furthermore, we may have to introduce a *regularisation prescription* to make the quantum theory finite. After quantising the theory, we can derive *path integral* expressions for matrix elements of time ordered products of field operators. In the path integral formalism, the gauge fixing condition and any regularisation prescription are represented by the explicit way, in which we define the integration measure on the space of "paths" (classical trajectories). Therefore, the path integral formalism is taken as the starting point for lattice formulations of field theories. A good introduction to the path integral formulation of field theories can be found in [28].

The whole physical content of a field theory can be extracted from Greens functions. In the path integral formalism, the Greens functions are related to functional derivatives of the *partition functional* Z. Consider a field theory with fields $\Phi_i,\ i = 1 \dots N$. To obtain the correct statistics, the components of fermion fields have to be represented by *Grassmann numbers*. Let $\mathbf{\Phi} = (\Phi_i,\ i = 1 \ldots N)$ denote the complete field content of the theory and let $\mathcal{S} = \{\mathbf{\Phi}\}$ be a space of sufficiently "well behaved" field configurations. For example, $\mathcal{S}$ could be a space of smooth functions, which vanish sufficiently fast at infinity. For each field configuration $\mathbf{\Phi}$, we define the *dual field* $\bar{\mathbf{\Phi}}$ in such a way that $\bar{\mathbf{\Phi}}(x)\mathbf{\Phi}(x)$ is a real Lorentz scalar and invariant under local gauge transformations. In general, the components of $\bar{\mathbf{\Phi}}$ will be a combination of the complex conjugated components Φ_i^* of $\mathbf{\Phi}$. By writing

$$(\mathbf{\Phi}_1, \mathbf{\Phi}_2) = \int d^4x \, \bar{\mathbf{\Phi}}_1(x)\mathbf{\Phi}_2(x) \tag{3.28}$$

we introduce a hermitian product $(\,\cdot\,,\,\cdot\,)$ on $\mathcal{S}$, which is invariant under Poincaré and local gauge transformations. For QCD, we would choose

$$\begin{aligned} \mathbf{\Phi} = (A^a_\mu, \psi^f_{i\alpha}) \qquad &, \qquad \bar{\mathbf{\Phi}} = (A^\mu_a, \bar{\psi}^f_{i\alpha}) \quad , \\ (\mathbf{\Phi}, \mathbf{\Phi}') = \int d^4x \, &\left(\bar{\psi}(x)\psi'(x) + A^a_\mu(x) A'^\mu_a(x)\right) \quad . \end{aligned} \tag{3.29}$$

The partition functional Z is formally defined as the path integral over $\mathcal{S}$,

$$Z[\mathbf{J}] = \int_{\mathcal{S}} [d\mathbf{\Phi}] \, e^{iS[\mathbf{\Phi}] - i(\mathbf{J},\mathbf{\Phi}) - i(\mathbf{\Phi},\mathbf{J})} \quad , \tag{3.30}$$

with $\mathbf{J} \in \mathcal{S}$ and

$$S[\mathbf{\Phi}] = \int d^4x \, \mathcal{L}(\mathbf{\Phi}(x), (\partial\mathbf{\Phi})(x)) \quad . \tag{3.31}$$

The path integrals over fermion fields are Grassmann integrals.

What is the relation between Greens functions and the partition functional Z? In the operator formalism, we define the two point Greens function as

$$G_{ij}(x, y; T) = \mathrm{Tr}\left(e^{-iHT} \mathrm{T}\{\Phi_i(x)\bar{\Phi}_j(y)\}\right) \quad , \tag{3.32}$$

where $0 < x^0, y^0 < T$ and the 'T' denotes time ordering (large times to the left). In free field theories, G is also called the *Feynman propagator*. It should be understood as a distribution, which means that only such expressions are well defined, in which the arguments x and y of G are integrated out with sufficiently well behaved functions. In the path integral formalism, G is related to Z by

$$G_{ij}(x, y; T) = \frac{1}{Z[0]} \left[\frac{i\delta}{\delta \bar{J}_i(x)} \frac{i\delta}{\delta J_j(y)} Z[\mathbf{J}] \right]_{\mathbf{J}=0} = \int_{\mathcal{S}_T} [d\mathbf{\Phi}] \, \Phi_i(x) \, \bar{\Phi}_j(y) \, e^{iS[\mathbf{\Phi}]} \quad . \tag{3.33}$$

$\mathcal{S}_T$ denotes the subspace of field configurations, where all fields vanish outside the time interval $[0, T]$, with periodic boundary conditions for Boson fields and anti-periodic boundary conditions for Fermion fields. Greens functions of more than two fields are obtained by applying more functional derivatives to the partition functional Z. However, if the action $S[\mathbf{\Phi}]$ can be written as $(\mathbf{\Phi}, M\mathbf{\Phi})$ for some operator M, we can express every $2n$ point Greens function in terms of two point Greens functions. The general formula is

$$\mathrm{Tr}\left(e^{-iHT}\mathrm{T}\{\Phi_{i_1}\cdots\Phi_{i_n}\bar{\Phi}_{j_1}\cdots\bar{\Phi}_{j_n}\}\right) = \sum_{(\mathbf{p},\mathbf{q})}\sigma_{(\mathbf{p},\mathbf{q})}G_{p_1q_1}\cdots G_{p_nq_n} \quad , \tag{3.34}$$

where the sum runs over all possible pairings or *contractions* of the fields on the left hand side and $\sigma_{(\mathbf{p},\mathbf{q})}$ is the sign we pick up by bringing the fields on the left hand side in the order $\Phi_{p_1}\bar{\Phi}_{q_1}\cdots\Phi_{p_n}\bar{\Phi}_{q_n}$. Each interchange of two Fermion fields gives a factor of -1. In diagrammatic representations of contractions, the factor $\sigma_{(\mathbf{p},\mathbf{q})}$ can be determined by counting the closed Fermion loops in the diagram. An odd number of fermion loops corresponds to a factor of -1. The equation (3.34) is also known as *Wick's theorem*.

Greens functions like the Feynman propagator describe the evolution of the fields along the real time axis. However, to extract physically meaningful quantities like decay amplitudes or S matrix elements, it is necessary to consider the evolution of fields in a slightly imaginary time direction $(1-i\varepsilon)t$ or even along the negative imaginary time axis. For example, in *section 2.3* we learnt how to extract physically meaningful quantities from euclidean correlation functions, which are traces of field operators evolved in negative imaginary time. In the operator formalism, we define the *euclidean two point Greens function* G^{E}_{ij} as

$$G^{\mathrm{E}}_{ij}(x,y;T) = \mathrm{Tr}\left(e^{-HT}\mathrm{T}\{\Phi^{\mathrm{E}}_i(x)\bar{\Phi}^{\mathrm{E}}_j(y)\}\right) \quad , \tag{3.35}$$

where $0 < x^0, y^0 < T$. The euclidean field operators $\mathbf{\Phi}^{\mathrm{E}}$ are defined by

$$\mathbf{\Phi}^{\mathrm{E}}(\tau,\mathbf{x}) = e^{H\tau}\mathbf{\Phi}(0,\mathbf{x})e^{-H\tau} \quad , \quad \bar{\mathbf{\Phi}}^{\mathrm{E}}(\tau,\mathbf{x}) = e^{H\tau}\bar{\mathbf{\Phi}}(0,\mathbf{x})e^{-H\tau} \quad . \tag{3.36}$$

Note that the euclidean dual fields $\bar{\mathbf{\Phi}}^{\mathrm{E}}$ are no longer obtained from $\mathbf{\Phi}^{\mathrm{E}}$ by hermitian conjugation, but by hermitian conjugation *and* a time reflection $(\tau \to -\tau)$.[2] We can also write down path integral expressions for euclidean Greens functions. Assume that we have chosen a space $\mathcal{S}^{\mathrm{E}}$ of field configurations, where all fields $\mathbf{\Phi}$, as functions of the time variable, can be analytically continued to the whole complex plane. Furthermore, we require that the fields $\mathbf{\Phi}(x^0,\mathbf{x})$ vanish fast enough for $x^0 \to \pm i\infty$. We define a new action functional S' by taking the contour of the time integral in S along the negative imaginary time axis.

$$S'[\mathbf{\Phi}] = \int_{+i\infty}^{-i\infty} dx^0 \int d^3\mathbf{x}\ \mathcal{L}(\mathbf{\Phi}(x),(\partial\mathbf{\Phi})(x)) \quad . \tag{3.37}$$

Then, the euclidean two point Greens function is given by the path integral

$$G^{\mathrm{E}}_{ij}(x,y;T) = \mathcal{N}\int_{\mathcal{S}^{\mathrm{E}}_T}[d\mathbf{\Phi}]\ \Phi_i(-ix^0,\mathbf{x})\bar{\Phi}_j(-iy^0,\mathbf{y})\ e^{iS'[\mathbf{\Phi}]} \quad . \tag{3.38}$$

[2] The concept of *reflection positivity* follows from this remark.

$\mathcal{N}$ is a normalisation factor, that we will fix later, and $\mathcal{S}_T^{\mathrm{E}}$ denotes the subspace of field configurations, where all fields vanish outside the *imaginary* time interval $[-iT, 0]$, with periodic (Bosons) or anti-periodic (Fermions) boundary conditions. Note that the dual fields $\bar{\mathbf{\Phi}}(\tau, \mathbf{x})$ are anti-analytic functions of τ, i.e. power series in τ^*, because they are combinations of the complex conjugated components $[\Phi_i(\tau, \mathbf{x})]^*$. To obtain higher euclidean Greens functions, we have to put more factors of the form $\Phi_i(-ix^0, \mathbf{x})$ in the integrand.

The integral along the imaginary time axis, which appears in the definition of S' is still a bit clumsy. We can get rid of it by introducing a *Wick rotation operator* W on $\mathcal{S}$.

$$(W\mathbf{\Phi})(x^0, \mathbf{x}) = \mathbf{\Phi}(ix^0, \mathbf{x}) \qquad , \qquad (\overline{W\mathbf{\Phi}})(x^0, \mathbf{x}) = \bar{\mathbf{\Phi}}(ix^0, \mathbf{x}) \quad . \tag{3.39}$$

We define a *euclidean Lagrangian* $\mathcal{L}_{\mathrm{E}}$ and a *euclidean action* S_{E} through

$$S_{\mathrm{E}}[\mathbf{\Phi}] = \int d^4x\, \mathcal{L}_{\mathrm{E}}(\mathbf{\Phi}(x), (\partial\mathbf{\Phi})(x)) = -\int d^4x\, \mathcal{L}(\mathbf{\Phi}(x), (\partial^{\mathrm{E}}\mathbf{\Phi})(x)) \quad . \tag{3.40}$$

Note that the time integral is taken along the real time axis. The *euclidean space-time derivatives* are defined as

$$\partial_0^{\mathrm{E}} = i\partial_0 \qquad , \qquad \partial_i^{\mathrm{E}} = \partial_i \quad . \tag{3.41}$$

They satisfy the operator identity

$$\partial W = W\partial^{\mathrm{E}} \quad . \tag{3.42}$$

From this, it follows immediately, that

$$\begin{aligned} iS'[W\mathbf{\Phi}] &= i\int_{+i\infty}^{-i\infty} dx^0 \int d^3\mathbf{x}\ \mathcal{L}(W\mathbf{\Phi}(x), (\partial W\mathbf{\Phi})(x)) \\ &= i\int_{+i\infty}^{-i\infty} dx^0 \int d^3\mathbf{x}\ \mathcal{L}(W\mathbf{\Phi}(x), (W\partial^{\mathrm{E}}\mathbf{\Phi})(x)) \\ &= -\int_{-\infty}^{+\infty} dx^0 \int d^3\mathbf{x}\ \mathcal{L}_{\mathrm{E}}(\mathbf{\Phi}(x), (\partial\mathbf{\Phi})(x)) \\ &= -S_{\mathrm{E}}[\mathbf{\Phi}] \quad . \end{aligned} \tag{3.43}$$

We can express the euclidean two point Greens function in terms of S_{E} by performing a change of variables in the path integral (3.38).

$$\begin{aligned} G_{ij}^{\mathrm{E}}(x, y; T) &= \mathcal{N}\int_{\mathcal{S}_T^{\mathrm{E}}} [d\mathbf{\Phi}]\ (W^{-1}\Phi_i)(x)(\overline{W^{-1}\Phi_j})(y)\ e^{iS'[\mathbf{\Phi}]} \\ &= \mathcal{N}\int_{\mathcal{S}_T^{\mathrm{E}}} \det(W)[d\mathbf{\Phi}]\ \Phi_i(x)\bar{\Phi}_j(y)\ e^{iS'[W\mathbf{\Phi}]} \\ &= \mathcal{N}\det(W)\int_{\mathcal{S}_T^{\mathrm{E}}} [d\mathbf{\Phi}]\ \Phi_i(x)\bar{\Phi}_j(y)\ e^{-S_{\mathrm{E}}[\mathbf{\Phi}]} \quad . \end{aligned} \tag{3.44}$$

In the second line, we changed the integration 'variables' of the functional integral from $\mathbf{\Phi}$ to $W^{-1}\mathbf{\Phi}$. The functional determinant $\det(W)$ is the corresponding Jacobian. In the last line, we used (3.43). Higher euclidean Greens functions can be treated in the same way. We can even define a *euclidean partition functional* $Z_{\mathrm{E}}[\mathbf{J}]$, whose functional derivatives are euclidean Greens functions. Let

$$Z_{\mathrm{E}}[\mathbf{J}] = \int_{\mathcal{S}_T^{\mathrm{E}}} [d\mathbf{\Phi}]\, e^{-S_{\mathrm{E}}[\mathbf{\Phi}]+(\mathbf{J},\mathbf{\Phi})+(\mathbf{\Phi},\mathbf{J})} \quad . \tag{3.45}$$

Then, by fixing the the normalisation constant $\mathcal{N}$ appropriately, the euclidean Greens function (3.44) can be written as

$$G^{\mathrm{E}}_{ij}(x,y;T) = \frac{1}{Z_{\mathrm{E}}[0]} \left[\frac{\delta}{\delta \bar{J}_i(x)} \frac{\delta}{\delta J_j(y)} Z_{\mathrm{E}}[\mathbf{J}] \right]_{\mathbf{J}=0} \quad . \tag{3.46}$$

Higher euclidean Greens function can be obtained by applying more functional derivatives.

Formally, this looks all very nice, but we have left out one important step: We have not yet defined what we mean by the functional integral (3.30). Unfortunately, there is no canonical way to define a functional integral. More precisely, there is no integration measure on the infinite dimensional space $\mathcal{S}$ of field configurations, which has all the properties we know from finite dimensional integration. Thus, we have to provide an explicit definition of the partition functional Z. As we mentioned above, the arbitrariness in the definition of Z just reflects our freedom to choose different gauge fixing conditions and regularisation methods in the (operator) quantisation of the theory.

In a free field theory, the action functional has the form

$$S_0[\mathbf{\Phi}] = (\mathbf{\Phi}, M\mathbf{\Phi}) \quad , \tag{3.47}$$

where M is some hermitian operator on $\mathcal{S}$. In this case, we can define the partition functional through a functional version of the Gauss integral. Let $\mathbf{v}, \mathbf{b} \in \mathbb{C}^n$ and let K be a hermitian, non-singular, positive definite $n \times n$ matrix. Then, the Gaussian integration formula tells us that

$$\int d^n\mathbf{v}\, \exp\left(\zeta(-\mathbf{v}^\dagger K \mathbf{v} + \mathbf{b}^\dagger \mathbf{v} + \mathbf{v}^\dagger \mathbf{b})\right) = \frac{\pi^n}{\det(\zeta K)} \exp(\zeta \mathbf{b}^\dagger K^{-1} \mathbf{b}) \quad , \tag{3.48}$$

where ζ is a complex phase with $\mathrm{Re}\,\zeta > 0$. The integrals over the complex components of $\mathbf{v}$ are integrals over the whole complex plane. A formula similar to (3.48) holds for Grassmann integrals. Let $\boldsymbol{\theta}$ and $\boldsymbol{\eta}$ be n component vectors of complex Grassmann variables and K the same as above. Then,

$$\int d^n\boldsymbol{\theta}\, \exp\left(\zeta(-\boldsymbol{\theta}^\dagger K \boldsymbol{\theta} + \boldsymbol{\eta}^\dagger \boldsymbol{\theta} + \boldsymbol{\theta}^\dagger \boldsymbol{\eta})\right) = \det(\zeta K) \exp(\zeta \boldsymbol{\eta}^\dagger K^{-1} \boldsymbol{\eta}) \quad . \tag{3.49}$$

We can formulate infinite-dimensional versions of (3.48) and (3.49) in the following way: Let K be a hermitian, non-singular, positive definite operator on $\mathcal{S}$. Then, making the formal substitution $\zeta = -i$ in (3.48) and (3.49), we *define* the following functional Gauss integrals for bosonic and fermionic fields:

$$\text{bosonic fields:} \qquad \int_{\mathcal{S}} [d\mathbf{\Phi}]\, e^{i(\mathbf{\Phi},K\mathbf{\Phi})-i(\mathbf{J},\mathbf{\Phi})-i(\mathbf{\Phi},\mathbf{J})} \equiv \frac{1}{\det(-iK)}\, e^{-i(\mathbf{J},K^{-1}\mathbf{J})} \quad , \tag{3.50a}$$

$$\text{fermionic fields:} \qquad \int_{\mathcal{S}} [d\mathbf{\Phi}]\, e^{i(\mathbf{\Phi},K\mathbf{\Phi})-i(\mathbf{J},\mathbf{\Phi})-i(\mathbf{\Phi},\mathbf{J}))} \equiv \det(-iK)\, e^{-i(\mathbf{J},K^{-1}\mathbf{J})} \quad . \tag{3.50b}$$

The above definitions are still ambiguous, because there is also no canonical way to define a functional determinant, i.e. the determinant of an operator in an infinite-dimensional space. However, for a free field theory, the partition functional has the form

$$Z_0[\mathbf{J}] = \int_{\mathcal{S}} [d\mathbf{\Phi}]\, e^{i(\mathbf{\Phi},K\mathbf{\Phi})-i(\mathbf{J},\mathbf{\Phi})-i(\mathbf{\Phi},\mathbf{J})} \quad . \tag{3.51}$$

In that case, we can directly apply the functional Gauss integrals (3.50) and the functional determinant is just an overall constant, which cancels in the expressions for Greens functions. For the propagator (3.32) we can immediately obtain

$$G_{ij}(x,y;T) = \left[\frac{i\delta}{\delta \bar{J}_i(x)} \frac{i\delta}{\delta J_j(y)} e^{-i(\mathbf{J},K^{-1}\mathbf{J})} \right]_{\mathbf{J}=0} = i\, \mathcal{K}^{-1}_{ij}(x,y) \quad , \tag{3.52}$$

where the inverse kernel function $\mathcal{K}^{-1}$ is defined as

$$\mathcal{K}^{-1}_{ij}(x,y) = \frac{\delta}{\delta J_i(x)} \frac{\delta}{\delta \bar{J}_j(y)} (\mathbf{J}, K^{-1}\mathbf{J}) \quad . \tag{3.53}$$

Higher Greens functions can be calculated from this propagator by applying Wick's theorem (3.34).

For interacting field theories, the definition of the partition functional is more difficult. There, the Lagrangian cannot be written in the form (3.47), because of *interaction terms*, that contain local products of three or more fields. However, in the limit where the *coupling constants* vanish, we should re-obtain the free theory, which is defined through the partition functional (3.51). In *perturbation theory*, this is realised as follows: First, the interaction terms in the Lagrangian are split off by writing

$$\mathcal{L} = \mathcal{L}_0 + \mathcal{L}_{\text{int}} \quad . \tag{3.54}$$

Now, $\mathcal{L}_{\text{int}}$ contains all interaction terms and $\mathcal{L}_0$ is the Lagrangian of a free field theory. Formally, we can substitute (3.54) in (3.30) and expand the exponential with $\mathcal{L}_{\text{int}}$ into a power series.

$$\begin{aligned} Z[\mathbf{J}] = \int_{\mathcal{S}} [d\mathbf{\Phi}]\, e^{iS_0[\mathbf{\Phi}]-i(\mathbf{J},\mathbf{\Phi})-i(\mathbf{\Phi},\mathbf{J})} \bigg(1 &+ i \int d^4 z_1\, \mathcal{L}_{\text{int}}(z_1) \\ &+ \frac{i^2}{2} \int d^4 z_1 d^4 z_2\, \mathcal{L}_{\text{int}}(z_1)\mathcal{L}_{\text{int}}(z_2) + \dots \bigg) \quad . \end{aligned} \tag{3.55}$$

Each individual term in the expansion can be written as a functional derivative of the *free* partition functional $Z_0[\mathbf{J}]$, evaluated at $\mathbf{J} = 0$. As we have already seen, Z_0 is well defined through the functional Gauss integral (3.51). However, to calculate Greens functions in the interacting theory, we have to perform the *vertex integrals* over z_1, z_2, etc. In general, these integrals are divergent, and some ad hoc prescription has to be introduced to make them finite. This prescription is the *regularisation scheme* for divergent loop integrals, that was already mentioned in *section 2.2*. Having defined $Z[\mathbf{J}]$ in this way, it is obvious that we re-obtain the free theory in the limit where all coupling constants go to zero. In that case, all terms in the expansion (3.55) vanish, except the first, which is precisely the free partition functional $Z_0[\mathbf{J}]$.

In the *lattice regularisation* of field theories, we take a different path. Rather than using an analytic formula for the functional integral (3.30), we reduce it to a finite dimensional integral. This is achieved by replacing the continuous space and time coordinates with a four dimensional cubic lattice of finite space-time volume and with a non-zero lattice spacing a. A certain field configuration is now fully described by specifying the field components at each lattice site.[3] Thus, the space $\mathcal{S}$ of field configurations becomes finite dimensional. Operators acting on $\mathcal{S}$ are represented as finite-dimensional complex matrices and the path integral (3.30) is well defined, being an integral over a finite dimensional space. It's independent integration variables are the field components at each lattice site.

For small coupling constants, the physical properties of a lattice regularised theory should agree with perturbative calculations, that use continuum regularisation methods like dimensional regularisation. In particular, the correct free field theory should be re-obtained in the case, where all coupling constants vanish. This is not always the case, and depends on the explicit way, in which the lattice equivalent of the action functional S is chosen. Operators like space-time derivatives, which appear in the continuum action and act on the continuum fields have to be identified with matrices acting on the lattice fields. For any such identification, it has to be checked explicitly, whether the correct free field theory is re-obtained, if we set all coupling constants to zero and take the continuum limit $a \to 0$. This can be done by comparing the pole structures of the propagators G_{ij} obtained from the partition functional (3.51) with those from the continuum limit of the lattice theory.

Another problem is the convergence of the path integral. Even though the discretisation of space-time allows us to define the partition functional as a finite dimensional integral, this integral can still be divergent. The action functional S will usually be bounded from below, but go to infinity, if the field components become large. Thus, the integrand in (3.30) oscillates heavily for large values of the integration variables, and the path integral diverges. To assure the convergence of the path integral, the integrand

[3] In the lattice formulation of gauge theories, it is more convenient to associate the gauge fields not with individual lattice sites, but with connections or *links* between two adjacent lattice sites. This does, however, not invalidate any of the following arguments.

should fall off exponentially for large excitations of the fields. This is usually not the case for the partition functional in Minkowski space, but it is true for the *euclidean partition functional* (3.45), if the euclidean action (3.40) is real and bounded from below. It turns out that in many field theories, and in particular in QCD, the euclidean action has this property. Therefore, the lattice regularised euclidean partition functional of those theories is a mathematically well defined quantity and euclidean Greens functions can be extracted from it. Furthermore, due to the exponential damping, significant contributions to the overall value of Z_{E} come only from a small volume of the (finite dimensional) space of field configurations. This fact allows the very efficient use of a certain class of numerical integration techniques called *Monte Carlo* integration. All the numerical work on lattice QCD is based on the idea of applying Monte Carlo integration techniques to calculate euclidean Greens functions in lattice regularised QCD.

3.3 Lattice Formulation of QCD

In this section, we will apply the systematics developed in the last section to the Lagrangian constructed in *section 3.1*, and provide a lattice formulation of QCD.

The first step is to construct the euclidean Lagrangian $\mathcal{L}_{\mathrm{E}}$. In (3.40) this was essentially done by replacing in the Minkowski space Lagrangian $\mathcal{L}$ the time derivative ∂_0 with $i\partial_0$. For the QCD Lagrangian, there is one more thing to consider. In Minkowski space, we wrote the QCD Lagrangian in terms of the covariant derivative (3.14), which is related to the connectors $U(x, y)$ by (3.17). We also want to express the euclidean Lagrangian in terms of a covariant derivative of the form (3.17). If our gauge group is to remain unitary, this means that the time components of the gauge fields have to pick up a factor of i, too. Therefore, we define the time components of the euclidean gauge field operators with an additional factor of i.

$$A_0^{\mathrm{E}a}(\tau, \mathbf{x}) = e^{H\tau}\, iA_0^a(0, \mathbf{x})\, e^{-H\tau} \quad . \tag{3.56}$$

Consequently, they have to be represented in the path integral by imaginary valued fields. We may write them as iA_0^a, where A_0^a is a real valued field. Therefore, with the definition (3.56) for the euclidean gauge field operators, the time components of the gauge fields also pick up a factor of i, and we obtain the (negative) euclidean Lagrangian from the Minkowski Lagrangian (3.25) by making the following replacements:

$$\partial_0 \to i\partial_0 \qquad , \qquad A_0^a \to iA_0^a \quad . \tag{3.57}$$

We first split the Lagrangian (3.25) in a gauge term $\mathcal{L}^{\mathrm{g}}$ and a quark term $\mathcal{L}^{\mathrm{q}}$.

$$\mathcal{L}^{\mathrm{g}} = -\frac{1}{4} F^a_{\mu\nu} F_a^{\mu\nu} \qquad , \qquad \mathcal{L}^{\mathrm{q}} = \bar{\psi}\big[i\gamma^\mu(\partial_\mu - igA^a_\mu T^a) - m\big]\psi \quad , \tag{3.58}$$

and then make the replacements (3.57) in each of the terms separately. The euclidean quark Lagrangian is

$$\begin{aligned}\mathcal{L}_{\mathrm{E}}^{\mathrm{q}} &= -\bar{\psi}\big(i\gamma^0[(i\partial_0) - ig(iA_\mu^a)T^a] + i\gamma^j[\partial_j - igA_\mu^a T^a] - m\big)\psi \\ &= \bar{\psi}\big(\gamma^0[\partial_0 - igA_\mu^a T^a] - i\gamma^j[\partial_j - igA_\mu^a T^a] + m\big)\psi \\ &= \bar{\psi}(\gamma^0 D_0 - i\gamma^j D_j + m)\psi \quad ,\end{aligned} \tag{3.59}$$

where the covariant derivatives D_μ are the same as in (3.14). To make this look nicer, we define the euclidean gamma matrices

$$\gamma_0^E = \gamma^0 \qquad , \qquad \gamma_j^E = -i\gamma^j \quad . \tag{3.60}$$

They satisfy

$$\{\gamma_\mu^{\mathrm{E}}, \gamma_\nu^{\mathrm{E}}\} = 2\delta_{\mu\nu} \qquad , \qquad \gamma_\mu^{\mathrm{E}\,\dagger} = \gamma_\mu^{\mathrm{E}} \quad . \tag{3.61}$$

Then, we may write the euclidean quark Lagrangian as

$$\mathcal{L}_{\mathrm{E}}^{\mathrm{q}} = \bar{\psi}(\gamma_\mu^{\mathrm{E}} D_\mu + m)\psi \quad . \tag{3.62}$$

Note that the two μ indices are simply summed over, without one being raised by contraction with the metric tensor. To obtain the (negative) euclidean gauge Lagrangian $\mathcal{L}_{\mathrm{E}}^{\mathrm{g}}$, we have to make the replacements (3.57) in the field strength tensor (3.20). We see that the components F_{0i}^a pick up a factor of i, while the spacial components F_{ij}^a remain unchanged. Therefore

$$\begin{aligned}\mathcal{L}_{\mathrm{E}}^{\mathrm{g}} &= \frac{1}{4}\big(2(iF_{0i}^a)(iF_a^{0i}) + F_{ij}^a F_a^{ij}\big) \\ &= \frac{1}{4}\big(2F_{0i}^a F_{0i}^a + F_{ij}^a F_{ij}^a\big) \\ &= \frac{1}{4}F_{\mu\nu}^a F_{\mu\nu}^a \quad .\end{aligned} \tag{3.63}$$

Again, we end up with a simple sum over lower indices, and not a contraction of upper and lower indices. By putting (3.63) and (3.62) together, we get the euclidean QCD Lagrangian

$$\mathcal{L}_{\mathrm{E}} = \frac{1}{4}F_{\mu\nu}^a F_{\mu\nu}^a + \bar{\psi}(\gamma_\mu^{\mathrm{E}} D_\mu + m)\psi \quad . \tag{3.64}$$

$\mathcal{L}_{\mathrm{E}}$ is still invariant under the local gauge transformations (3.9), but it is no longer invariant under Lorentz transformations. It is, however, invariant under $SO(4)$ transformations of the euclidean space-time, if we choose the $SO(4)$ transformation behaviour of the spinors appropriately. In fact, this is the reason why we speak of a *euclidean* theory at all. The Lorentz group leaves the Minkowski product invariant, and in the same way the $SO(4)$ transformations leave the euclidean product invariant. This is what we mean, if we say that a field theory is formulated on a space-time with euclidean

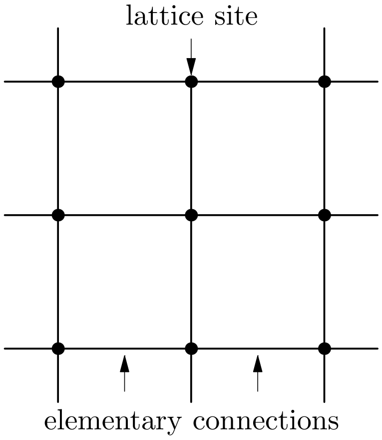

Figure 3.1: A typical choice for elementary connections between neighbouring lattice sites.

metric. From now on, products between four vectors denote *euclidean products*, i.e. $px \equiv \sum_\mu p_\mu x_\mu$ etc.

The next step is to discretise the euclidean space-time, along with the fields that live on it. We replace the continuous space-time with a finite four dimensional cubic lattice, with an extent T in the (euclidean) time direction, an extent L in all spacial directions and a lattice spacing a. Thus, the space-time coordinates x, y, etc. become discrete variables or *position indices*, which identify individual *lattice sites*. The lattice spacing a is a quantity of mass dimension -1. We can use it to define the unit energy of the lattice theory. Therefore, all quantities like masses, field components, space-time coordinates, momenta etc. can be described by dimensionless variables. To re-obtain the correct dimensionful quantity, we only have to multiply with the right power of a. From now on, we will use these *lattice units* for all quantities we define on the lattice. For example, in lattice units, the space-time coordinates x of the lattice sites are integer numbers, and so are the space and time extents L and T of the lattice. Even though we always have $a = 1$ in lattice units, we can still take the continuum limit. We only have to rescale the parameters that depend on a. For example, the value of L in lattice units approaches infinity in the continuum limit, even if we keep the spacial volume fixed.

Now, we have to implement the fields of QCD on our lattice. For the quark fields, this is done in the obvious way: With each lattice site x, we associate a complete set of quark fields $\psi^f_{j\alpha}(x)$, where $\alpha = 1 \ldots 4$ is the spinor, $j = 1 \ldots 3$ the colour and $f = 1 \ldots n_f$ the flavour index. Each field component is a complex Grassmann number. The gauge fields are treated in a different way. As we already saw in *section 3.1*, they can be viewed as coefficients, that determine the infinitesimal connectors $U(x, x + \varepsilon)$. On the lattice, we treat the connectors U themselves as dynamical degrees of freedom, and not the gauge fields A^a_μ. First, we define *elementary connections* between neighbouring lattice sites. There are different ways to define the neighbourhood of a lattice site, but the most common choice is the one shown in *figure 3.1*. Let x and y be two neighbouring lattice sites, in the sense of *figure 3.1*. The connectors $U(x, y)$ associated with pairs (x, y) of *neighbouring* lattice sites are called *gauge links*. In the lattice regularised theory, they are treated as dynamical degrees of freedom and replace the gauge fields A^a_μ. Consequently, the path integrals over the gauge fields are replaced by integrals over the gauge links U. Since they are elements of a compact Lie group, the integrals run over the whole group manifold. If we want to preserve gauge symmetry, the integration measure dU on the group manifold has to be invariant under gauge transformations. It turns out, that, for compact groups, this requirement already fixes the measure up to an irrelevant normalisation constant. This measure is called the *Haar measure*, and we will use it in all integrals over gauge links. Further information on integration over group manifolds can be found in [29].

Through the discretisation of space-time, the space of (lattice) field configurations has become finite-dimensional. Now, we have to define an action S_{lat} on this space. Like the Lagrangian (3.64), we may split it into a quark term $S^{\text{q}}_{\text{lat}}$ and a gauge term $S^{\text{g}}_{\text{lat}}$. To discretise an action of the form (3.31), the obvious approach is to replace the field derivatives in the Lagrangian with differences of the field components. (We don't have to divide by the lattice spacing a, because we are using lattice units, where $a = 1$.) However, as we want to re-obtain all symmetries of the Lagrangian (3.64) in the continuum limit, it seems a good idea to break as few of them as possible. This is the reason why we implemented the gauge fields through the gauge links U. It allows us to maintain an exact local gauge symmetry. On the lattice, a local gauge transformation assigns to each lattice site x an $SU(3)$ matrix $\Lambda(x)$. Therefore, the local gauge group $\mathcal{G}^{\text{lat}}_{\text{loc}}$ of the lattice regularised theory is a compact semi-simple Lie group, namely

$$\mathcal{G}^{\text{lat}}_{\text{loc}} = SU(N_c) \times SU(N_c) \times \ldots \times SU(N_c) \quad , \tag{3.65}$$

with one factor $SU(N_c)$ for each lattice site. The quark fields on each lattice site transform according to (3.9), while the gauge links transform like the connectors in (3.16). Thus, we define the *covariant lattice derivative* Δ_μ as

$$(\Delta_\mu \psi)(x) = \frac{1}{2}\big[U(x, x+\hat{\mu})\psi(x+\hat{\mu}) - U(x, x-\hat{\mu})\psi(x-\hat{\mu})\big] \quad . \tag{3.66}$$

From the transformation behaviour of the quark fields and gauge links under local gauge transformations follows immediately, that $(\Delta_\mu \psi)(x)$ also transforms like a quark field, in accordance with the property (3.12) of the continuum covariant derivative. Therefore, our first guess for the lattice quark action is:

$$S^{\text{q}}_{\text{lat}}[U, \psi] = \sum_x \bar{\psi}(x)\big[(\gamma^{\text{E}}_\mu \Delta_\mu + m)\psi\big](x) \equiv \sum_{x,y} \bar{\psi}(x) M(x, y) \psi(y) \quad . \tag{3.67}$$

In the last step, we have defined M as the matrix representation of the lattice operator $(\gamma^{\text{E}}_\mu \Delta_\mu + m)$. It carries flavour, colour, spinor and position indices. In (3.67), we have written out the position indices (x, y) and left all other indices implicit. Note also, that M, like the covariant lattice derivative Δ depends implicitly on the gauge links U.

Does the action (3.67) have the correct continuum limit? Assume that we have chosen $U = \mathbb{1}$ for all gauge links. Then, the matrix M acts on a field configuration ψ as

$$(M\psi)(x) = \sum_\mu \frac{1}{2}\gamma_\mu^{\mathrm{E}}\big(\psi(x+\hat{\mu}) - \psi(x-\hat{\mu})\big) + m\psi(x) \quad . \tag{3.68}$$

In this case, we should obtain the free Dirac field in the continuum limit. The euclidean two point Greens function of the free Dirac field is

$$G^{\mathrm{E}}(x,y) = \int \frac{d^4p}{(2\pi)^4}\,\tilde{G}^{\mathrm{E}}(p)e^{-ip(x-y)} \quad , \tag{3.69}$$

with

$$\tilde{G}^{\mathrm{E}}(p) = [ip_\mu\gamma_\mu^{\mathrm{E}} + m]^{-1} = \frac{-ip_\mu\gamma_\mu^{\mathrm{E}} + m}{p^2+m^2} \quad . \tag{3.70}$$

Remember, that products of four vectors are now *euclidean products*, i.e. $px = \sum_\mu p_\mu x_\mu$. The value of the integral in (3.69) is completely determined by the poles of the momentum space propagator (3.70). As function of the time component p_0, the momentum space propagator $\tilde{G}^{\mathrm{E}}(p_0,\mathbf{p})$ has two poles at $p_0 = \pm i\sqrt{\mathbf{p}^2+m^2}$.

To obtain the lattice two point Greens function, we have to invert the matrix M. It's eigenvectors are the normal modes

$$\psi_p(x) = \chi\, e^{ipx} \quad , \tag{3.71}$$

where χ is an arbitrary vector in flavour, colour and spinor space. The allowed values for the *lattice momenta* p are

$$\begin{aligned} p_0 &= 2\pi\frac{n_0}{T} \qquad \text{with} \quad n_0 = -\frac{T}{2},\ldots,+\frac{T}{2} \quad , \\ p_i &= 2\pi\frac{n_i}{L} \qquad \text{with} \quad n_i = -\frac{L}{2},\ldots,+\frac{L}{2} \quad . \end{aligned} \tag{3.72}$$

They form a four dimensional cubic lattice, which is also called the *reciprocal lattice*. It has an extent π in all four directions. The lattice two point Greens function is

$$G^{\mathrm{lat}}(x,y) = M^{-1}(x,y) = \frac{1}{L^3T}\sum_p \tilde{G}^{\mathrm{lat}}(p)\, e^{-ip(x-y)} \quad , \tag{3.73}$$

where the sum runs over the discrete momenta given in (3.72). The lattice propagator in momentum space is

$$\tilde{G}^{\mathrm{lat}}(p) = \left[i\sum_\mu \gamma_\mu^{\mathrm{E}}\sin(p_\mu) + m\right]^{-1} \quad . \tag{3.74}$$

For $|p_\mu| \ll 1$, we can use the approximation $\sin(p_\mu) \approx p_\mu$ and obtain the same expression as in (3.70). However, the allowed values for the momentum components reach up to

π, where the sine function has another zero point. In the continuum limit, the lattice momenta become continuous variables. Then, the lattice propagator (3.74) has, in addition to the poles of (3.70), 16 extra poles. For $m = 0$ they lie in the corners of the four dimensional hypercube, which contains the allowed lattice momenta p. In the LSZ formalism, the poles of the two point Greens function (in momentum space) are identified with one particle states. Thus, our lattice theory has 16 additional types of quarks. This is the famous *Fermion doubling problem.* In any case, with the quark action (3.67), the physical properties of the lattice theory are different from the properties of the free Dirac field, even in the continuum limit.

One possible solution to the fermion doubling problem was proposed by Wilson and consists in adding a new term, the *Wilson term*, to the quark action (3.67). We define the lattice operator $\Box$ as

$$(\Box\psi)(x) = \frac{1}{2}\sum_{\mu}\left[U(x,x+\hat{\mu})\psi(x+\hat{\mu}) + U(x,x-\hat{\mu})\psi(x-\hat{\mu}) - 2\psi(x)\right] \quad . \qquad (3.75)$$

Then, the Wilson quark action $S^{\mathrm{q}}_{\mathrm{W}}$ and the Wilson matrix M^{W} are defined through

$$\begin{aligned} S^{\mathrm{q}}_{\mathrm{W}}[U,\psi] &= \sum_{x,y}\bar{\psi}(x)M^{\mathrm{W}}(x,y)\psi(y) \\ &= S^{\mathrm{q}}_{\mathrm{lat}}[U,\psi] - \sum_{x}\bar{\psi}(x)(\Box\psi)(x) \\ &= \sum_{x}\bar{\psi}(x)\left[(\gamma^{\mathrm{E}}_{\mu}\Delta_{\mu} - \Box + m)\psi\right](x) \quad . \end{aligned} \qquad (3.76)$$

If we define κ as

$$\kappa = \frac{1}{2ma+8} \quad , \qquad (3.77)$$

we can write M^{W} as

$$\begin{aligned} (M^{\mathrm{W}}\psi)(x) = \frac{1}{2}\Big[& \quad (\gamma^{\mathrm{E}}_{\mu} - \mathbb{1}){\textstyle\sum_{\mu}}U(x,x+\hat{\mu})\psi(x+\hat{\mu}) \\ & - (\gamma^{\mathrm{E}}_{\mu} + \mathbb{1}){\textstyle\sum_{\mu}}U(x,x-\hat{\mu})\psi(x-\hat{\mu}) + \frac{1}{\kappa}\psi(x)\Big] \quad . \end{aligned} \qquad (3.78)$$

For this lattice action, the free ($U = \mathbb{1}$) momentum space propagator is

$$\tilde{G}^{\mathrm{W}}(p) = \left[\frac{1}{2\kappa} + \sum_{\mu}\left(i\gamma^{\mathrm{E}}_{\mu}\sin(p_{\mu}) - \cos(p_{\mu})\right)\right]^{-1} \quad . \qquad (3.79)$$

The additional 16 poles have disappeared because of the cosine term. Thus, if all gauge links are chosen as $\mathbb{1}$, the momentum space propagator of the Wilson action has, in the continuum limit, the same pole structure as the propagator (3.70) of the free Dirac field.

However, we have made a sacrifice for this achievement. As we saw at the end of *section 3.1*, the QCD Lagrangian is, in the limit of vanishing quark masses, invariant

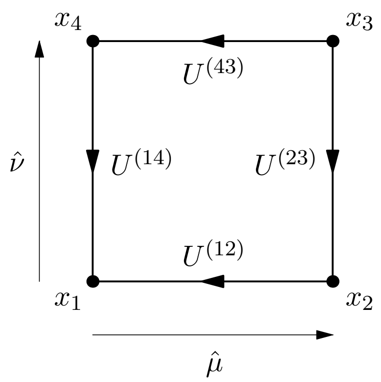

Figure 3.2: Elementary plaquette with gauge links.

under the *chiral symmetry transformations* (3.27). This symmetry is broken explicitly by the Wilson term in (3.83). It is restored in the continuum limit, but it's explicit breaking can still lead to problems in calculations, where chiral symmetry is of central importance.

So far, we just talked about the quark part of the lattice action. Now, we have to construct a lattice action for the gauge fields. The one, which is most commonly used, was also proposed by Wilson and is called *Wilson action* or *plaquette action*. We denote it by $S^{\mathrm{g}}_{\mathrm{W}}$. It's continuum limit should be the euclidean gauge action $S^{\mathrm{g}}_{\mathrm{E}}$ obtained from the Lagrangian (3.63). $\mathcal{L}^{\mathrm{g}}_{\mathrm{E}}$ is expressed in terms of the fields strength tensor $F_{\mu\nu}(x)$, which is a matrix in colour space. In (3.19), we obtained $F_{\mu\nu}$ from the commutator of two covariant derivatives. On the lattice, this commutator can be approximated as follows: Let x_1, x_2, x_3 and x_4 be neighbouring lattice sites, that span an elementary square or *plaquette*, as shown in *figure 3.2*. If we approximate D_μ by the covariant lattice *forward* derivative,

$$(D_\mu\psi)(x) \approx (U(x, x+\hat{\mu})\psi(x+\hat{\mu}) - \psi(x)) \quad , \tag{3.80}$$

we obtain

$$([D_\mu, D_\nu]\psi)(x_1) \approx (U^{(12)}U^{(23)} - U^{(14)}U^{(43)})\psi(x_3) \quad . \tag{3.81}$$

As indicated in *figure 3.2*, we use the abbreviation $U^{(ij)} \equiv U(x_i, x_j)$. Equation (3.81) suggests, that we should take the matrix $(U^{(12)}U^{(23)} - U^{(14)}U^{(43)})$ as value for $-igF_{\mu\nu}$ at one of the x_i. We will use x_1 here. Thus,

$$\begin{aligned}
\frac{1}{2}\,\mathrm{Tr}[F^\dagger_{\mu\nu}(x_1)F_{\mu\nu}(x_1)] &\approx \frac{1}{2g^2}\,\mathrm{Tr}\left[(U^{(12)}U^{(23)} - U^{(14)}U^{(43)})^\dagger(U^{(12)}U^{(23)} - U^{(14)}U^{(43)})\right] \\
&= \frac{1}{2g^2}\,\mathrm{Tr}\left[(U^{(32)}U^{(21)} - U^{(34)}U^{(41)})(U^{(12)}U^{(23)} - U^{(14)}U^{(43)})\right] \\
&= \frac{1}{2g^2}\,\mathrm{Tr}[2\mathbb{1} - U_\square - U^\dagger_\square] \\
&= \frac{1}{g^2}\,\mathrm{Re}\,\mathrm{Tr}(\mathbb{1} - U_\square) \quad ,
\end{aligned} \tag{3.82}$$

where $U_\Box = U^{(12)}U^{(23)}U^{(34)}U^{(41)}$. Note that, in (3.82), we have not summed over the indices μ and ν. To do this, we would have to sum over all plaquettes with their lower left corner at x_1. In a sum over μ and ν, each plaquette is counted twice, because we obtain the same plaquette, if we swap μ and ν. In the action we also have to do the space-time integration, i.e. sum over all lattice sites, so that we simply end up with twice the sum over all plaquettes. Thus, we define the Wilson action as

$$S_{\mathrm{W}}^{\mathrm{g}}[U] = \frac{\beta}{3} \sum_{\Box} \mathrm{Re}\,\mathrm{Tr}(\mathbb{1} - U_\Box) \quad , \tag{3.83}$$

where the sum runs over all plaquettes on the lattice. By convention, the parameter β is defined as

$$\beta = \frac{2N_c}{g^2} = \frac{6}{g^2} \quad . \tag{3.84}$$

It can be shown, that the action (3.83) yields, in the continuum limit, the correct free gauge theory, as given by the Lagrangian (3.63).

The complete lattice QCD action is the sum of the actions (3.76) and (3.83).

$$S_{\mathrm{W}}[U,\psi] = S_{\mathrm{W}}^{\mathrm{g}}[U] + S_{\mathrm{W}}^{\mathrm{q}}[U,\psi] \quad . \tag{3.85}$$

It can be shown that this action is renormalisable and yields, in the continuum limit, an asymptotically free theory with the same gauge symmetry as QCD. In the regime, where it can be solved in lattice perturbation theory, it's physical predictions are equal to those obtained in continuum regularisation schemes like dimensional regularisation. Therefore, it is taken as a starting point for many non-perturbative calculations in lattice QCD.

Chapter 4

Numerical Methods

In the last chapter, we provided a lattice regularised definition of the euclidean QCD partition functional. As we pointed out before, the lattice regularisation method has the great advantage, that it allows us to calculate euclidean Greens functions numerically, and this even at low energy scales, where perturbative methods fail. In this chapter, I will describe the numerical methods, which are required for the calculation of euclidean Greens functions on the lattice.

The first obstacle in the numerical computation of Greens functions are the path integrals over the quark fields. They must be treated in a semi-analytic way by introducing an *effective gauge action*. This is discussed in the first section. In *section 4.2*, we introduce the basic concepts of the *Monte Carlo integration* method. We will see that the problem of calculating path integrals over lattice gauge fields can be reduced to generating *ensembles* of gauge configurations with the correct statistical distribution. In *section 4.3* we discuss various numerical algorithms, that can be used to generate these ensembles. The last step in a lattice simulation is to determine parameters like masses, form factors or matrix elements by fitting the numerical results to theoretical curves like those from *section 2.3*. In *section 4.4*, I describe how these fits are done and how the (theoretical) errors on the parameters can be estimated.

4.1 The Effective Gauge Action

In *section 3.2*, we saw that euclidean Greens functions can be calculated from path integral expressions like the one in (3.32). In *section 3.3*, we provided an explicit definition of the euclidean partition functional of QCD, by formulating the theory on a finite four-dimensional lattice. From now on, all considerations are done for a lattice in euclidean space-time. Let us therefore introduce some new notations. The lattice quark fields carry flavour, colour, spinor and position indices. As we already mentioned in *section 3.1*, we use the letters f, g, h for flavour, i, j, k for colour, α, β, γ for spinor and x, y, z for position indices. To pick out a single component of the quark field ψ at lattice site x, we write $\psi^f_{i\alpha}(x)$. With so many indices, it is a good idea to group them into multi-indices. We use capital letters X, Y, Z for multi-indices in colour, spinor and position space. We continue to use the word "function" for objects that depend on position indices and the word "functional" for functions of vectors in flavour, colour, spinor and position space. Products $\bar{\eta}\psi$ of a quark field ψ and a bar conjugated field $\bar{\eta}$ are understood as contraction of all indices, including position indices, i.e.

$$\bar{\eta}\psi = \sum_f \sum_X \bar{\eta}^f_X \psi^f_X \quad . \tag{4.1}$$

With these conventions, we are ready to go. To calculate lattice Greens functions of the quark fields, we define the lattice partition functional

$$Z[\eta] = \int [dU] \int [d\psi] \, e^{-S_{\mathrm{W}}[U,\psi]+\bar{\eta}\psi+\bar{\psi}\eta} \quad . \tag{4.2}$$

The path integrals over the gauge links U and the quark fields ψ in (4.2) are finite dimensional integrals. The Wilson action can be written as

$$S_{\mathrm{W}}[U,\psi] = S^{\mathrm{g}}_{\mathrm{W}}[U] + \bar{\psi} M_U \psi \quad . \tag{4.3}$$

M_U denotes the Wilson matrix (3.78), which is a matrix in flavour, colour, spinor and position space and depends on the gauge configuration U.

In (4.2), the path integral over the gauge links can be done numerically, by methods we will discuss later on. The path integral over the quark fields is more problematic from the numerical point of view, because the components of ψ are Grassmann numbers. It is, however, possible to deal with them analytically. For a given gauge configuration U, we define the functional Z_U as

$$Z_U[\eta] = \int [d\psi] \, e^{-\bar{\psi} M_U \psi + \bar{\eta}\psi + \bar{\psi}\eta} \quad . \tag{4.4}$$

Then, (4.2) can be written as

$$Z[\eta] = \int [dU] \, Z_U[\eta] \, e^{-S^{\mathrm{g}}_{\mathrm{W}}[U]} \quad . \tag{4.5}$$

Note that the exponential contains only the gauge action $S^{\mathrm{g}}_{\mathrm{W}}$. To extract Greens functions of the quark fields, we derive with respect to the components of η. For example, the two point function is

$$G^{fg}_{XY} = \frac{1}{Z[0]} \left[\frac{\partial}{\partial \bar{\eta}^f_X} \frac{\partial}{\partial \eta^g_Y} Z[\eta] \right]_{\eta=0} = \frac{1}{Z[0]} \int [dU] \, e^{-S^{\mathrm{g}}_{\mathrm{W}}[U]} \left[\frac{\partial}{\partial \bar{\eta}^f_X} \frac{\partial}{\partial \eta^g_Y} Z_U[\eta] \right]_{\eta=0} \quad . \tag{4.6}$$

To obtain higher Greens functions, we have to take more derivatives. However, for a fixed *gauge background* U, the functional $Z_U[\eta]$ can be calculated by means of the Gaussian integration formula (3.49) for Grassmann numbers.

$$Z_U[\eta] = \det(M_U)\, e^{\bar{\eta} M_U^{-1} \eta} \quad . \tag{4.7}$$

Furthermore, we can apply Wick's theorem (3.34) to express all n-th order partial derivatives of $Z_U[\eta]$ (at $\eta = 0$) in terms of it's second derivatives. As we discussed in *section 3.2*, the result is a sum over all pairings or *contractions* of the n partial derivative operators, each term of the sum being a product of second derivatives evaluated at $\eta = 0$. However, from (4.7), we see immediately that

$$\frac{1}{Z_U[0]} \left[\frac{\partial}{\partial \bar{\eta}_X^f} \frac{\partial}{\partial \eta_Y^g} Z_U[\eta] \right]_{\eta=0} = (M_U^{-1})_{XY}^{fg} \quad . \tag{4.8}$$

Therefore, all Greens functions of quark fields can be written as sums of path integrals of the following form:

$$\left\langle \Gamma_{X_1 Y_1 \cdots X_n Y_n}^{f_1 g_1 \cdots f_n g_n} \right\rangle = \frac{1}{Z} \int [dU]\, \Gamma_{X_1 Y_1 \cdots X_n Y_n}^{f_1 g_1 \cdots f_n g_n}[U] \;\det(M_U) e^{-S_{\mathrm{W}}^{\mathrm{g}}[U]} \quad , \tag{4.9a}$$

with

$$Z = \int [dU] \;\det(M_U)\, e^{-S_{\mathrm{W}}^{\mathrm{g}}[U]} \quad , \tag{4.9b}$$

and

$$\Gamma_{X_1 Y_1 \cdots X_n Y_n}^{f_1 g_1 \cdots f_n g_n}[U] = (M_U^{-1})_{X_1 Y_1}^{f_1 g_1} \cdots (M_U^{-1})_{X_n Y_n}^{f_n g_n} \quad . \tag{4.9c}$$

The possible contractions are often represented diagrammatically, in analogy to the Feynman diagrams of perturbation theory. Each diagram corresponds to a function like (4.9c). We therefore use the word *diagram* as a synonym for functions of the from (4.9c). For any such function Γ, we define the the angular bracket $\langle \Gamma \rangle$ in accordance with (4.9a) and call it the *expectation value* of the diagram Γ.

If we consider only two flavours with a degenerate mass m, the flavour structure of the Wilson matrix becomes very simple. We can write

$$M_U^{fg} = Q_U\, \delta^{fg} \quad , \tag{4.10}$$

where Q_U is a matrix in colour, spinor and position space, but not in flavour space. The matrix Q_U has an important property, which it inherits from M_U. We can obtain it's hermitian conjugate, by simply multiplying with γ_5 matrices.

$$Q_U^\dagger = \gamma_5 Q_U \gamma_5 \quad . \tag{4.11}$$

Note that the hermitian conjugation applies to all indices, including the position indices. The same equation holds for M_U, and it follows immediately from the explicit form of the Wilson matrix given through (3.78). By taking the determinant on both sides of (4.11), we see that

$$(\det Q_U)^* = \det Q_U^\dagger = \det Q_U \quad . \tag{4.12}$$

Consequently, the determinant $\det Q_U$ is real. Thus, for two degenerate flavours, the expectation values, through which all quark Greens functions can be expressed, are even simpler. Using $\det M_U = (\det Q_U)^2 = \det(Q_U Q_U^\dagger)$, we can write them as

$$\langle \Gamma_{X_1Y_1\cdots X_nY_n} \rangle = \frac{1}{Z} \int [dU]\, \Gamma_{X_1Y_1\cdots X_nY_n}[U]\ \det(Q_U Q_U^\dagger) e^{-S_\mathrm{W}^\mathrm{g}[U]} \quad , \tag{4.13a}$$

with

$$Z = \int [dU]\ \det(Q_U Q_U^\dagger)\, e^{-S_\mathrm{W}^\mathrm{g}[U]} \quad , \tag{4.13b}$$

and

$$\Gamma_{X_1Y_1\cdots X_nY_n}[U] = (Q_U^{-1})_{X_1Y_1} \cdots (Q_U^{-1})_{X_nY_n} \quad . \tag{4.13c}$$

In principle, the expectation values $\langle \Gamma \rangle$ can be calculated with a numerical integration technique called *Monte Carlo integration*, which will be discussed in the next section. But even without knowing the technical details of this integration method, we can anticipate, that the evaluation of the *quark determinant* $\det Q_U$ will cause problems. In recent computations, the dimension of the quark field vector ψ (including the position indices) is of order 10^7. Therefore, the quark determinant is a sum of $10^7!$ terms, each term being a product of 10^7 numbers. A good deal of optimisation is possible due to the fact that Q_U is *sparse*, i.e. contains many zeros, but the explicit calculation of $\det Q_U$ remains very time consuming. In the past, this problem was usually dealt with, by assuming that the quark determinant effectively just yields an irrelevant overall factor. This approximation is equivalent to ignoring all fermion loops in a perturbative QCD calculation, and is known as the *quenched approximation*.

In the calculation I present in *chapter 5*, the quark determinant *is* taken into account. In this case, one speaks of an *unquenched* of *full QCD* calculation. The numerical effort, that is required to include the quark determinant in the calculation, can be greatly reduced by writing it as a path integral over a set of auxiliary *bosonic* fields $\phi_{i\alpha}(x)$. These fields are also called *pseudo-fermion fields* and carry colour, spinor and position indices, but no flavour indices. Using the formula (3.48) for complex Gauss integrals, we can write

$$\begin{aligned} \det(Q_U Q_U^\dagger) &\propto \int [d\phi]\ \exp\big(- \phi^\dagger [Q_U Q_U^\dagger]^{-1} \phi \big) \\ &= \int [d\phi]\ \exp\big(- (Q_U^{-1}\phi)^\dagger (Q_U^{-1}\phi) \big) \quad , \end{aligned} \tag{4.14}$$

where products like $\phi_1^\dagger\phi_2$ imply the contraction of colour, spinor and position indices. If we define the *effective gauge action* $S^{\mathrm{g}}_{\mathrm{eff}}$ as

$$S^{\mathrm{g}}_{\mathrm{eff}}[U,\phi] = S^{\mathrm{g}}_{\mathrm{W}}[U] + (Q_U^{-1}\phi)^\dagger(Q_U^{-1}\phi) \quad , \tag{4.15}$$

we can write the diagrams (4.13) as

$$\langle\Gamma_{X_1Y_1\cdots X_nY_n}\rangle = \frac{1}{Z}\int[dU]\int[d\phi]\,\Gamma_{X_1Y_1\cdots X_nY_n}[U]\,e^{-S^{\mathrm{g}}_{\mathrm{eff}}[U,\phi]} \quad . \tag{4.16a}$$

with

$$Z = \int[dU]\int[d\phi]\,e^{-S^{\mathrm{g}}_{\mathrm{eff}}[U,\phi]} \quad , \tag{4.16b}$$

and $\Gamma_{X_1Y_1\cdots X_nY_n}[U]$ as in (4.13c). From (4.15), we see immediately, that the effective gauge action $S^{\mathrm{g}}_{\mathrm{eff}}$ is real and positive. This guarantees, that the path integral (4.16) converges, and it is the reason why we restrict our considerations to two *degenerate* flavours. For non-degenerate flavours, the positivity of the effective gauge action, and thus the convergence of the path integral, would no longer be guaranteed.

Let's summarise this. In the path integral expression (4.16), the quark determinant has disappeared. Instead, we have picked up a set of pseudo-fermion fields ϕ, which further increase the dimension of the integral. Furthermore, the inverse quark matrix Q_U^{-1} appears in the action. Still, from the numerical point of view, it is much more efficient to calculate the path integral (4.16), rather than evaluating the quark determinant explicitly in the path integral (4.13). The main reason for this is, that, as we will see in the next section, Monte Carlo integration techniques can be applied very efficiently to high dimensional integrals of the form (4.16). Furthermore, there are efficient algorithms to invert sparse matrices like Q_U. Note that we do not need the whole matrix Q_U^{-1}, but only the vector $Q_U^{-1}\phi$ and some other components of Q_U^{-1}, which appear explicitly in the path integral (4.16). It is therefore sufficient to solve a few linear equations of the form $Q_U\chi = \phi$, where ϕ and the gauge configuration U are given. Solutions of such equations can be calculated much faster than the whole inverse quark matrix Q_U^{-1}, especially, if the matrix Q_U is sparse. The step of solving the equation $Q_U\chi = \phi$ for a particular choice of ϕ and U is called a *partial inversion*, while finding the whole matrix Q_U^{-1} is called a *full inversion*. The partial inversions for the calculation in *chapter 5* were done with the *stabilised biconjugate gradient* method. A description of this and other inversion algorithms can be found in [30].

4.2 Monte Carlo Integration

In this section, we will discuss the basic concepts of the Monte Carlo integration technique, with emphasis on their application to lattice path integrals. For the sake of notational simplicity, we consider a general set of lattice field variables $\mathbf{\Phi}$, with components Φ_X. As in *section 4.1*, the multi-indices X, Y, Z embrace field component and position indices. All our considerations are directly applicable to path integrals of the form (4.16). Note however, that the possible values for the individual gauge links $U(x, x+\mu)$ are elements of the $SU(3)$ group. Therefore, integrals over and statistical distributions of link variables are defined with respect to the Haar measure (see [29]), which is the natural measure on compact group manifolds. For the pseudo-fermion field components ϕ_X, the space of possible values is simply the complex plane with it's normal measure.

Let $\mathcal{S}$ be the (finite-dimensional) space of lattice field configurations $\mathbf{\Phi}$. Let F be a sufficiently smooth, real valued function on $\mathcal{S}$. We call F an *observable*. Furthermore, let S be a real, positive *action* on $\mathcal{S}$. In analogy to (4.16), we define the *expectation value* of the observable F as

$$\langle F \rangle = \frac{1}{Z} \int [d\mathbf{\Phi}]\, F[\mathbf{\Phi}]\, e^{-S[\mathbf{\Phi}]} \quad , \tag{4.17a}$$

with

$$Z = \int [d\mathbf{\Phi}]\, e^{-S[\mathbf{\Phi}]} \quad . \tag{4.17b}$$

In the previous section, we saw that the computation of lattice Greens functions boils down to calculating expectation values of the form (4.17) for properly chosen observables F. For example, to calculate $\langle \Gamma \rangle$ from (4.16), we would choose $F = \Gamma$ and $S[\mathbf{\Phi}] \equiv S^{\mathrm{g}}_{\mathrm{eff}}[U]$.

To solve the integrals in (4.17) numerically, conventional methods would be very inefficient. Because of the factor $\exp(-S[\mathbf{\Phi}])$, only a small area of the space $\mathcal{S}$ of field configurations will contribute significantly to the overall value of the integral. More precisely, only that area will contribute, where $S[\mathbf{\Phi}]$ is close to it's minimum. Anywhere else, the integrand is strongly suppressed by the exponential factor. If we tried to approximate the integral by taking sample values at field configurations, which are distributed equally in $\mathcal{S}$, we would get zero contributions from most of them. The idea of Monte Carlo integration is, to choose the sample configurations randomly, and absorb the factor $\exp(-S[\mathbf{\Phi}])$ into their statistical distribution. This way, almost all samples yield significant contributions, and we don't waste time by calculating zeros.

Therefore, the central task in a Monte Carlo integration is to generate a set or *ensemble* $\mathcal{E}$ of n field configurations $\mathbf{\Phi}^{(1)}, \ldots, \mathbf{\Phi}^{(n)}$, which approximates a random distribution with a statistical density or *weight* given by

$$w_{\mathrm{c}}[\mathbf{\Phi}] = \frac{1}{Z}\, e^{-S[\mathbf{\Phi}]} \quad . \tag{4.18}$$

The index 'c' stands for *canonical* and refers to an analogy of (4.17) to the canonical partition function in statistical mechanics. The factor Z is the one from (4.17b). It assures that w_c is normalised like a probability density, i.e.

$$\int [d\mathbf{\Phi}]\, w_c[\mathbf{\Phi}] = 1 \quad . \tag{4.19}$$

Once we have generated an ensemble $\mathcal{E}$ of configurations $\mathbf{\Phi}^{(k)}$, $k = 1 \ldots n$, which is distributed according to the density function w_c, we can approximate the expectation value (4.17) by

$$\langle F \rangle \approx \frac{1}{n} \sum_{k=1}^{n} F[\mathbf{\Phi}^{(k)}] \quad . \tag{4.20}$$

From a more mathematical point of view, the field configurations $\mathbf{\Phi}^{(k)}$ are *random variables*, which are distributed according to w_c. Consequently, the numbers $F[\mathbf{\Phi}^{(k)}]$, $i = 1 \ldots n$ and their average $\langle F \rangle$ are random variables, too. In the limit of large n, the distribution of $\langle F \rangle$ becomes strongly peaked around a single value, namely, the value of the integral (4.17). However, for a finite n, $\langle F \rangle$ has still a non-vanishing standard deviation, which represents the uncertainty of the approximation (4.20). This uncertainty due to finite statistics is the main source of the *theoretical errors* of lattice simulations.

There is another pitfall, if we want to use the Monte Carlo integration technique to calculate the diagrams Γ from (4.16). The integral (4.17) is well defined for any smooth function F, but the diagrams Γ from (4.13c) are not smooth. They have “poles” at gauge configurations U, for which the quark matrix Q_U is singular. The path integral (4.13a) is still well defined, because the factor $\det(Q_U)$ cancels these poles and makes the integrand regular. Therefore, a finite ensemble of gauge configurations U, that is distributed according to the effective gauge action (4.15), will not contain any configurations, for which Q_U is singular. However, it may still have configurations, for which the $\det Q_U$ is very small. In numerical computations, the components of the inverse quark matrix are usually calculated with iterative inversion algorithms. If the quark matrix is “almost” singular, i.e. $\det(Q_U) \ll 1$, these algorithms will not converge fast enough or even not converge at all. It turns out that in ensembles distributed according to the effective gauge action (4.15), such *exceptional configurations* occur more frequently, if we decrease the quark mass m and the value of β. Therefore, most lattice simulations have to be done in an *unphysical region*, where the quarks are too heavy and β too big. The results thus obtained then have to be extrapolated to the physical region.

4.3 Simulation Algorithms

In this section, we discuss different numerical algorithms, that can be used to generate finite ensembles of field configurations, that approximate a random distribution of the form (4.18). Generally, a finite set $\mathcal{E}$ of field configurations $\mathbf{\Phi}$ is created by a (pseudo) random process, which chooses randomly for a given configuration $\mathbf{\Phi}^{(k)}$ the next configuration $\mathbf{\Phi}^{(k+1)}$, according to a *transition probability distribution* $P[\mathbf{\Phi}^{(k+1)}, \mathbf{\Phi}^{(k)}]$. This step is called an *updating step*. If we consider P as a function of only one of it's arguments, while keeping the other one fixed, it is just another weight function. Therefore, it should satisfy the following normalisation condition:

$$\int [d\mathbf{\Phi}]\, P[\mathbf{\Phi}, \mathbf{\Phi}'] = \int [d\mathbf{\Phi}']\, P[\mathbf{\Phi}, \mathbf{\Phi}'] = 1 \quad . \tag{4.21}$$

To make sure that any field configuration can, in principle, be reached from any other configuration, we further require, that for any pair of field configurations $\mathbf{\Phi}$ and $\mathbf{\Phi}'$

$$P[\mathbf{\Phi}, \mathbf{\Phi}'] > 0 \quad . \tag{4.22}$$

This condition is called *strong ergodicity*. An updating step, which is described by a transition probability distribution P satisfying (4.21) and (4.22), is called a *Markow update* or *Markow process*. A sequence of field configurations, in which each configuration is generated from the previous one by a Markow update, is called a *Markow chain*.

Any transition probability distribution P induces an operator on the space of weight functions $w[\mathbf{\Phi}]$ by

$$(Pw)[\mathbf{\Phi}] = \int [d\mathbf{\Phi}']\, P[\mathbf{\Phi}, \mathbf{\Phi}']w[\mathbf{\Phi}'] \quad . \tag{4.23}$$

The practical meaning of this operator is the following: Assume we have a finite ensemble $\mathcal{E}$ which is distributed randomly according to a density function w. Now, we generate a new ensemble by performing an updating step for each configuration in the ensemble. In other words, we choose randomly for each configuration $\mathbf{\Phi}^{(k)}$ a new configuration $\mathbf{\Psi}^{(k)}$ according to the probability density $P[\mathbf{\Psi}^{(k)}, \mathbf{\Phi}^{(k)}]$. Then, our new ensemble $\mathcal{E}' = \{\mathbf{\Psi}^{(k)}\}$ is distributed according to the density function Pw.

Now assume that we have generated an ensemble $\mathcal{E} = \{\mathbf{\Phi}^{(k)},\ k = 1 \ldots N\}$ of field configurations by subsequent updating steps, starting from some arbitrarily chosen configuration $\mathbf{\Phi}^{(0)}$. We define the sub-ensembles $\mathcal{E}_n^r \subset \mathcal{E}$ as $\mathcal{E}_n^r = \{\mathbf{\Phi}^{(k)},\ k = r \ldots n + r\}$ with $n + r \leq N$. If the sub-ensemble $\mathcal{E}_n^0$ is distributed according to a weight function w, then any other sub-ensemble $\mathcal{E}_n^r$ is distributed according to $P^r w$. To get an ensemble distributed according to the canonical density function w_c, we only have to choose the transition probability distribution P in such a way that

$$\lim_{r\to\infty} P^r w = w_\mathrm{c} \tag{4.24}$$

for a sensible class of initial density functions w. Then, for a sufficiently large r, the sub-ensemble $\mathcal{E}_n^r$ will be distributed according to w_c. In other words, if we generate $\mathcal{E}$ with a transition probability distribution that satisfies (4.24), we obtain a canonically distributed ensemble simply by chopping off some configurations at the beginning.

For a given transition probability distribution P, the condition (4.24) is generally quite hard to check. There is, however, a stronger condition, which is sufficient for

(4.24) and can be verified much more easily. First, note that (4.24) implies, that w_c is a fixed point of the operator P, i.e.

$$\int [d\mathbf{\Phi}'] \, P[\mathbf{\Phi}, \mathbf{\Phi}'] w_c[\mathbf{\Phi}'] = w_c[\mathbf{\Phi}] \quad . \tag{4.25}$$

Furthermore, it can be shown [31] for Markow processes, that the fixed point w_c is unique and that (4.24) follows from (4.25). On the other hand, a sufficient condition for (4.25) is *detailed balance*,

$$P[\mathbf{\Phi}, \mathbf{\Phi}'] w_c[\mathbf{\Phi}'] = P[\mathbf{\Phi}', \mathbf{\Phi}] w_c[\mathbf{\Phi}] \quad , \tag{4.26}$$

as can be seen by integrating over $\mathbf{\Phi}'$ on both sides of (4.26) and using the normalisation condition (4.21) on the right hand side. Thus, for a Markow process, the condition (4.26) of detailed balance is sufficient to assure (4.24), and usually it can be verified much more easily.

We see that our task of generating a canonically distributed ensemble boils down to implementing a numerical algorithm simulating a Markow process that satisfies detailed balance (4.26). The two most important classes of such algorithms are the *Metropolis* and the *Langevin* algorithms. Here, we will briefly discuss the basic concepts of both classes. The algorithm, that was actually used to generate the gauge configurations for the calculation in *chapter 5*, is a *Hybrid Monte Carlo algorithm*. It is a combination of both, the ideas of Metropolis *and* Langevin algorithms. Technical details of the simulation, in which the gauge configurations for *chapter 5* were generated, can be found in [32].

Let's start with the Metropolis algorithm. Here, the basic idea is to link an arbitrary Markow process, which we call the *trial process* and which does not satisfy detailed balance, with a subsequent *accept-reject step*. Assume that we have a trial process, which chooses randomly for a given configuration $\mathbf{\Phi}$ a new configuration $\mathbf{\Phi}'$, according to a probability distribution $P^{\text{trial}}[\mathbf{\Phi}', \mathbf{\Phi}]$. In a second *selection process*, we make a random choice, whether we accept or reject the new configuration $\mathbf{\Phi}'$. If the configuration is rejected, we invoke the trial process again to generate a new trial configuration, which is then passed on to the selection process again. This procedure is repeated, until some configuration $\mathbf{\Phi}''$ is accepted by the selection process. Then, the update is declared as finished, and $\mathbf{\Phi}''$ is added to the Markow chain. It can be shown, that the overall process satisfies detailed balance, if the acceptance probability is chosen in the following way:

$$p^{\text{accept}}[\mathbf{\Phi}', \mathbf{\Phi}] = \min\left\{1, \frac{P^{\text{trial}}[\mathbf{\Phi}, \mathbf{\Phi}'] w_c[\mathbf{\Phi}']}{P^{\text{trial}}[\mathbf{\Phi}', \mathbf{\Phi}] w_c[\mathbf{\Phi}]}\right\} \quad . \tag{4.27}$$

Note that, for any given pair of configurations $\mathbf{\Phi}$ and $\mathbf{\Phi}'$, the quantity $p^{\text{accept}}[\mathbf{\Phi}', \mathbf{\Phi}]$ is an ordinary probability, i.e. a number between 0 and 1. On the other hand, P^{trial} is a probability *distribution* or *density*. To obtain an ordinary probability from P^{trial}, one of it's arguments has to be integrated out.

The implementation of the selection process on a computer is pretty straightforward. All we have to do is compare the quotient in (4.27) with a random number r, that is equally distributed in the interval $[0, 1]$. Such equally distributed random numbers can be picked from a list or generated on demand by one of the many well known pseudo-random number generators. For further information on algorithms, that generate equally distributed random numbers, see for example [30]. Note however, that in the selection process for a transition $\mathbf{\Phi} \to \mathbf{\Phi}'$, we have to evaluate the density function w_c at the new trial configuration $\mathbf{\Phi}'$. Thus, we have to calculate $S[\mathbf{\Phi}']$, and this can be a very time consuming step. For example, to calculate the effective action (4.15) for a new configuration of the gauge links U and the pseudo-fermion fields ϕ, we have to solve the equation $Q_U\chi = \phi$ for χ. Thus, if the evaluation of $w_\mathrm{c}[\mathbf{\Phi}']$ for a new trial configuration $\mathbf{\Phi}'$ takes so much time, it is even more annoying, if this configuration is then rejected. The efficiency of a given implementation of the Metropolis algorithm depends greatly on it's *acceptance rate*, i.e. the percentage of trial configurations, which are accepted in the selection process.

To improve the acceptance rate, one has to choose the trial process cleverly. For example, we could generate a new trial configuration $\mathbf{\Phi}'$, by simply choosing equally distributed random numbers for all it's components Φ'_X. This corresponds to generating configurations, which are distributed equally in the configuration space $\mathcal{S}$. The acceptance rate for this trial process would, however, be extremely low. Remember that we want to generate a distribution of configurations, whose density is strongly peaked around the minimum of the action S. For an equally distributed random configuration $\mathbf{\Phi}'$, the factor $\exp(-S[\mathbf{\Phi}'])$ will usually be much smaller than one, and the configuration is hardly ever accepted. Assume that we already have a configuration $\mathbf{\Phi}$, where $\exp(-S[\mathbf{\Phi}])$ is of order 1. To generate from $\mathbf{\Phi}$ a configuration $\mathbf{\Phi}'$, for which the exponential factor is also of order one, we might try to change $\mathbf{\Phi}$ just a little bit. For example, we could just change the components of $\mathbf{\Phi}$ at an individual lattice site x, or even just a single component Φ_X. This is also called a *local update*. However, if we do this, our trial process does no longer satisfy the condition (4.22) of strong ergodicity. We can no longer reach any configuration from $\mathbf{\Phi}$ in one step. For the ensemble, this means that subsequent configurations will always lie very close together in configuration space, and we may not reach distant areas, where the action $S[\mathbf{\Phi}]$ is also small. One way to re-establish strong ergodicity is to define the actual update step as a whole series of local updates. We can subsequently perform local updates at every lattice site, but insert an accept-reject step after each *local* update. This is also called a *sweep*.

As a sketch of the basic ideas and variations of the Metropolis algorithm, the above discussion will have to suffice. Detailed information can be found in the related literature, for example in chapter 7 of [33]. We will now move on to the second class of update processes, the *Langevin algorithms*. Here, the basic idea is to introduce *classical* equations of motion for the lattice fields. New field configurations are then generated from a given one by evolving the system along it's classical trajectory for some finite time step τ. It should be stressed that the classical equations of motion are in no way related to the physical dynamics of the system, and the time τ is a *fictional*, i.e. non-physical time. It's just a trick to generate new field configurations, that happens to look like physics, too. Remember, that our task is to generate from a given field configuration $\mathbf{\Phi}$ a new configuration $\mathbf{\Phi}'$, according to a probability distribution $P[\mathbf{\Phi}', \mathbf{\Phi}]$, that satisfies detailed balance (4.26). In Langevin algorithms, this is achieved in the following way: We start by introducing conjugate momenta Π_X for every lattice field component Φ_X. Then, each of these momenta is chosen randomly according to a Gaussian distribution with a standard deviation of 1. Thus, the state of the system is characterised by the point $(\mathbf{\Pi}, \mathbf{\Phi})$ in the classical phase space. Now, we let the system evolve according to the canonical equations of motion

$$\frac{d\Phi_X}{d\tau} = \frac{\partial H}{\partial \Pi_X} \qquad , \qquad \frac{d\Pi_X}{d\tau} = -\frac{\partial H}{\partial \Phi_X} \quad , \tag{4.28}$$

determined by the classical Hamiltonian

$$H[\mathbf{\Pi}, \mathbf{\Phi}] = \frac{1}{2} \sum_X \Pi_X^2 + S[\mathbf{\Phi}] \quad . \tag{4.29}$$

Let $(\mathbf{\Pi}', \mathbf{\Phi}')$ be the state we obtain after a finite 'time' τ. Obviously, the new field configuration $\mathbf{\Phi}'$ depends on the initial field configuration $\mathbf{\Phi}$ and the momenta $\mathbf{\Pi}$, which were chosen randomly. Therefore, $\mathbf{\Phi}'$ is a random variable, too, which is described by a probability distribution $P[\mathbf{\Phi}, \mathbf{\Phi}']$. It can be shown[1], that this distribution satisfies detailed balance.

The technical problems in the numerical implementation of Langevin algorithms are obvious: We have to solve the canonical equations of motion (4.28) numerically. To do this, the simplest approach is to divide the time interval $[0, \tau]$ into small sub-intervals of size $\Delta\tau$ and use linear approximations for the time dependence of $\mathbf{\Pi}$ and $\mathbf{\Phi}$ in each of the sub-intervals. A very popular application of this strategy is the *leap frog* algorithm, in which some accuracy is gained by evaluating the fields and momenta at different times, offset from each other by $\Delta\tau/2$. In any case, the *step size* $\Delta\tau$ has to be small, if we want our solution of the equations of motion (4.28) to be precise and the condition of detailed balance to hold. In fact, it is shown in [33], that for numerical solutions of the equations of motion, the condition of detailed balance holds only up to terms proportional to $\Delta\tau$. While the step size $\Delta\tau$ has to be small, we need, at the same time, a large value for τ. If we make τ too small, subsequent field configurations will again be very similar, and we might not reach all important areas of the configuration space with our finite ensemble. A large τ and a small step size mean that we end up with a large number of iteration steps. But, as we can see from (4.28) and (4.29), we have to calculate the derivatives $\partial S/\partial\Phi_X$ in each iteration step. Like the evaluation of the action S itself, this is very time consuming. In practice, it is therefore very difficult to implement Langevin algorithms, that satisfy our requirements on speed and accuracy.

[1] see chapter 7 of [33]

A very elegant way to circumvent the accuracy problems of Langevin algorithms is to use them as a trial processes for Metropolis algorithms. This is the idea behind the so called *hybrid Monte Carlo algorithms*. For a given configuration $\mathbf{\Phi}$, we generate Gaussian distributed momenta $\mathbf{\Pi}$. Next, we use a Langevin algorithm to generate a new configuration $\mathbf{\Phi'}$ and new momenta $\mathbf{\Pi}'$, by solving the equations of motion numerically with a step size $\Delta\tau$. Then, we invoke an accept-reject step with an acceptance probability

$$p_{\mathrm{HMC}}^{\mathrm{accept}} = \min\{1, e^{-(H[\mathbf{\Pi}',\mathbf{\Phi}']-H[\mathbf{\Pi},\mathbf{\Phi}])}\} \quad . \tag{4.30}$$

If the new configuration is rejected, we keep the old one, generate new momenta and start over again. If it is accepted, we add it to our ensemble. It can be shown, that the probability distribution of the configurations thus generated satisfies detailed balance exactly, independent of our choice for the numerical step size $\Delta\tau$. The proof can be found in [33]. A poor approximation of the classical equations of motion will only result in a low acceptance rate. This is the great advantage of hybrid Monte Carlo algorithms: Errors in the numerical solution of the equations of motion do not lead to accuracy problems. Instead, the step size $\Delta\tau$ can be used to maximise the efficiency of the overall process. Maximal performance is usually reached at acceptance rates of ca. 80%.

4.4 Curve Fitting and Error Estimates

In *section 2.3* we saw how to extract particle masses and matrix elements from euclidean correlation functions $C(t)$. With the lattice formulation of QCD and the Monte Carlo integration method, we can calculate $C(t)$ numerically, at least for integer values of t. Note that the correlation functions from *section 2.3* are just special cases of Greens functions, where the spacial arguments are fixed or summed over. In *section 4.1*, we saw that Greens functions can be expressed in terms of the expectation values from (4.16). These expectation values are finite dimensional integrals and can be calculated numerically with the Monte Carlo method. Assume we have generated an ensemble $\mathcal{E} = \{U_1, \ldots, U_N\}$ of gauge configurations distributed according to the effective gauge action (4.15). (The corresponding configurations of the pseudo-fermion fields are no longer needed at this stage.) Then, the expectation values $\langle\Gamma\rangle$ are approximated, in accordance with (4.17), by an average of the form

$$\langle \Gamma_{X_1 Y_1 \cdots X_n Y_n} \rangle \approx \frac{1}{N} \sum_{k=1}^{N} \Gamma_{X_1 Y_1 \cdots X_n Y_n}[U] \quad . \tag{4.31}$$

By changing the order of sums, we can also approximate the correlation function $C(t)$ by an average over gauge configurations:

$$C(t) \approx \bar{C}(t) = \frac{1}{N} \sum_{k=1}^{N} C_k(t) \quad , \tag{4.32}$$

where each term $C_k(t)$ is a combination of components of different diagrams Γ. The uncertainty $\sigma(t)$ of the approximation can be estimated in the usual way:

$$\sigma^2(t) = \frac{1}{N(N-1)} \sum_{k=1}^{N} \left(C_k(t) - \bar{C}(t) \right)^2 \quad . \tag{4.33}$$

The numerical lattice simulation gives us the values of $\bar{C}(t)$ only for integer values of t between 0 and T. In *section 2.3*, we found analytic expressions for correlation functions. The free parameters of these expressions are related to physical quantities like particle masses or form factors. Thus, to extract physical quantities from our numerical data, we have to compare it to a "theoretical" curve or *fit function*. The parameters of the fit function are then determined by the requirement, that the discrepancy between the function values and the "measured" data is minimised. So first, we have to define a quantity χ^2, which measures the discrepancy between fit function and data. Remember that our data points $\bar{C}(t)$ have statistical uncertainties $\sigma(t)$, which our measure for the discrepancy between curve and data should take into account.[2] Let $f(t;\mathbf{a})$ be a fit function with N_p adjustable parameters $a_1, \ldots a_{N_p}$. Then, we can measure the discrepancy between curve and data by adding up the squared the differences $(\bar{C}(t) - f(t,\mathbf{a}))^2$ between function values and data points. The errors are accounted for by weighting each difference with a factor of $1/\sigma$. This sum is also called the *weighted sum of square residuals* (WSSR). We define

$$\chi^2(\mathbf{a}) = \sum_{i=1}^{N_t} \frac{(\bar{C}(t_i) - f(t_i,\mathbf{a}))^2}{\sigma^2(t_i)} \quad , \tag{4.34}$$

where the $t_i,\ i = 1 \ldots N_t$ denote those time values, for which numerical results for $\bar{C}$ and σ are available. Optimal agreement between data and curve is considered to be reached for those parameter values $\mathbf{a}$, which minimise χ^2.

In practice, the minimum of χ^2 can be found by iteration, starting from some initial set of parameters $\mathbf{a}^{(0)}$. If we are far from the minimum, the best strategy is usually to change, in each iteration step, the parameters $a_p^{(k)}$ by amounts

$$\delta a_p^{(k)} = a_p^{(k+1)} - a_p^{(k)} \quad , \tag{4.35}$$

which are proportional to the partial derivatives of χ^2. This strategy is known as the *steepest descent method*. Close to the minimum, it is more efficient to use a quadratic approximation for χ^2. The minimum of this approximation can be found essentially by inverting the Hessian (second derivative) matrix of χ^2. It should lie close to the real minimum and is therefore taken as the starting point of the next iteration step. This method is known as the *inverse Hessian method*. An algorithm, which combines the

[2] It is also possible to define a χ^2 function, that accounts for the correlations between different data points. Further information about such *correlated fits* can be found in [34].

virtues of both methods, is the *Marquardt-Levenberg algorithm*. It estimates, how close we are to the minimum of χ^2, and interpolates smoothly between the steepest descent and the inverse Hessian method. This algorithm was used for the fits in *chapter 5*, and I will now describe it in detail.

We start with some definitions. Let

$$\Delta(t;\mathbf{a}) = \bar{C}(t) - f(t,\mathbf{a}) \quad , \tag{4.36}$$

$$\beta_p(\mathbf{a}) = -\frac{1}{2}\frac{\partial\chi^2}{\partial a_p}(\mathbf{a}) = \sum_{i=1}^{N_t} \frac{\Delta(t_i;\mathbf{a})}{\sigma^2(t_i)}\frac{\partial f}{\partial a_p}(t_i;\mathbf{a}) \quad , \tag{4.37}$$

$$\alpha_{pq}(\mathbf{a}) = \frac{1}{2}\frac{\partial^2\chi^2}{\partial a_p \partial a_q} = \sum_{i=1}^{N_t}\left(\frac{1}{\sigma^2(t_i)}\frac{\partial f}{\partial a_p}(t_i;\mathbf{a})\frac{\partial f}{\partial a_q}(t_i;\mathbf{a}) - \frac{\Delta(t_i;\mathbf{a})}{\sigma^2(t_i)}\frac{\partial^2 f}{\partial a_p \partial a_q}(t_i;\mathbf{a})\right) \quad . \tag{4.38}$$

Then, the quadratic approximation of χ^2 around a given set of parameters $\mathbf{a}^{(k)}$ can then be written as

$$\chi^2(\mathbf{a}) \approx \chi^2(\mathbf{a}^{(k)}) - 2\sum_p \beta_p^{(k)}(a_p - a_p^{(k)}) + \sum_{p,q}(a_p - a_p^{(k)})\alpha_{pq}^{(k)}(a_q - a_q^{(k)}) \quad , \tag{4.39}$$

with $\beta_p^{(k)} = \beta_p(a^{(k)})$ and $\alpha_{pq}^{(k)} = \alpha_{pq}(a^{(k)})$. In the inverse Hessian method, we would choose the next parameter set $\mathbf{a}^{(k+1)}$ as the minimum of the approximation (4.39). Thus, $\delta\mathbf{a}^{(k)}$ would have to satisfy

$$\sum_q \alpha_{pq}^{(k)}\delta a_q^{(k)} = \beta_p^{(k)} \quad . \tag{4.40}$$

In the steepest descent method, we would simply choose $\delta a_p^{(k)} \propto \beta_p^{(k)}$. Making a particularly natural choice for the proportionality factors, we define

$$\delta a_p^{(k)} = \frac{1}{\lambda^{(k)}\alpha_{pp}^{(k)}}\beta_p^{(k)} \quad , \tag{4.41}$$

where $\lambda^{(k)}$ is a dimensionless scale factor. The factor $\alpha_{pp}^{(k)}$ is included for dimensional reasons. To interpolate between (4.40) and (4.41), we define

$$\alpha'^{(k)}_{pq} = (1 + \lambda^{(k)}\delta_{pq})\alpha_{pq}^{(k)} \quad , \tag{4.42}$$

and choose $\delta\mathbf{a}^{(k)}$ as solution of the linear equation

$$\sum_q \alpha'^{(k)}_{pq}\delta a_q^{(k)} = \beta_p^{(k)} \quad . \tag{4.43}$$

For $\lambda = 0$, this is just the equation (4.40). For large λ, the matrix $\alpha'^{(k)}$ is dominated by it's diagonal entries, and we effectively get (4.41). Thus, by varying $\lambda^{(k)}$, we interpolate smoothly between the steepest descent and the inverse Hessian method. Now, for appropriate start values $\mathbf{a}^{(0)}$ and $\lambda^{(0)}$, the minimum of χ^2 can be found by the following recursion:

(i) Calculate $\chi^2(\mathbf{a}^{(k)})$ according to (4.34)

(ii) Calculate $\alpha'^{(k)}$ and $\boldsymbol{\beta}^{(k)}$ according to (4.42) and (4.37).

(iii) Determine $\delta\mathbf{a}^{(k)}$ by solving (4.43).

(iv) Calculate $\chi^2(\mathbf{a}^{(k)} + \delta\mathbf{a}^{(k)})$. If

$$\chi^2(\mathbf{a}^{(k)} + \delta\mathbf{a}^{(k)}) > \chi^2(\mathbf{a}^{(k)}) \quad ,$$

keep the old parameters and increase λ by some factor $r > 1$, i.e. let $\mathbf{a}^{(k+1)} = \mathbf{a}^{(k)}$ and $\lambda^{(k+1)} = r\lambda^{(k)}$. If

$$\chi^2(\mathbf{a}^{(k)} + \delta\mathbf{a}^{(k)}) \leq \chi^2(\mathbf{a}^{(k)}) \quad ,$$

let $\mathbf{a}^{(k+1)} = \mathbf{a}^{(k)} + \delta\mathbf{a}^{(k)}$ and $\lambda^{(k+1)} = \lambda^{(k)}/r$.

(v) Start again from step (i), with k replaced by $k + 1$.

A typical choice for r is 10. If the algorithm converges, the values of λ will approach zero. The convergence is not guaranteed in general, but depends on our choice for the initial parameters $\mathbf{a}^{(0)}$. In practice, the recursion is aborted, if λ falls below some sufficiently small limit λ^{min}. Note that it is not sufficient to observe the change in the values of χ^2. If λ gets very large, the value of χ^2 will stop changing significantly, just because the proportionality factor in (4.41) vanishes. This does, however, not mean that we are anywhere near the minimum.

Now let $\mathbf{a}$ be the set of parameters that minimises χ^2. The goodness of the fit can be measured by the *reduced chi square* value $\chi^2(\mathbf{a})/\nu$, where $\nu = N_t - N_p$ is the number of degrees of freedom of the fit. For a good fit, the reduced chi square value should be approximately 1.

If, for a given t, the $C_k(t)$ were *independent* random numbers, we could estimate the *errors* on the parameters a_p directly from the inverse Hessian $\alpha^{-1}(\mathbf{a})$. For a good fit, the parameter covariance matrix V is approximated by

$$V_{pq} = \text{cov}(a_p, a_q) \approx \alpha^{-1}_{pq}(\mathbf{a}) \quad . \tag{4.44}$$

The errors of the parameters are just the square roots of the diagonal entries.

$$\Delta a_p = \sqrt{V_{pp}} \quad . \tag{4.45}$$

In practice, the $C_k(t)$ can not be viewed as independent random numbers. Remember, that they are calculated from gauge configurations U_k, which were generated by a Markow process, where the probability distribution for the k-th configuration U_k depends on the previous configuration U_{k-1}. Thus, subsequent elements of the Markow chain are *correlated*, and the $C_k(t)$ inherit this feature. Generally, we assume that significant correlations exist only between sample values $C_k(t)$ and $C_\ell(t)$ with $|k-\ell| \leq \tau$ for some finite τ, which is called the *correlation length* of the sample. As a consequence of this correlation, our estimates (4.32) and (4.33) for $C(t)$ and $\sigma(t)$ will be *biased*, if the sample size n is not much larger than the correlation length τ. Assume that the first value $C_1(t)$ of our sample lies slightly above $C(t)$. If there is a positive correlation between subsequent sample values, it is more likely, that the next few sample values $C_2(t)$, $C_3(t)$, etc. lie above $C(t)$, too. Therefore, our estimate (4.32) for $C(t)$ will be too big and the estimate for (4.33) for $\sigma(t)$ too small. Consequently, there will also be a bias on our results for the parameters $\mathbf{a}$.

We can (partially) remove the bias on our estimates with a statistical tool called the *jackknife method*. The basic idea is to divide our sample of size N into n blocks of m data values. The averages over each block can be viewed as independent random numbers, if $m > \tau$. To remove the bias on our estimates, we subsequently remove individual blocks from our sample and observe the change in the estimates. Let $\mathbf{C}$ denote the complete sample, i.e. the whole set of values $C_k(t_i)$ with $k = 1 \dots N$ and $i = 1 \dots N_t$. The parameters that minimise χ^2 can be viewed as functions $\mathbf{a}(\mathbf{C})$. We define n sub-samples $\mathbf{C}_r,\ r = 1 \dots n$ by removing, for each time t_i, blocks of m data values from the sample.

$$\mathbf{C}_r = \{C_k(t_i) | i = 1 \dots N_t;\ k = 1 \dots m(r-1), mr+1 \dots N\} \quad , \tag{4.46}$$

with $m \cdot n = N$ and $r = 1 \dots n$. Let $\bar{\mathbf{a}}(\mathbf{C})$ be the average of the parameter values $\mathbf{a}$ estimated on the sub-samples $\mathbf{C}_r$, i.e.

$$\bar{\mathbf{a}}(\mathbf{C}) = \frac{1}{n} \sum_{r=1}^{n} \mathbf{a}(\mathbf{C}_r) \tag{4.47}$$

In practice, the parameter estimates $\mathbf{a}(\mathbf{C})$ and $\mathbf{a}(\mathbf{C}_r)$ have to be determined in separate fits. The *jackknife estimates* for the parameters $\mathbf{a}$ are defined as

$$\mathbf{a}^{\mathrm{jk}} = n\,\mathbf{a}(\mathbf{C}) - (n-1)\bar{\mathbf{a}}(\mathbf{C}) \quad . \tag{4.48}$$

The jackknife estimates for the errors Δa_p^{jk} of the parameters a_p are defined by

$$(\Delta a_p^{\mathrm{jk}})^2 = \frac{n-1}{n} \sum_{r=1}^{n} \big(a_p(\mathbf{C}_r) - \bar{\mathbf{a}}(\mathbf{C})\big)^2 \quad . \tag{4.49}$$

It can be shown (Quenouille, 1956) that the jackknife method removes a bias of order n^{-1}. We will use this method for the error estimates in *chapter 5*.

Chapter 5

Two Pion Propagators on the Lattice

After all the preparations, we are now ready for the calculation of the two pion propagators. While the analysis of two pion states with a total isospin of 2 is pretty straightforward, we will see that the isospin 0 states require the computation of *disconnected diagrams*, which are more problematic. With the naive methods we use for one particle states, the calculation of the disconnected diagrams would require a large number of partial quark matrix inversions and is impracticable with the current computing power. A possible workaround is the use of a different type of quark propagators called *wall propagators*. To test this method, we will use both, ordinary propagators and wall propagators, to simulate one pion states and two pion states with isospin 2. From the numerical results, we will extract the *two pion energy shift*, i.e. the difference between the energy of the two pion state and twice the energy of the one pion state.

In the first section, we introduce the composite operators that we use to create the states we are interested in. Furthermore, we define Greens functions, that describe their propagation. In *section 5.2* we define correlation functions, from which physical quantities like the energy of the two pion state can be extracted. We relate these correlation functions to the Greens functions from *section 5.1* and show how they can be calculated with different types of quark propagators. In *section 5.3*, the results of the numerical simulation are presented.

5.1 Meson Operators and Greens Functions

In our simulation, the quark fields come in two degenerate quark flavours: the 'up' fields $u_A(x)$ and the 'down' fields $d_A(x)$. The index A is a multi-index in colour and spinor space. Throughout this chapter, we will use capital letters A, B, C for such multi-indices. Furthermore, all considerations in this chapter are done in *euclidean* space. Thus, all gamma matrices, field operators and Greens functions are euclidean ones. We will suppress the superscript 'E' for all these objects. From the fields u and d, we have to construct local composite operators in such a way, that the lightest states these operators create from the vacuum are the meson states we are interested in. As we discussed in *section 2.3*, this is done by choosing the *symmetry properties* of the composite operators appropriately.

As we are interested in the two pion energy shift, we have to calculate the energies of one and two pion states on the lattice. Due to the problem of exceptional gauge configurations, that we addressed at the end of *section 4.2*, our calculations must be done in the "unphysical" region of large quark masses, i.e. for small values of the parameter κ defined in (3.77). If possible, we should therefore extrapolate our results for the energy shift to the chiral limit.[1] The simplest way to do such an extrapolation is the following: First, we have to find the *critical kappa value* κ_c, for which the quark masses of the lattice theory vanish. κ_c can be found with a linear extrapolation of the pion mass. Remember that the pions are the Goldstone bosons related to the spontaneous breakdown of chiral symmetry, and therefore become massless in the chiral limit. Thus, we calculate the pion mass for different kappa values, plot the results against $1/\kappa$ and fit a linear function through them. The zero point of the fit function is $1/\kappa_c$. To extrapolate some other lattice observable O, we also calculate it for different kappa values, plot it against $1/\kappa$ and fit it, for lack of deeper knowledge of it's κ dependence, with a linear function. The value of this function at $1/\kappa_c$ is then taken as the extrapolated value of O. More sophisticated extrapolation methods will exploit analytic relations between different lattice observables or knowledge of their κ dependence.

Note that all energies we calculate on the lattice are obtained in *lattice units*, i.e. in units of the energy scale a^{-1} set by the lattice spacing a. In every lattice simulation, the lattice spacing has to be determined by matching the *lattice value* of some dimensionful observable to it's physical value. As we are interested in the chiral limit, we should use an observable that remains nonzero in the limit $\kappa \to \kappa_c$. That rules out the pion mass, but the mass of the rho meson is a possible and very popular choice. Neglecting cutoff effects, the lattice spacing is given by

$$\frac{1}{a} = \frac{m_\rho^{\text{lat}}}{m_\rho^{\text{phys}}} \quad , \tag{5.1}$$

where m_ρ^{lat} is the (dimensionless) lattice value and m_ρ^{phys} the physical value of the rho mass. A more sophisticated method to determine the lattice spacing is presented in [35]. There too, the rho mass is required as a reference value. Therefore, we will now introduce composite operators that create rho mesons and states of one and two pions.

Let's start with the one pion states. In (1.6), we already expressed the states of the pion multiplet in terms of pseudo-scalar quark-antiquark states (spin 0 and parity -1).

[1] As the dominant contributions to the pion mass comes from the binding energies between the constituent quarks, setting the quark masses to zero is a valid approximation.

The flavour structure in (1.6) assures the correct symmetry properties under isospin transformations. To construct a pseudo-scalar operator from a local product of a quark and an anti-quark operator, we have to contract the spinor indices with an appropriate matrix in spinor space. Possible choices for the *interpolating operator* are γ_5 or $\gamma_0\gamma_5$. We define the one pion operators π^+, π^0 and π^- as

$$\pi^+(x) = -\,\bar{d}(x)\gamma_0\gamma_5 u(x) \quad , \tag{5.2a}$$

$$\pi^0(x) = \frac{1}{\sqrt{2}}\big(\bar{u}(x)\gamma_0\gamma_5 u(x) - \bar{d}(x)\gamma_0\gamma_5 d(x)\big) \quad , \tag{5.2b}$$

$$\pi^-(x) = +\,\bar{u}(x)\gamma_0\gamma_5 d(x) \quad . \tag{5.2c}$$

Here, we consider the gamma matrices as matrices in spinor *and* colour space, i.e.

$$(\gamma_\mu)_{AB} \equiv (\gamma_\mu)_{(i,\alpha)(j,\beta)} = \delta_{ij}(\gamma_\mu)_{\alpha\beta} \quad , \tag{5.3}$$

where $(\gamma_\mu)_{\alpha\beta}$ denotes the components of the ordinary (euclidean) gamma matrices in spinor space. Thus, the colour indices in (5.2) are contracted, too. The hermitian conjugates of the pion operators satisfy

$$\pi^{-\dagger}(x) = \pi^+(x) \qquad , \qquad \pi^{0\dagger}(x) = -\pi^0(x) \quad . \tag{5.4}$$

This follows immediately from the properties (3.61) of the euclidean gamma matrices.

The rho mesons are vector particles. Like the pions, they have an isospin of 1 and a parity of -1, but their (spacial) spin is 1. Thus, for operators that create rho mesons, we can use the same flavour structure as in (5.2). We only have to take a different interpolating operator. To get an operator with spin 1 and parity -1, we can use any linear combination of the spacial gamma matrices γ_k ($k = 1, 2, 3$). We define

$$\rho^+(x) = -\sum_k \bar{d}(x)\gamma_k u(x) \quad , \tag{5.5a}$$

$$\rho^0(x) = \frac{1}{\sqrt{2}}\sum_k \big(\bar{u}(x)\gamma_k u(x) - \bar{d}(x)\gamma_k d(x)\big) \quad , \tag{5.5b}$$

$$\rho^-(x) = +\sum_k \bar{u}(x)\gamma_k d(x) \quad . \tag{5.5c}$$

Like the pion operators, they satisfy

$$\rho^{-\dagger}(x) = \rho^+(x) \qquad , \qquad \rho^{0\dagger}(x) = -\rho^0(x) \quad . \tag{5.6}$$

Finally, we need operators that create two pion states. Since our motivation is to understand the (lattice) propagation of two pion states created in neutral kaon decays, we are only concerned with the isospin eigenstates $|\pi\pi, 0\rangle$ and $|\pi\pi, 2\rangle$ from *section 1.2*. Thus, we need operators with $I_3 = 0$ and $I = 0, 2$. To construct them, we can basically copy equation (1.18). For two pion states, where the pions are localised at different points x and y in space-time, we define the operators

$$J_0(x,y) = \frac{1}{\sqrt{3}}\pi^+(x)\pi^-(y) + \frac{1}{\sqrt{3}}\pi^-(x)\pi^+(y) - \frac{1}{\sqrt{3}}\pi^0(x)\pi^0(y) \quad , \tag{5.7a}$$

$$J_2(x,y) = \frac{1}{\sqrt{6}}\pi^+(x)\pi^-(y) + \frac{1}{\sqrt{6}}\pi^-(x)\pi^+(y) + \sqrt{\frac{2}{3}}\pi^0(x)\pi^0(y) \quad . \tag{5.7b}$$

The indices '0' and '2' refer to the value of I. From (5.4) we see immediately, that

$$J_0^\dagger(x,y) = J_0(y,x) \qquad , \qquad J_2^\dagger(x,y) = J_2(y,x) \quad . \tag{5.8}$$

With the meson operators at hand, we proceed and define the following (euclidean) Greens functions:

$$G_\rho(x,y) = \mathrm{Tr}\left(e^{-HT}\mathrm{T}\{\rho^-(x)\rho^+(y)\}\right) \quad , \tag{5.9a}$$

$$G_\pi(x,y) = \mathrm{Tr}\left(e^{-HT}\mathrm{T}\{\pi^-(x)\pi^+(y)\}\right) \quad , \tag{5.9b}$$

$$G_{\pi\pi,2}(x_1,x_2,y_1,y_2) = \mathrm{Tr}\left(e^{-HT}\mathrm{T}\{J_2(x_1,x_2)J_2(y_2,y_1)\}\right) \quad , \tag{5.9c}$$

$$G_{\pi\pi,0}(x_1,x_2,y_1,y_2) = \mathrm{Tr}\left(e^{-HT}\mathrm{T}\{J_0(x_1,x_2)J_0(y_2,y_1)\}\right) \quad . \tag{5.9d}$$

G_ρ and G_π describe the propagation of a rho meson and a pion, while $G_{\pi\pi,2}$ and $G_{\pi\pi,0}$ describe the propagation of a two pion state with isospin 2 and 0, respectively. Due to their bosonic character, the pion and rho operators commute within the time ordered product. Thus, it follows immediately that all the Greens functions in (5.9) are real.

Following the procedures described in *sections 3.2, 3.3 and 4.1*, we can express the lattice regularised versions of the Greens functions in terms of expectation values of the form

$$\langle F \rangle = \int_{\mathcal{S}} [dU]\; F[U] e^{-S^{\mathrm{g}}_{\mathrm{eff}}[U]} \quad , \tag{5.10}$$

where F is some function of the gauge links U. Usually, it is a combination of components of the inverse quark matrix Q_U^{-1}. An important feature of this expectation value is, that it is zero for all observables F, that are not invariant under local gauge transformations. To see this, we factor out from the path integral (5.10) an integral over elements Λ of the local gauge group (3.65). Let $\bar{\mathcal{S}} \subset \mathcal{S}$ denote a subset of gauge configurations, which can not be transformed into each other by local gauge transformations. Then, we may write (5.10) as

$$\langle F \rangle = \int_{\bar{\mathcal{S}}} [d\bar{U}] \int_{\mathcal{G}^{\mathrm{lat}}_{\mathrm{loc}}} [d\Lambda]\; F[\Lambda\bar{U}] e^{-S^{\mathrm{g}}_{\mathrm{eff}}[\bar{U}]} \quad , \tag{5.11}$$

where the gauge transformed field configuration $\Lambda\bar{U}$ is defined in accordance with (3.16). The gauge transformation Λ does not appear in the action, because the action is gauge invariant. Now, let F_i ($i = 1 \dots n$) denote a set of observables, that transform under some non-trivial representation $\mathcal{D}$ of the local gauge group $\mathcal{G}_{\rm loc}^{\rm lat}$, i.e.

$$F_i[\Lambda U] = \sum_j \mathcal{D}_{ij}(\Lambda) F_j[U] \quad . \tag{5.12}$$

Without restriction, we may assume that $\mathcal{D}$ is an *irreducible* representation. According to (5.11), the expectation values of the F_i are given by

$$\langle F_i \rangle = \int_{\bar{\mathcal{S}}} [d\bar{U}] e^{-S_{\rm eff}^{\rm g}[\bar{U}]} \sum_j \left(\int_{\mathcal{G}_{\rm loc}^{\rm lat}} [d\Lambda]\, \mathcal{D}_{ij}(\Lambda) \right) F_j[\bar{U}] \quad . \tag{5.13}$$

However, for compact semi-simple Lie groups it can be shown that the integral $\int [d\Lambda]\ \mathcal{D}(\Lambda)$ is zero for all irreducible representations $\mathcal{D}$ except the singlet representation. Therefore, the expectation value (5.10) is only non-zero for gauge invariant observables F.

To calculate the Greens functions (5.9), we first introduce some new notations. From now on, we let $S^{[U]}$ denote the inverse quark matrix Q_U^{-1} and call it the *quark propagator* in the gauge background U. To select a specific component of $S^{[U]}$ with position indices x and y and colour/spinor multi-indices A and B, we write $S_{AB}^{[U]}(x,y)$. Using the same notation for Q_U, the components of $S^{[U]}$ are defined by the equation

$$\sum_{B,y} (Q_U)_{AB}(x,y)\ S_{BC}^{[U]}(y,z) = \delta_{AB}\delta(x,y) \quad , \tag{5.14}$$

where $\delta(x,y)$ is the Kronecker delta for position indices. If the quark propagator appears in an expectation value $\langle \cdots \rangle$, the gauge links U are integrated out, so we will drop the superscript $[U]$ there. Usually, we also leave the colour and spinor indices implicit. Thus, for given x and y, $S(x,y)$ denotes a matrix in colour and spinor space. Traces and hermitian conjugates of these objects do not affect the position indices. In the case of hermitian conjugation, we make this clear by placing the dagger behind the position arguments. From the property (4.11) of the quark matrix it follows that

$$S(y,x) = \gamma_5 S(x,y)^\dagger \gamma_5 \quad . \tag{5.15}$$

Our strategy for calculating the Greens functions (5.9) consists of three steps:

1. Apply Wick's theorem to find the diagrams Γ, that contribute to a given Greens function G. Each diagram is a product of quark propagators $S(x,y)$.

2. To calculate the expectation values of the diagrams numerically, generate a sufficiently large ensemble of properly distributed gauge configurations U.

Figure 5.1: Diagrams contributing to the two point Greens functions (5.9a) and (5.9b).

3. Evaluate the products of quark propagators for each gauge configuration U. The quark propagators are obtained by inverting the quark matrix Q_U^{-1}. Then, add up all diagrams and take the average over all gauge configurations. The result is (approximately) the desired value of G.

After generating the gauge configurations, the most time consuming procedure is the computation of the quark propagators, which requires partial inversions of the quark matrix Q_U^{-1}. For most computations, it is impossible to calculate all components of Q_U^{-1}, i.e. perform a full inversion of the quark matrix. We therefore have to restrict the arguments of the Greens function cleverly, so that we need only a few partial inversions. We will return to this issue in the next section.

For graphical representations of the diagrams from step 1, we use the following conventions: The position indices x and y are represented by dots (*vertices*). For a contraction between a quark field q at x and a bar conjugated field $\bar{q}$ at y, we draw a solid line (fermion line) between the vertices x and y, with a middle arrow pointing from x to y. Thus, for each line between the vertices x and y, the corresponding function Γ contains a factor $S(x,y)$. The topological structure of the diagram determines, how the colour and spinor indices of the propagators are contracted. For the Greens functions (5.9), there is exactly one quark field q and one bar conjugate $\bar{q}$ associated with each position index. Thus, every vertex has exactly one incoming and one outgoing fermion line. The colour and spinor indices of the related propagators have to be contracted with the interpolating operator associated with the vertex, i.e. with $\sum_k \gamma_k$ for G_ρ and with $\gamma_0\gamma_5$ for G_π and $G_{\pi\pi,2}$.

For the two point functions G_ρ and G_π, there are two different types of diagrams. They are shown in *figure 5.1*. However, the contributions of the "bubble" diagram (*figure 5.1b*) cancel because of the flavour structure of the meson operators (5.2) and (5.5). Thus, we obtain for the two point Greens functions

$$G_\rho(x,y) = \sum_k \left\langle \mathrm{Tr}\left(S(x,y)\gamma_k S(y,x)\gamma_k \right) \right\rangle \quad , \tag{5.16a}$$

$$G_\pi(x,y) = \left\langle \mathrm{Tr}\left(S(x,y)\gamma_0\gamma_5 S(y,x)\gamma_0\gamma_5 \right) \right\rangle \quad . \tag{5.16b}$$

The minus signs from the fermion loops are cancelled by the minus signs in the definitions of π^+ and ρ^+.

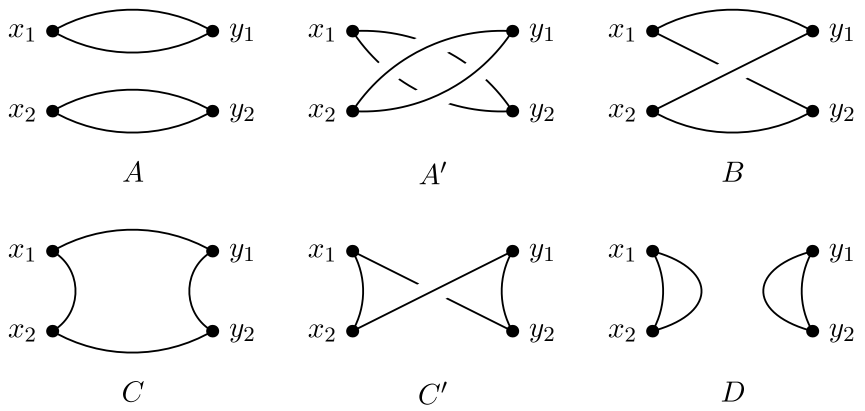

Figure 5.2: Diagrams contributing to the four point Greens functions (5.9c) and (5.9d).

The calculation of the four point functions is more complicated. If we substitute (5.2) and (5.7) into (5.9c) and (5.9d), we obtain terms of the form

$$\mathrm{Tr}\left(e^{-HT}\mathrm{T}\{\bar{q}(x_1)\gamma_0\gamma_5 q(x_1)\ \bar{q}(x_2)\gamma_0\gamma_5 q(x_2)\ \bar{q}(y_2)\gamma_0\gamma_5 q(y_2)\ \bar{q}(y_1)\gamma_0\gamma_5 q(y_1)\}\right) \quad , \tag{5.17}$$

where each of the qs is either a u or a d field. Applying Wick's theorem to each of the terms individually, we encounter six[2] different types of diagrams, which we denote as Γ_A, $\Gamma_{A'}$, Γ_B, Γ_C, $\Gamma_{C'}$ and Γ_D. Graphical representations of these diagrams are shown in *figure 5.2*. To reduce the number of diagrams, we left out the orientations of the fermion lines. Adding them in the diagrams A, A' and D yields nothing new. For the diagrams B, C and C', there are two distinct ways to choose the orientations: a clockwise and a counterclockwise. From the property (5.15), it follows immediately that the clockwise and counterclockwise diagrams are related to each other by complex conjugation. As the Greens functions (5.9) are real, both orientations have to appear with the same coefficient. In other words, we need only the real parts of the diagrams B, C and C', which are independent of their orientation.

In terms of quark propagators, the diagrams from *figure 5.2* can be written as

$$\Gamma_A = \mathrm{Tr}\left(S(x_1,y_1)\gamma_0\gamma_5 S(y_1,x_1)\gamma_0\gamma_5\right)\mathrm{Tr}\left(S(x_2,y_2)\gamma_0\gamma_5 S(y_2,x_2)\gamma_0\gamma_5\right) \quad , \tag{5.18a}$$

$$\Gamma_{A'} = \mathrm{Tr}\left(S(x_1,y_2)\gamma_0\gamma_5 S(y_2,x_1)\gamma_0\gamma_5\right)\mathrm{Tr}\left(S(x_2,y_1)\gamma_0\gamma_5 S(y_1,x_2)\gamma_0\gamma_5\right) \quad , \tag{5.18b}$$

$$\mathrm{Re}\,\Gamma_B = -\,\mathrm{Re}\left[\mathrm{Tr}\left(S(x_1,y_1)\gamma_0\gamma_5 S(y_1,x_2)\gamma_0\gamma_5 S(x_2,y_2)\gamma_0\gamma_5 S(y_2,x_1)\gamma_0\gamma_5\right)\right] \quad , \tag{5.18c}$$

$$\mathrm{Re}\,\Gamma_C = -\,\mathrm{Re}\left[\mathrm{Tr}\left(S(x_1,y_1)\gamma_0\gamma_5 S(y_1,y_2)\gamma_0\gamma_5 S(y_2,x_2)\gamma_0\gamma_5 S(x_2,x_1)\gamma_0\gamma_5\right)\right] \quad , \tag{5.18d}$$

$$\mathrm{Re}\,\Gamma_{C'} = -\,\mathrm{Re}\left[\mathrm{Tr}\left(S(x_1,y_2)\gamma_0\gamma_5 S(y_2,y_1)\gamma_0\gamma_5 S(y_1,x_2)\gamma_0\gamma_5 S(x_2,x_1)\gamma_0\gamma_5\right)\right] \quad , \tag{5.18e}$$

$$\Gamma_D = \mathrm{Tr}\left(S(x_1,x_2)\gamma_0\gamma_5 S(x_2,x_1)\gamma_0\gamma_5\right)\mathrm{Tr}\left(S(y_1,y_2)\gamma_0\gamma_5 S(y_2,y_1)\gamma_0\gamma_5\right) \quad . \tag{5.18f}$$

[2]In addition to those six, we also find bubble diagrams like *figure 5.1b*. However, as for the two point functions, their contributions cancel because of the flavour structure of the pion operators (5.2).

Remember that, according to Wick's theorem, we pick up a factor of -1 for every fermion loop. Therefore, Γ_B, Γ_C and $\Gamma_{C'}$ have an extra minus sign.

Now, the four point Greens functions $G_{\pi\pi,2}$ and $G_{\pi\pi,0}$ can be expressed in terms of the diagrams (5.18). For $G_{\pi\pi,2}$, the diagrams of type C, C' and D cancel, and we obtain

$$G_{\pi\pi,2} = \langle \Gamma_A + \Gamma_{A'} + 2\,\mathrm{Re}\,\Gamma_B \rangle \quad . \tag{5.19}$$

The expression for $G_{\pi\pi,0}$ is more complicated and contains all six types of diagrams. We will not calculate it here, because in this work, we are only concerned with isospin 2 states.

5.2 Correlation Functions and Quark Propagators

If we wanted to find, by numerical computation, the values of the Greens functions (5.9) for all combinations of the position indices x_1, x_2 etc., we would have to perform a full inversion of the quark matrix for each gauge configuration U of our ensemble. As we mentioned earlier, this is usually impossible due to the high dimensionality of the quark matrix. However, in *section 2.3*, we extracted energies and form factors from *correlation functions* C, that depend only on a single time index t. In this section, we define correlation functions, from which the rho mass, the pion mass and the energy of the two pion state can be extracted. We express them in terms of the Greens functions (5.9), and we will see that they can be calculated with only a few partial inversions per gauge configuration.

First, we define new meson operators $\tilde{\pi}$, $\tilde{\rho}$ and $\tilde{J}$, that create states with a fixed spacial lattice momentum. They are obtained from the operators (5.2), (5.5) and (5.7) by discrete spacial Fourier transforms.

$$\tilde{\pi}^I(\mathbf{p},t) = \sum_{\mathbf{x}} e^{i\mathbf{p}\mathbf{x}} \pi^I(x)|_{x^0=t} \qquad \text{with } I = +,0,- \quad , \tag{5.20a}$$

$$\tilde{\rho}^I(\mathbf{p},t) = \sum_{\mathbf{x}} e^{i\mathbf{p}\mathbf{x}} \rho^I(x)|_{x^0=t} \qquad \text{with } I = +,0,- \quad , \tag{5.20b}$$

$$\tilde{J}_I(\mathbf{p}_1,t_1;\mathbf{p}_2,t_2) = \sum_{\mathbf{x}_1,\mathbf{x}_2} e^{i\mathbf{p}_1\mathbf{x}_1} e^{i\mathbf{p}_2\mathbf{x}_2} J_I(x_1,x_2)|_{x_1^0=t_1,x_2^0=t_2} \quad \text{with } I = 0,2 \quad . \tag{5.20c}$$

The possible values for the lattice momenta are given in (3.72). Now, we define the *local* correlation functions as

$$C_\rho^{\mathrm{loc}}(t) = \mathrm{Tr}\left(e^{-HT}\tilde{\rho}^-(\mathbf{0},t)\rho^+(0)\right) = \sum_{\mathbf{x}} G_\rho\big((t,\mathbf{x}),0\big) \quad , \tag{5.21a}$$

$$C_\pi^{\mathrm{loc}}(t) = \mathrm{Tr}\left(e^{-HT}\tilde{\pi}^-(\mathbf{0},t)\pi^+(0)\right) = \sum_{\mathbf{x}} G_\pi\big((t,\mathbf{x}),0\big) \quad , \tag{5.21b}$$

$$C_{\pi\pi,2}^{\mathrm{loc}}(t) = \mathrm{Tr}\left(e^{-HT}\tilde{J}_2(\mathbf{0},t;\mathbf{0},t)J_2(0,0)\right) = \sum_{\mathbf{x}_1,\mathbf{x}_2} G_{\pi\pi,2}\big((t,\mathbf{x}_1),(t,\mathbf{x}_2),0,0\big) \quad . \tag{5.21c}$$

The operators at time t annihilate zero momentum states, while the local operators at $t = 0$ create pions localised at $\mathbf{x} = 0$, i.e. superpositions of all possible momentum eigenstates. Therefore, we say that the pions are created with a *point source*. This is not exactly the situation we discussed in *section 2.3*, but we can still be sure that only zero momentum states contribute to the correlation functions (5.21), because for all other states the matrix elements of the Fourier transformed operators vanish. By calculations analogous to those in *section 2.3*, we can show that for $0 \ll t \ll T$

$$C_\rho^{\mathrm{loc}}(t) = A_\rho^{\mathrm{loc}} \cosh\left(m_\rho^{\mathrm{loc}}(t - T/2)\right) \quad , \tag{5.22a}$$

$$C_\pi^{\mathrm{loc}}(t) = A_\pi^{\mathrm{loc}} \cosh\left(m_\pi^{\mathrm{loc}}(t - T/2)\right) \quad , \tag{5.22b}$$

$$C_{\pi\pi,2}^{\mathrm{loc}}(t) = A_{\pi\pi,2}^{\mathrm{loc}} \cosh\left(E_{\pi\pi,2}^{\mathrm{loc}}(t - T/2)\right) + D_{\pi\pi,2}^{\mathrm{loc}} \quad . \tag{5.22c}$$

m_π^{loc} and m_ρ^{loc} are the pi and rho meson masses. We directly obtain the masses of the particles, because we are working with momentum zero states. $E_{\pi\pi,2}^{\mathrm{loc}}$ is the energy of the two pion state with isospin 2 and total momentum 0. The coefficients A_ρ^{loc}, A_π^{loc} and $A_{\pi\pi,2}^{\mathrm{loc}}$ are related to form factors of the meson operators. Here, we are only interested in the energy shift

$$\Delta E_{\pi\pi,2} = E_{\pi\pi,2} - 2m_\pi \quad , \tag{5.23}$$

so we will not further specify them. As in (2.32), the constant $D_{\pi\pi,2}^{\mathrm{loc}}$ is related to diagonal matrix elements of the operators $\tilde{J}_2(\mathbf{0}, t; \mathbf{0}, t)$ and $J_2(0, 0)$. The leading term in $D_{\pi\pi,2}^{\mathrm{loc}}$ is proportional to $e^{-m_\pi T}$. For the two point correlation functions C_ρ^{loc} and C_π^{loc}, the contributions from diagonal matrix elements can be neglected.

To compute the local correlation functions (5.21), we only need those values of the quark propagator, where one position index is zero. This can be seen directly from the equations (5.16) and (5.19) for the Greens functions G_ρ, G_π and $G_{\pi\pi,2}$. However, $S^{[U]}(x, 0)$ and $S^{[U]}(0, x)$ are related to each other by equation (5.15). Thus, we only have to calculate the *local propagators*

$$S_{\mathrm{loc}}^{[U]}(x) \equiv S^{[U]}(x, 0) \tag{5.24}$$

for all x and all gauge configurations U of our ensemble. According to (5.14), $S_{\mathrm{loc}}^{[U]}(x)$ is related to the quark matrix Q_U by

$$\sum_x Q_U(y, x)\, S_{\mathrm{loc}}^{[U]}(x) = \delta(y, 0) \cdot \mathbb{1} \quad , \tag{5.25}$$

where $\mathbb{1}$ denotes the identity matrix in colour and spinor space. Ignoring the fact that $Q_U(y, x)$ and $S_{\mathrm{loc}}^{[U]}(x)$ are still matrices in colour and spinor space, we may view (5.24) as an L^3T-dimensional system of linear equations. It can be solved for $S_{\mathrm{loc}}^{[U]}(x)$ numerically with iterative algorithms like the biconjugate gradient method. To do this, individual sub-matrices of Q_U in colour and spinor space have to be inverted, too. As they are only low dimensional and not sparse, this is usually done with other methods like LU or singular value decomposition. From now on, solving an equation like (5.24) is what we mean by a *partial inversion*. Thus, the local correlation functions (5.21) can be calculated with just one partial inversion per gauge configuration.

Note that the reason, why we only need the local propagators $S^{[U]}_{\text{loc}}(x)$ to calculate the four point correlation function $C_{\pi\pi,2}$ is, because only the diagrams of type A, A' and B contribute to the four point Greens function $G_{\pi\pi,2}$. As we can see in (5.18), the expressions for Γ_A, $\Gamma_{A'}$ and Γ_B contain only the propagators $S^{[U]}(x_i, y_j)$ and $S^{[U]}(y_i, x_j)$ with $i, j = 1, 2$. Thus, if we set $y_1 = y_2 = 0$, we only need the local propagator and it's hermitian conjugate, which is related to $S^{[U]}(0, x)$ by (5.15). For the diagrams Γ_C, $\Gamma_{C'}$ and Γ_D, this trick no longer works. There, we also encounter the propagators $S^{[U]}(x_1, x_2)$, $S^{[U]}(y_1, y_2)$ etc. A two pion correlation function for isospin 0 states would have contributions from the diagrams Γ_C, $\Gamma_{C'}$ and Γ_D. Thus, even if we defined it in analogy to (5.22c), we would need a full inversion of the quark matrix to calculate it. A possible solution to this problem is the use of *wall propagators*, like those we will define later in this section. However, we are not concerned with isospin 0 states here. The main objective of this work is to "test" the wall propagators on unquenched gauge configurations by computing two pion correlation functions for isospin 2 states and comparing the results with those obtained from local propagators.

First, we define a new set of "wall" correlation functions.

$$C^{\text{w}}_\rho(t) = \text{Tr}\left(e^{-HT}\tilde{\rho}^-(\mathbf{0}, t)\tilde{\rho}^+(\mathbf{0}, 0)\right) = \sum_{\mathbf{x},\mathbf{y}} G_\rho\big((t, \mathbf{x}), (0, \mathbf{y})\big) \quad , \tag{5.26a}$$

$$C^{\text{w}}_\pi(t) = \text{Tr}\left(e^{-HT}\tilde{\pi}^-(\mathbf{0}, t)\tilde{\pi}^+(\mathbf{0}, 0)\right) = \sum_{\mathbf{x},\mathbf{y}} G_\pi\big((t, \mathbf{x}), (0, \mathbf{y})\big) \quad , \tag{5.26b}$$

$$\begin{aligned} C^{\text{w}}_{\pi\pi,2}(t) &= \text{Tr}\left(e^{-HT}\tilde{J}_2(\mathbf{0}, t; \mathbf{0}, t+1)\tilde{J}_2(\mathbf{0}, 1; \mathbf{0}, 0)\right) \\ &= \sum_{\mathbf{x}_1,\mathbf{x}_2}\sum_{\mathbf{y}_1,\mathbf{y}_2} G_{\pi\pi,2}\big((t, \mathbf{x}_1), (t+1, \mathbf{x}_2), (0, \mathbf{y}_1), (1, \mathbf{y}_2)\big) \quad . \end{aligned} \tag{5.26c}$$

Because of the sums over the spacial planes at $t = 0$ and 1, we also speak of a *wall source*. The reason for the curious shift in the time arguments of $G_{\pi\pi,2}$ will soon become apparent. In perfect analogy to the calculations in *section 2.3*, we find

$$C^{\text{w}}_\rho(t) = A^{\text{w}}_\rho \cosh\left(m^{\text{w}}_\rho(t - T/2)\right) \quad , \tag{5.27a}$$

$$C^{\text{w}}_\pi(t) = A^{\text{w}}_\pi \cosh\left(m^{\text{w}}_\pi(t - T/2)\right) \quad , \tag{5.27b}$$

$$C^{\text{w}}_{\pi\pi,2}(t) = A^{\text{w}}_{\pi\pi,2} \cosh\left(E^{\text{w}}_{\pi\pi,2}(t - T/2)\right) + D^{\text{w}}_{\pi\pi,2} \quad . \tag{5.27c}$$

The coefficients A^{w}_ρ, A^{w}_π, $A^{\text{w}}_{\pi\pi,2}$ and the constant $D^{\text{w}}_{\pi\pi,2}$ are different from those in (5.22), because we have used different meson operators. However, the particle masses m^{w}_ρ and m^{w}_π and the two pion energy $E^{\text{w}}_{\pi\pi,2}$ should agree with those from (5.22) within the numerical precision.

To calculate the correlation functions (5.26) with the method discussed above, we would need the quark propagators $S^{[U]}(x, y)$ for all gauge configurations U, all values of

x and all values of y with $y^0 = 0, 1$. This would require $L^3 = \mathcal{O}(10^3)$ partial inversions per gauge configuration — far too many for today's computing power. In this situation, too, wall propagators are a possible solution. We define the wall propagator for the time slice t as

$$S^{[U]}_{\mathrm{w},t}(x) = \sum_{\mathbf{y}} S\big(x, (t, \mathbf{y})\big) \tag{5.28}$$

From (5.15) it follows that

$$\sum_{\mathbf{x}} S^{[U]}_{\mathrm{w},t_1}\big((t_2, \mathbf{x})\big) = \sum_{\mathbf{x}} \gamma_5 S^{[U]}_{\mathrm{w},t_2}\big((t_1, \mathbf{x})\big)^{\dagger} \gamma_5 \quad . \tag{5.29}$$

According to (5.14), $S^{[U]}_{\mathrm{w},t}$ is related to the quark matrix Q_U by

$$\sum_{x} Q_U(y, x) S^{[U]}_{\mathrm{w},t}(x) = \sum_{\mathbf{z}} \delta(t, y^0) \delta(\mathbf{z}, \mathbf{y}) \cdot \mathbb{1} \quad , \tag{5.30}$$

where $\mathbb{1}$ denotes again the identity matrix in colour and spinor space. Like (5.25), this is a system of linear equations in position space and can be solved with one partial inversion of the quark matrix.

What can we do with the wall propagators? Consider the following expectation value:

$$\begin{aligned} &\sum_{\mathbf{x},\mathbf{y}} \left\langle \mathrm{Tr}\left[S_{\mathrm{w},0}\big((t, \mathbf{x})\big)\gamma_0\gamma_5 S_{\mathrm{w},t}\big((0, \mathbf{y})\big)\gamma_0\gamma_5\right]\right\rangle \\ &\qquad = \sum_{\mathbf{x}_1,\mathbf{x}_2} \sum_{\mathbf{y}_1,\mathbf{y}_2} \left\langle \mathrm{Tr}\left[S\big((t, \mathbf{x}_1), (0, \mathbf{y}_1)\big)\gamma_0\gamma_5 S\big((0, \mathbf{y}_2), (t, \mathbf{x}_2)\big)\gamma_0\gamma_5\right]\right\rangle \quad . \end{aligned} \tag{5.31}$$

Because of (5.29), we only need the values of $S_{\mathrm{w},0}$ to calculate the left hand side. On the right hand side, the term in angular brackets is gauge invariant only for $\mathbf{x}_1 = \mathbf{x}_2$ and $\mathbf{y}_1 = \mathbf{y}_2$. As we saw in *section 5.1*, only expectation values of gauge invariant observables can be nonzero. Thus, the "loose ends" of the wall propagators tie up and the right hand side of (5.31) reduces to

$$\sum_{\mathbf{x},\mathbf{y}} \left\langle \mathrm{Tr}\left[S\big((t, \mathbf{x}), (0, \mathbf{y})\big)\gamma_0\gamma_5 S\big((0, \mathbf{y}), (t, \mathbf{x})\big)\gamma_0\gamma_5\right]\right\rangle = C^{\mathrm{w}}_{\pi}(t) \quad , \tag{5.32}$$

where the last equality follows from (5.26b) and (5.16b). Consequently, the use of wall propagators allows us to calculate the correlation function C_π with only one partial inversion per gauge configuration. A similar trick can be used for C_ρ and $C_{\pi\pi,2}$. For the two point functions, we obtain

$$C^{\mathrm{w}}_{\rho}(t) = \sum_{\mathbf{x},\mathbf{y}} \left\langle \mathrm{Tr}\left[S_{\mathrm{w},0}\big((t, \mathbf{x})\big)\gamma_k S_{\mathrm{w},t}\big((0, \mathbf{y})\big)\gamma_k\right]\right\rangle \quad , \tag{5.33a}$$

$$C^{\mathrm{w}}_{\pi}(t) = \sum_{\mathbf{x},\mathbf{y}} \left\langle \mathrm{Tr}\left[S_{\mathrm{w},0}\big((t, \mathbf{x})\big)\gamma_0\gamma_5 S_{\mathrm{w},t}\big((0, \mathbf{y})\big)\gamma_0\gamma_5\right]\right\rangle \quad . \tag{5.33b}$$

The expression for the four point function $C_{\pi\pi,2}$ is a bit lengthy. We define

$$C^{\mathrm{w}}_{A}(t) = \sum_{\mathbf{x}_1,\mathbf{x}_2}\sum_{\mathbf{y}_1,\mathbf{y}_2}\Big\langle \quad \mathrm{Tr}\left[S_{\mathrm{w},0}\big((t,\mathbf{x}_1)\big)\gamma_0\gamma_5 S_{\mathrm{w},t}\big((0,\mathbf{y}_1)\big)\gamma_0\gamma_5\right] \cdot \mathrm{Tr}\left[S_{\mathrm{w},1}\big((t+1,\mathbf{x}_2)\big)\gamma_0\gamma_5 S_{\mathrm{w},t+1}\big((1,\mathbf{y}_2)\big)\gamma_0\gamma_5\right]\Big\rangle \quad , \tag{5.34a}$$

$$C^{\mathrm{w}}_{A'}(t) = \sum_{\mathbf{x}_1,\mathbf{x}_2}\sum_{\mathbf{y}_1,\mathbf{y}_2}\Big\langle \quad \mathrm{Tr}\left[S_{\mathrm{w},0}\big((t+1,\mathbf{x}_2)\big)\gamma_0\gamma_5 S_{\mathrm{w},t+1}\big((0,\mathbf{y}_1)\big)\gamma_0\gamma_5\right] \cdot \mathrm{Tr}\left[S_{\mathrm{w},1}\big((t,\mathbf{x}_1)\big)\gamma_0\gamma_5 S_{\mathrm{w},t}\big((1,\mathbf{y}_2)\big)\gamma_0\gamma_5\right]\Big\rangle \quad , \tag{5.34b}$$

$$C^{\mathrm{w}}_{B}(t) = -\sum_{\mathbf{x}_1,\mathbf{x}_2}\sum_{\mathbf{y}_1,\mathbf{y}_2}\Big\langle \mathrm{Tr}\Big[\quad S_{\mathrm{w},0}\big((t+1,\mathbf{x}_2)\big)\gamma_0\gamma_5 S_{\mathrm{w},t+1}\big((1,\mathbf{y}_2)\big)\gamma_0\gamma_5 \cdot S_{\mathrm{w},1}\big((t,\mathbf{x}_1)\big)\gamma_0\gamma_5 S_{\mathrm{w},t}\big((0,\mathbf{y}_1)\big)\gamma_0\gamma_5\Big]\Big\rangle \quad . \tag{5.34c}$$

Then, in accordance with (5.19), the whole four point correlation function can be written as

$$C^{\mathrm{w}}_{\pi\pi,2} = C^{\mathrm{w}}_{A} + C^{\mathrm{w}}_{A'} + 2\,\mathrm{Re}\,C^{\mathrm{w}}_{B} \quad . \tag{5.35}$$

Now, we see the reason for our particular choice of the time arguments. We have to put all four vertices on different time slices, so that the loose ends of the wall propagators tie up, for each diagram, in way we want it. Using (5.29), the functions (5.34) can be calculated with two partial inversions per gauge configuration. We only have to compute $S_{\mathrm{w},0}$ and $S_{\mathrm{w},1}$.

In practice, we cannot calculate the expectation values in (5.33) and (5.34) exactly. We have to approximate them by an average over gauge configurations. In this average, the contributions from non-gauge-invariant diagrams tend to cancel each other, but for a finite ensemble of gauge configurations, the cancellation is not exact. Thus, by using wall propagators, we generate additional *noise* in our results. On the other hand, the extra sum over the spacial planes at $t = 0$ (for the two point functions) and $t = 0$ and 1 (for the four point function) reduces the statistical errors on the correlation function values. This might compensate the noise introduced by the wall propagators.

5.3 Results of the Simulation

The wall propagator method was first introduced by M. Fukugita in [6], where it was applied to gauge configurations generated in the *quenched approximation*. Since the paper was published in 1995, the generation of *full QCD* gauge configurations has become feasible due to a rapid improvement of computing power. In this work, the wall propagator method is applied to unquenched gauge configurations. Similar calculations were done by the CP-PACS collaboration [36], using full QCD gauge configurations generated with an RG-improved gauge action and a mean field improved clover quark action.

Our calculations are based on unquenched gauge configurations generated by the SPQcdR Collaboration, using the plaquette gauge action and the Wilson quark action. We have ensembles on two different lattices with $T = 48$ and $L = 16$ and 24, respectively. Ensembles of 100 configurations (on the small volume) and 50 configurations (on the large volume) were generated for

$$\beta = 5.8 \tag{5.36}$$

and the following kappa values:

$$\kappa = 0.1535,\ 0.1538,\ 0.1540,\ 0.1541 \quad . \tag{5.37}$$

Further technical information on the generation of the gauge configurations can be found in the related paper [32] of the SPQcdR Collaboration. In this paper, the *mass scale* $1/a$ corresponding to the beta value (5.36) is determined as

$$\frac{1}{a} = 3.0\,\text{GeV} \pm 0.1\,\text{GeV} \quad . \tag{5.38}$$

Thus, the extents of the two spacial volumes are $16a \approx 1.1\,\text{fm}$ and $24a \approx 1.6\,\text{fm}$.

To calculate the correlation functions (5.21) and (5.26), the propagators S_{loc}, $S_{\text{w},0}$ and $S_{\text{w},1}$ are computed for each gauge configuration. The partial inversions were done with the biconjugate gradient method (see [30]). Then, the fit functions (5.22) and (5.27) are fitted to the numerical results. However, in deriving these functions (see *section 2.3*), we only included contributions from the lowest energy eigenstates (with the correct symmetries). For $t \approx 0$ and $t \approx T$, contributions from higher energy eigenstates cannot be neglected. Thus, we have to choose the boundaries of the fit range at some distance to $t = 0$ and $t = T$. A convenient way to determine the range, where contributions from higher energy eigenstates are negligible, are *plateau plots* like the one shown in *figure 5.3*. For every correlation function $C(t)$, we define the corresponding *plateau function* as

$$P(t) = \ln \frac{C(t)}{C(t+1)} \quad . \tag{5.39}$$

For $t \gg T/2$ or $t \ll T/2$, the cosh functions in (5.22) and (5.27) behave like simple exponentials. (At this qualitative level, the constants $D^{\text{loc}}_{\pi\pi,2}$ and $D_{\pi\pi,2}$ can be completely neglected.) Thus, at some distance from the middle time slice, the plateau function remains constant. However, if t approaches 0 or T, the contributions from higher energy eigenstates become significant and the plateau function starts changing again. Thus, the outermost edges of the two plateaus of P are good choices for the boundaries of the fit range. If no plateaus can be seen in the plateau plot, this means that, for the considered correlation function, the time extent of the lattice is not sufficient to isolate the lowest energy eigenstate or that the statistical errors of the data points are too large. In this work, wherever plateaus could be seen at all, a reasonable choice for the fit range turned out to be $t \in [10, 38]$.

Let's first compare the pion masses obtained from point sources (C^{loc}_{π}) with those obtained from wall sources (C^{w}_{π}). *Table 5.1* shows the results of the fits. The errors

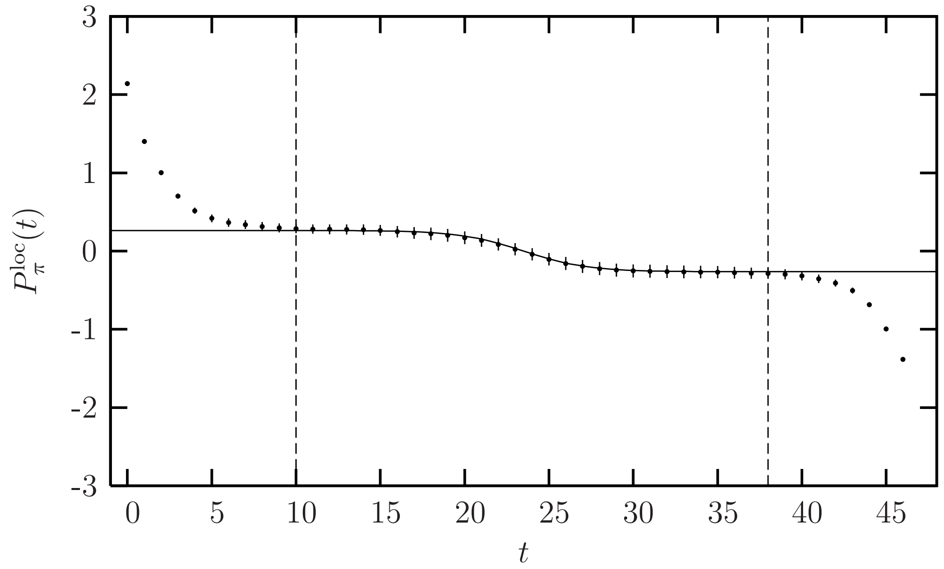

Figure 5.3: Plateau plot of $C_\pi^{\rm loc}$ on the big volume for $\kappa = 0.1535$ with a fit of (5.22b). The boundaries of the fit range, indicated by the dashed lines, are placed at the outermost edges of the two plateaus.

L	κ	$m_\pi^{\rm loc}$	rcs	$m_\pi^{\rm w}$	rcs
16	0.1535	0.3035(56)	1.37	0.2992(67)	1.60
	0.1538	0.2669(70)	1.18	0.2670(63)	1.04
	0.1540	0.2697(95)	0.39	0.2653(101)	0.43
	0.1541	0.2561(67)	0.56	0.2565(88)	0.28
24	0.1535	0.2639(35)	1.55	0.2681(22)	0.27
	0.1538	0.2338(43)	0.10	0.2318(29)	0.15
	0.1540	0.2227(17)	0.91	0.2239(15)	0.73
	0.1541	0.2238(54)	0.50	0.2376(45)	0.44

Table 5.1: Pion masses (in lattice units) obtained with point ($m_\pi^{\rm loc}$) and wall sources ($m_\pi^{\rm w}$) on both volumes ($L = 16, 24$) and for all kappa values. The numbers in brackets behind the pion masses are the statistical errors on the last digit. The columns labelled 'rcs' contain the reduced chi square values of the fits, in which the pion masses on the left were obtained.

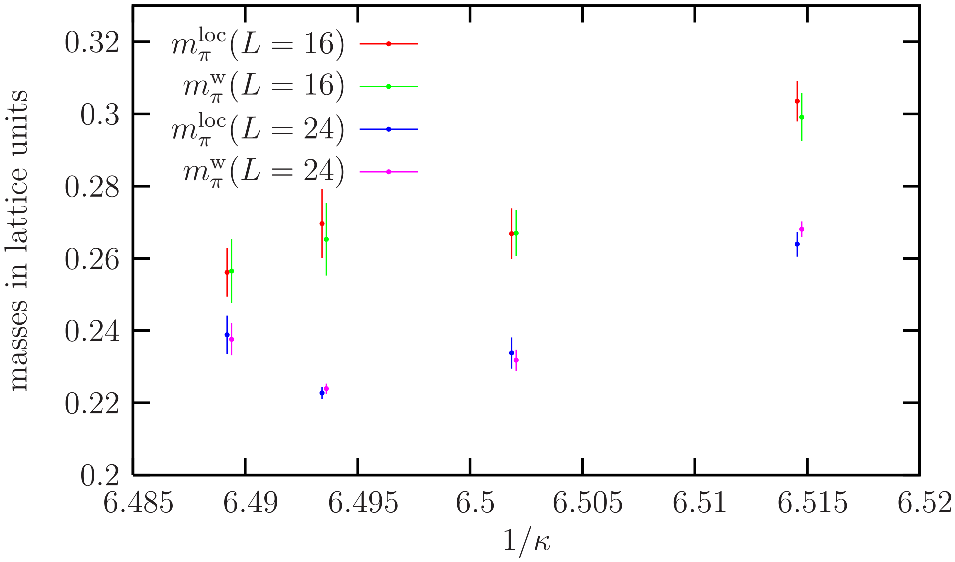

Figure 5.4: Plot of the pion masses from *table 5.1* against the inverse kappa value. Data points lying on top of each other were slightly shifted in the horizontal direction to make them distinguishable.

were determined with the jackknife method, as described in *section 4.4*. In *figure 5.4*, the pion masses are plotted against the inverse kappa value. Masses calculated for the same kappa value and on different volumes turn out to disagree significantly. These deviations are a manifestation of *finite volume effects*, which are still relevant for spacial volumes of order $(1\,\mathrm{fm})^3$. On the other hand, masses obtained from point sources (m_π^{loc}) and those obtained from wall sources (m_π^{w}) agree within the error bars. On the large volume, the statistical errors of the m_π^{w} values are smaller than those of m_π^{loc}. Thus, on the large volume, the noise generated by the wall propagators is overcompensated by the improvement due to the extra sum over the spacial plane at $t = 0$. On the small volume, less improvement is gained by the sum over the spacial plane, so there, the errors of the m_π^{w} values are still slightly bigger than those of the m_π^{loc} values. In *figure 5.4*, a κ dependence of the pion masses can be seen, too, but it is not distinct enough to allow any extrapolations.

For the rho masses and the energy of the two pion state, the use of wall propagators turns out to be more problematic. *Figure 5.5(a)* shows the plateau plot of C_ρ^{w} on the big volume for $\kappa = 0.1535$. Obviously, the data is far too noisy to extract the rho mass. The plateau plot for the corresponding *local* correlation function C_ρ^{loc} is shown in *figure 5.5(b)*. It has two distinct plateaus and the rho mass can be determined from it. For the two pion correlation functions $C_{\pi\pi,2}^{\mathrm{loc}}$ and $C_{\pi\pi,2}^{\mathrm{w}}$, the situation is exactly the same. The local correlation functions yield good results, while those calculated with wall propagators are too noisy to be of any use. It remains unclear, why the wall correlation functions for the rho meson and the two pion state are so much noisier than the pion function C_π^{w}.

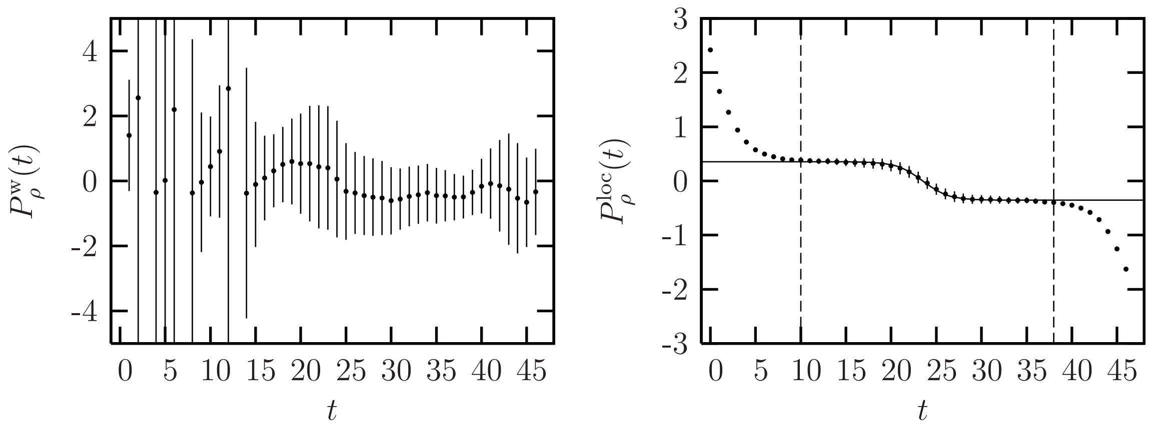

(a) (b)

Figure 5.5: Plateau plots of (a) C_ρ^{w} and (b) C_ρ^{loc} on the big volume for $\kappa = 0.1535$. The data in (a) is far too noisy to determine the rho mass. The missing data points come from negative values of C_ρ^{w}, for which the logarithms in (5.39) are not defined. In (b), the function (5.22a) has been fit to the data. The boundaries of the fit range are indicated by the dashed lines.

L	κ	m_ρ^{loc}	rcs
16	0.1535	0.403(11)	0.43
	0.1538	0.348(15)	0.11
	0.1540	0.376(17)	1.03
	0.1541	0.358(14)	1.03
24	0.1535	0.3545(42)	0.39
	0.1538	0.3275(62)	2.06
	0.1540	0.3263(59)	0.55
	0.1541	0.3248(66)	0.47

Table 5.2: Rho masses (in lattice units) obtained from local correlation functions C_ρ^{loc} on both volumes ($L = 16, 24$) and for all kappa values. The numbers in brackets behind the masses are the statistical errors on the last digit. The column labelled 'rcs' contains the reduced chi square values of the fits, in which the rho masses were obtained.

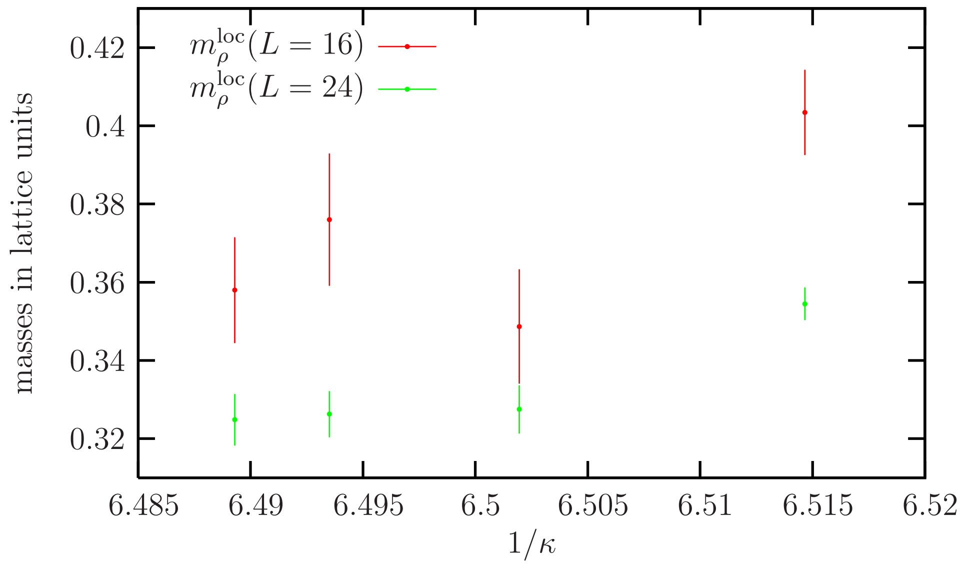

Figure 5.6: Plot of the rho masses from *table 5.2* against the inverse kappa value.

Table 5.2 shows the rho masses obtained by fitting (5.27b) to the numerical data for $C_\rho^{\rm loc}$. In *figure 5.6*, these masses are plotted against the inverse kappa value. As with the pion masses, we see a significant dependence on L due to finite volume effects. On each volume, the masses for the three largest kappa values agree within the errorbars. However, as our pion masses fail to show any distinct κ dependence, there is no reason to assume that we already found the values of the chiral limit.

The energies of the two pion state could only be extracted from the local correlation functions on the large volume. In all other cases, the plateau plots look like *figure 5.5(a)*. The fit values of $E_{\pi\pi,2}^{\rm loc}$ and the corresponding energy shifts are shown in *table 5.3*. In *figure 5.7*, the energy shifts are plotted against $1/\kappa$. As for the other observables, no distinct dependence on κ can be seen.

κ	$E_{\pi\pi,2}^{\rm loc}$	rcs	$E_{\pi\pi,2}^{\rm loc} - 2m_\pi^{\rm loc}$	$E_{\pi\pi,2}^{\rm loc} - 2m_\pi^{\rm w}$
0.1535	0.672(12)	1.68	0.144(14)	0.135(13)
0.1538	0.604(8)	0.40	0.137(12)	0.141(10)
0.1540	0.650(25)	1.51	0.204(25)	0.202(25)
0.1541	0.642(8)	0.09	0.164(13)	0.167(12)

Table 5.3: Energies (in lattice units) of the two pion state calculated on the large volume ($L=24$) with point sources. The energies in the second column were obtained by fitting (5.22c) to the numerical data. The third column contains the reduced chi square values of the fits. The last two columns hold the energy shifts obtained by subtracting twice the pion mass obtained from point and wall sources, respectively. The numbers in brackets are the statistical errors on the last digit.

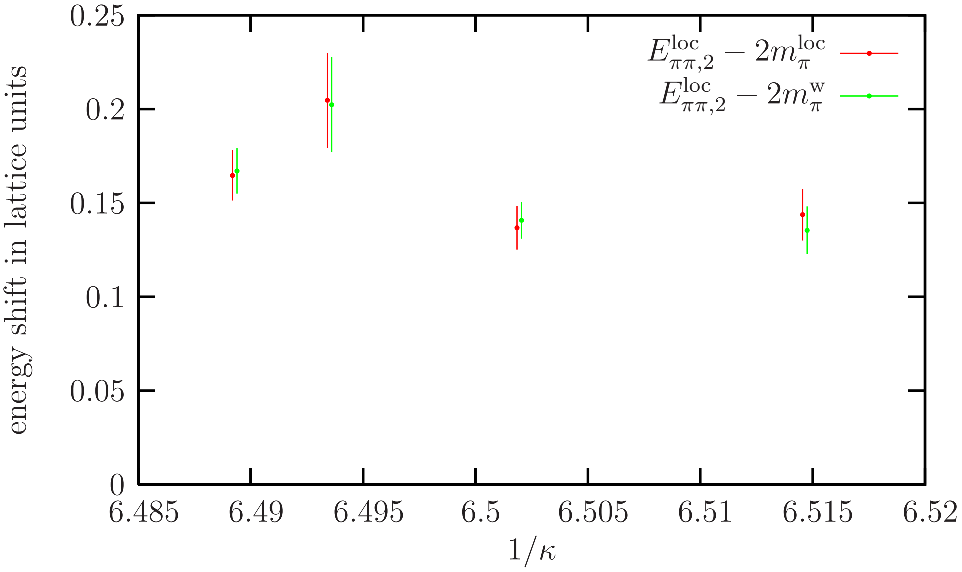

Figure 5.7: Plot of the energy shifts from *table 5.3* against the inverse kappa value. Data points lying on top of each other have been offset horizontally to make them distinguishable.

5.4 Conclusions

With the conventional method of local propagators, the energy shift of the two pion state could be extracted on the large volume. The range of kappa values was not large enough to allow an extrapolation to the chiral limit. With the wall propagator method, it was only possible to determine the pion masses.

The main observation is that the amount of noise generated by the wall propagators seems to vary significantly between different correlation functions. In the case of the pion two point correlation function C_π, the use of the wall source reduced the noise, while the noise was immensely increased in the case of C_ρ and $C_{\pi\pi,2}$. For the pion two point function, we still have the separation of the wall sources in time direction as a parameter to play with. It is possible, that some of the noise observed in the four point function is due to the fact that the wall propagators do not tie up properly. However, as the results for C^{w}_ρ are equally bad, there must be another reason for the great difference between the quality of the results for C^{w}_π on the one hand and C^{w}_ρ and $C^{\mathrm{w}}_{\pi\pi,2}$ on the other hand.

However, comparing our results to those presented in [36], we are led to the conclusion, that the application of wall propagators in the calculation of pion four point correlation functions is not possible for the simple gauge and quark actions we used in our calculation. Improvements like those applied in [36] appear to be necessary and worthwhile.

Bibliography

[1] **NA48** Collaboration, V. Fanti et al., "A New Measurement of Direct CP Violation in Two Pion Decays of the Neutral Kaon," *Phys. Lett.* **B465** (1999) 335, `hep-ex/9909022`.

[2] **KTeV** Collaboration, A. Alavi-Harati et al., "Observation of Direct CP Violation in $K_{S,L} \to \pi\pi$ Decays," *Phys. Rev. Lett.* **83** (1999) 22, `hep-ex/9905060`.

[3] C. W. Bernard, T. Draper, A. Soni, H. D. Politzer, M. B. Wise, "Application of Chiral Perturbation Theory to $K \to 2\pi$ Decays," *Phys. Rev.* **D32** (1985) 2343.

[4] P. Boucaud et al., "An Exploratory Lattice Study of $\Delta I = 3/2$ $K \to \pi\pi$ Decays at Next-to-Leading Order in the Chiral Expansion," `hep-lat/0412029`.

[5] C. J. D. Lin, G. Martinelli, E. Pallante, C. T. Sachrajda, G. Villadoro, "$K^+ \to \pi^+\pi^0$ Decays on Finite Volumes and at Next-to-Leading Order in the Chiral Expansion," *Nucl. Phys.* **B650** (2003) 301–355, `hep-lat/0208007`.

[6] M. Fukugita, Y. Kuramashi, M. Okawa, H. Mino A. Ukawa, "Hadron Scattering Lengths in Lattice QCD," *Phys. Rev.* **D52** (1995) 3003, `hep-lat/9501024`.

[7] J. W. Christenson, V. L. Fitch, R. Turlay, "Evidence for the 2π Decay of the K_2^0 Meson," *Phys. Rev. Lett.* **13** (1964) 138.

[8] D. Bećirević, D. Meloni, A. Retico, "An Estimate of the K^0-$\bar{K}^0$ Mixing Amplitude," *JHEP* **01** (2001) 012, `hep-lat/0012009`.

[9] **RBC** Collaboration, T. Blum et al., "$K \to \pi\pi$ Decays with Domain Wall Fermions: Lattice Matrix Elements," *Nucl. Phys. Proc. Suppl.* **94** (2001) 291, `hep-lat/0011042`.

[10] **CP-PACS** Collaboration, A. Ali Khan et al., "Kaon B Parameter from Quenched Domain-Wall QCD," *Phys. Rev.* **D64** (2001) 114506, `hep-lat/0105020`.

[11] Y. Nir, "CP Violation," *SLAC Summer Inst.* (1992) 81, `SLAC-PUB-5874`.

[12] L. L. Chau *Physics Reports* **95** (1983) 1.

[13] L. L. Chau, W.-Y. Keung *Phys. Rev. Lett.* **53** (1984) 1802.

[14] L. Wolfenstein *Phys. Rev. Lett.* **51** (1983) 1945.

[15] A. J. Buras, "CP Violation in B and K Decays: 2003," `hep-ph/0307203`.

[16] M. E. Peskin, D. V. Schroeder, *An Introduction to Quantum Field Theory.* Westview Press, 1995.

[17] **CKMfitter** Collaboration, J. Charles et al., "CP Violation and the CKM Matrix: Assessing the Impact of the Asymmetric B Factories," `hep-ph/0406184,` `http://www.slac.stanford.edu/xorg/ckmfitter/`.

[18] **BaBar** Collaboration, B. Aubert et al., "Measurement of the CP-violating Asymmetry Amplitude $\sin 2\beta$," *Phys. Rev. Lett.* **89** (2002) 201802, `hep-ex/0207042`.

[19] **Belle** Collaboration, K. Abe et al., "Improved Measurement of Mixing-induced CP Violation in the Neutral B Meson System," *Phys. Rev.* **D66** (2002) 071102.

[20] Y. Nir, "CP Violation: The CKM Matrix and New Physics," *Nucl. Phys. Proc. Suppl.* **B117** (2003) 111.

[21] A. J. Buras, "Weak Hamiltonian, CP Violation and Rare Decays," `hep-ph/9806471`.

[22] S. Capitani, "Lattice Perturbation Theory," *Phys. Rept.* **382** (2003) 113, `hep-lat/0211036`.

[23] L. Maiani, M. Testa *Phys. Lett.* **B245** (1990) 585.

[24] M. Lüscher *Nucl. Phys.* **B354** (1990) 531.

[25] L. Lellouch, M. Lüscher *Commun. Math. Phys.* **219** (2001) 31.

[26] H. Georgi, *Lie Algebras in Particle Physics.* Westview Press, second ed., 1999.

[27] J. Goldstone, A. Salam, S. Weinberg *Phys. Rev.* **127** (1962) 965.

[28] P. Ramond, *Field Theory: A Modern Primer.* Addison Wesley, 1990.

[29] J. F. Cornwell, *Group Theory in Physics.* Academic Press, 1984.

[30] W. H. Press, S. A. Teukolsky, W. T. Vetterling, B. P. Flannery, *Numerical Recipes in C++.* Cambridge University Press, second ed., 2003.

[31] G. Bhanot, "The Metropolis Algorithm," *Rep. Prog. Phys.* **51** (1988) 429.

[32] **SPQcdR** Collaboration, C. Bećirević et al. `hep-lat/0409110`.

[33] I. Montvay, M. Münster, *Quantum Fields on a Lattice.* Cambridge University Press, 1994.

[34] B. R. Martin, *Statistics for Physicists.* Academic Press, 1971.

[35] C. R. Allton et al. *Nucl. Phys.* **B489** (1997) 427, `hep-lat/9611021`.

[36] **CP-PACS** Collaboration, T. Yamazaki et al., "$I = 2$ Pion Pion Scattering Phase Shift in the Continuum Limit calculated with Two Flavor Full QCD," *Nucl. Phys. Proc. Suppl.* **129** (2004) 191, `hep-lat/0309155`.

Acknowledgments / Danksagung